UNIVERSITAT DE BARCELONA

CPEB4 function in macrophages

Clara Suñer Navarro

Universitat de Barcelona

Facultat de Farmàcia i Ciències de l'Alimentació

IRB Barcelona

Programa de Doctorat en Biomedicina

CPEB4 function in macrophages

Aquesta tesi ha estat realitzada per la Clara Suñer Navarro sota la direcció del Dr. Raúl Méndez de la Iglesia, a l'Institut de Recerca Biomèdica de Barcelona (IRB Barcelona).

Es presenta aquesta memòria per optar al títol de doctora per la Universitat de Barcelona en el Programa de Doctorat en Biomedicina.

Raúl Méndez de la Iglesia	Antonio Zorzano Olarte	Clara Suñer Navarro
Director de tesi	*Tutor de tesi*	*Doctoranda*

Barcelona 2018

Para los cuatro.

"Not only to be receiver,

but also to be provider"

Buddhist proverb

Preface

What is the meaning of life?

Throughout history, great efforts have been made trying to understand which is the significance of living or existence. Philosophical, scientific, theological and metaphysical approaches have proposed multiple answers to questions such as "Why are we here?", "What is life all about?", or "What is the purpose of existence?".

Scientific contributions have focused primarily on describing empirical facts about the universe, exploring the context and parameters concerning what life is and aiming to describe how it works. Though life definition is still a challenge, from the biologist point of view lifeforms are self-organizing systems that regulate their internal environments as to maintain this organized state, also known as homeostasis, and reproduce to continue life over multiple generations.

Importantly, homeostasis maintenance needs the capacity to sense and adapt to the external environment. Throughout this thesis, we will focus on a specific subset of mechanisms developed to respond to a certain stimulus. These mechanisms, if successful, return life to its homeostatic state but, upon failure, may lead to life-threating conditions.

I am afraid we will not provide a new answer to the question "What is the meaning of life?", however we will further describe its complexity and fragility and, one could extrapolate from that, how precious life is.

INDEX

Index

List of Figures

INTRODUCTION

RESULTS

DISCUSSION

MATERIALS AND METHODS

SUPPLEMENTARY FIGURES

ABBREVIATIONS

Abbreviations

A site – acceptor site

ActD – Actinomycin D

APA – alternative polyadenylation

ARE – AU rich element

ARE-BP – ARE binding protein

AREd – ARE-dominant mRNAs

BMDM – bone marrow derived macrophage

CCL – CC chemokine ligand

CDE – constitutive decay element

CDK – cyclind-dependent kinase

CDS – coding sequence

CLIP – cross linking and immunoprecipiation

COX2 – cyclooxygenase 2

CPE – cytoplasmic polyadenylation element

CPEB – cytoplasmic polyadenylation element binding protein

*Cpeb4*KO – Cpeb4 ubiquitous knowckout

*Cpeb4*MKO – myeloid-specific Cpeb4 knock-out

CPEc – CPE consensus

CPEd – CPE-dominant mRNAs

CPEnc – CPE non consensus

CPSF – cleavage and polyadenylation specificity factor

CSTF – cleavage stimulation factor

CTD – C terminal domain

CXCL – CXC chemokine ligand

DAMP – danger-associated molecular pattern

DC – dendritic cell

Diff Exp – differential expression

DNA – deoxyribonucleic acid

DSE – downstream sequence element

DT – differential translation

DUB – deubiquitinase enzyme

DUSP – dual-specificity protein phosphatase

E site – exit site

EDEN – embrionic deadenylation element

eEF – eukaryote elongation factor

eIF – eukaryote initiation factor

ELAV – embryonic lethal and abnormal vision

ER – endoplasmic reticulum

eRF – eukaryote release factor

ERK – extracellular signal-regulated kinase

HDAC – hitone deacetylase

HIF1α – hypoxia-inducible factor 1α

HSC – hematopoietic stem cell

HuR – Hu-antigen R

IFN – intereferon

IKK – IκB kinase

IL – interleukin

IL-1RA – Interleukin-1 receptor antagonist

iNOS – inducible nitric oxide synthase

IP – immunoprecipitation

IRES – internal ribosome entry site

IRF – intereferon regulatory factor

JNK – jun N-terminal kinase

LPS – Lipopolysaccharide

M-CSF – macrophage colony stimulating factor

MAPK – mitogen activated protein kinase

miRNAs – microRNA

MKO– myeloid-specific knock-out

MPS – mononuclear phagocytic system

mRNA – messenger RNA

mRNPs – messenger ribonucleoprotein particle

mTOR – mammalian/mechanistic target of rapamycin

NF-κB – nuclear factor κB

NMD – non sense mediated

NTD – N terminal domain

P site – peptidyl site

P-bodies – processing bodies

PABP – poly(A) binding protein

PAMP – pathogen-associated molecular pattern

PAP – poly(A) polymerase

PAR-iCLIP - photoactivatable ribonucleoside-enhanced crosslinking and immunoprecipitation

PAS – polyadenylation site

PG – prostaglandins

poly(A) – polyadenosine

PP2A – Protein Phosphatase 2A

PRR – pathogen recognition receptor

PTC – premature termination codon

PTMs – post-translational modificantions

PV - p value

QC – quality control

RBP – RNA binding protein

RIP-seq – RNA-immunoprecipitation and sequencing

RISC – RNA-induced silencing complex

RNA – ribonucleic acid

ROS – reactive oxygen species

RP – ribosome profilin

RRM – RNA recognition motif

RT-qPCR – real time quantitative polymerase chain reaction

SG – stress granules

siRNA – small interfering RNAs

SOCS – Signal transducer and activator of transcription

STAT – signal

TBP – TATA binding protein

TC – ternary complex

TE – translation efficiency

TLR – toll-like receptor

TNFAIP3 – TNF alpha induced protein 3

TOP – terminal oligopyrimidine

TSS – transcription start site

TTP - tristetraprolin

uORF- upstream open reading frame

UPR – unfolded protein response

ABSTRACT

Abstract

As innate immune cells, macrophages sense endogenous and exogenous danger signals and respond orchestrating inflammatory processes. For the rapid induction and efficient resolution of inflammatory responses, macrophages induce the expression of pro-inflammatory and anti-inflammatory mediators, which cross-regulate each other through feedback loops. This process requires tightly controlled gene expression at multiple levels. Recently, the regulation of mRNA deadenylation has emerged as a key regulator of the strength and, critically, the duration of transient inflammatory responses.

Cytoplasmic Polyadenylation Element Binding (CPEB1-4) family of RNA-binding proteins target mRNAs containing Cytoplasmic Polyadenylation Elements (CPEs) in their 3'UTR. CPEBs orchestrate the assembly of two types of ribonucleoprotein complexes (mRNPs) which can repress or stimulate the translation of target mRNAs by modulating the length of poly(A) tail. Several inflammatory mediators harbour CPEs in their 3'UTRs and are potential CPEB targets. Thus, we hypothesized that CPEBs could be an additional checkpoint to control inflammatory responses.

We find that CPEB4 is a novel player in macrophage response to LPS. Upon LPS treatment, CPEB4 is upregulated and its polyadenylation function is activated, a process mediated by the MAPK p38α and ERK1/2 and two AU Rich Element Binding Proteins (ARE-BPs). Interestingly, the pattern of CPEB4 expression and activity suggests that it participates in late LPS-response, when the resolution of inflammation occurs. Indeed, myeloid-specific *Cpeb4*KO mice display increased sensitivity to LPS-induced endotoxic shock. We identify CPEB4 target mRNAs by RNA-Immunoprecipitation and Sequencing (RIP-Seq), uncovering that CPEB4 regulates the expression of negative regulators of MAPK signalling, thus creating the negative feedback loop needed the resolution of inflammation. Moreover, we also describe how the interplay between CPEB4, HuR and TTP defines mRNA behaviour during the different temporal windows of inflammatory responses.

INTRODUCTION

Introduction

In this thesis we have studied CPEBs contribution to inflammatory responses. CPEBs, which stands for Cytoplasmic Polyadenylation Element Binding Proteins, are RNA binding proteins that can regulate mRNA translation by modulating the poly(A) tail of mRNAs. In this first part of the introduction we will summarize the process of protein synthesis, focusing on the lifecycle of mRNAs and how the poly(A) tail,together with other elements, can have an impact on mRNAs fate.

1. Regulation of protein synthesis

Organisms store biological information in their genomes which, except for certain viruses, are made of DNA. The genome can be divided into genes, DNA regions that encode for functional molecules, either proteins or RNAs, and intergenic regions. Gene expression comprises a group of molecular processes by which information from a gene is used to synthesize its functional gene product. For instance, protein expression is initiated by the transcription of a gene into an intermediary molecule called messenger RNA (mRNA), which is then translated into the sequence of amino acids that forms the protein (Crick 1958; Crick 1970). This course of events is known as the central dogma of molecular biology, and it efficiently explains how nucleotides in the DNA store information for protein composition **(Fig. 1)**.

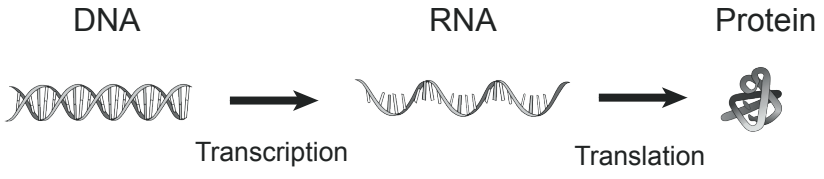

Figure 1. Central dogma of molecular biology. Modified from Barillot et al. 2012.

However, less than 2% of the human genome consists of protein-coding sequences (Brown 2011). So, what is the rest of our genome for? Besides other functions, our genome contains thousands of elements whose function is to regulate protein expression at the transcriptional, translational and also, post-translational level (Mayr 2017).

Since the statement of the Central Dogma, the elements that govern gene transcription have been widely studied. To date, we know that cis-regulatory elements on the DNA, trans-acting factors, chromatin structures or epigenetic modifications can govern gene transcription, indicating which genes need to be transcribed, to which extent or when. However, translational regulation has been less characterized. Importantly, each mRNA contains not only its protein-coding sequence but also regulatory elements. We know that these elements can govern mRNA translation, stability or localization; nevertheless, their impact on protein expression is, in many occasions, underestimated.

In this first part of the introduction we will summarize the process of protein synthesis, focusing on the lifecycle of mRNAs and the different regulatory elements that can have an impact on the fate of mRNAs.

1.1. pre-mRNA processing

The first processing events of pre-mRNAs occur concomitantly with transcription (Aguilera 2005). As soon as the first 20-30 nucleotides of the nascent pre-mRNA have been produced, the mRNA is capped at the 5' end (Topisirovic & Sonenberg 2011). The mature methylated cap (m7G-cap) is critical for mRNA protection from 5'-3' exonucleases, for mRNA nuclear export, and for cap-dependent mRNA translation initiation (Shatkin & Manley 2000),among other functions. These regulatory activities are mediated by cap-binding proteins: the nuclear cap binding protein complex (nCBC) in the nucleus and eukaryotic translation initiation factor 4E (eIF4E) in the cytosol.

Also concomitant with transcription, intronic sequences are removed from pre-mRNAs by a process named splicing (Papasaikas & Valcárcel 2015). Interestingly, this process allows the combinatorial removal of various intronic and/or exonic regions, potentially altering the exon composition of the mature mRNA. Consequently, alternatively spliced mRNA isoforms may differ in their regulation and function, as well as their encoded proteins **(Fig. 2a)**.

Once the polymerase has transcribed the entire gene, the 3' end of the pre-mRNA is processed. Except for replication-dependent histone mRNAs, this process consists of the endonucleolytic cleavage of the mRNA and the subsequent addition of a non-templated polyadenosine tract, named the poly(A) tail or poly(A) (Marzluff et al. 2008; Di Giammartino et al. 2011; Elkon et al. 2013). The location in the mRNA where this process occurs is defined by two specific regulatory elements in the pre-mRNA sequence, the polyadenylation signal (PAS, 5'-AAUAAA-3') and the downstream sequence element (DSE, U/GU-rich). These elements, in turn, will be recognized by the cleavage and polyadenylation specificity factor (CPSF) and the cleavage stimulating factor (CSTF), which together with other cleavage factors, will specify the cleavage site, often after a CA dinucleotide. After the cleavage event, a poly(A) polymerase (PAP) adds approximately 250 adenosines that will be coated by poly(A) binding proteins (PABP) **(Fig. 2b)**. Remarkably, PABPs coating and thus the poly(A) tail, is relevant for several mRNA processes: nuclear export, protection from 3'-5' degradation and mRNA translation (Proudfoot 2011; Eckmann et al. 2011; Jurado et al. 2014).

Importantly, once the tail has been synthesized, the length of the poly(A) tail can be dynamically modulated by deadenylases and polyadenylases (Zhang et al. 2010). Therefore, the population of mRNAs in a cell are heterogeneous in poly(A) tail length, ranging from 30 to 250 nucleotides, and modulation of their poly(A) tail is used to regulate mRNA translation and stability.

It is also worth mentioning that more than one half of all mammalian transcripts can be cleaved and polyadenylated at various sites, a process known as alternative cleavage and polyadenylation (APA). Depending on which site is used, transcripts will contain or exclude regulatory elements on their 3' untranslated region possibly altering mRNA behaviour at multiple levels (Elkon et al. 2013) **(Fig. 2c)**.

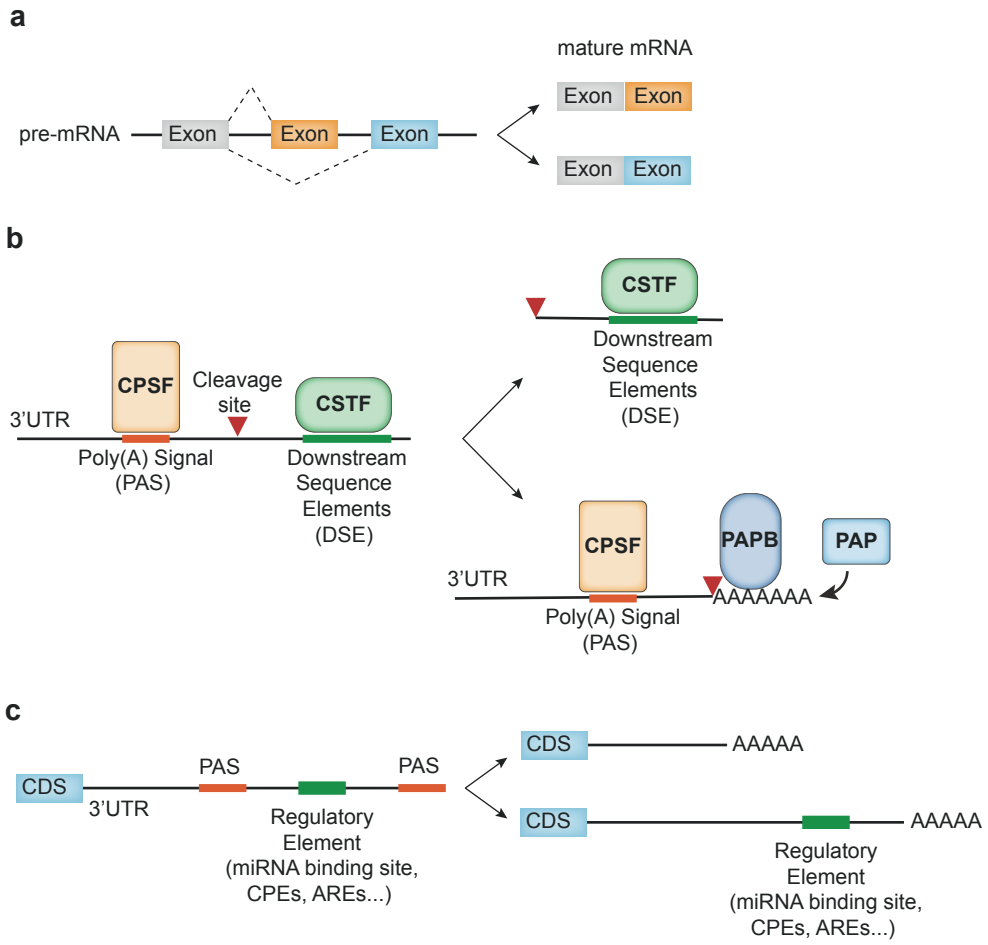

Figure 2. Pre-mRNA processing. (a) Schematic view of mRNA processing. **(b)** Examples of mRNAs generated by alternative splicing and alternative polyadenylation. **(c)** The PAS and the DSE define the cleavage site where the poly(A) tail will be added.

Finally, and before reaching the cytoplasm, mature transcripts can be enzymatically modified on specific nucleotides. More than 100 types of chemical modifications have been described (Peer et al. 2017; Roundtree et al. 2017), however, little is known about their biological function and distribution. Some of these have been shown to control mRNA expression and stability, mRNA structure or the susceptibility of mRNAs to interact with RNA binding proteins (RBPs) (Fu et al. 2014; Roignant & Soller 2017; Slobodin et al. 2017).

It is worth stressing that from the start of transcription, mRNA processing and functions are driven by cis-regulatory elements on the mRNA and the RBPs that they recruit. Consequently, cellular mRNAs are not "naked" nucleic acids, but they are constantly interacting with RBPs. Moreover, these interactions are dynamic, as they evolve during each phase of the mRNA's lifecycle. Thus, when we refer to mRNAs, we should be aware that we actual mean messenger ribonucleoprotein particles (mRNPs).

1.2. Mature mRNA structure

After all these processing steps, the mature mRNA body consists of a coding sequence (CDS) flanked by two untranslated regions (UTRs), with a m7G-cap at its 5' end and the poly(A) tail at its 3' end.

The CDS constitutes the region of the mRNA that will be translated into a protein by ribosomes. It starts with the AUG initiation codon and ends with one of the three stop codons UAA, UAG or UGA. In the last years, several studies have demonstrated that codon composition of the coding region can also impact translation, a concept known as codon optimality (Schuller & Green 2018). On the other hand, the 5' and 3'UTRs contain structural features or regulatory cis-acting sequences involved in the control of mRNA translation, storage, transport and decay. The 5' UTR regulatory motifs that influence mRNA translation include secondary structures, upstream open reading frames (uORFs), internal ribosome entry sites (IRES) and specific binding sites for RNA-binding proteins, among others (Leppek et al. 2018). The 3' UTR can also contain specific secondary structures and binding sites for regulatory proteins, as well as microRNA (miRNA) binding sites **(Fig. 3)**.

It is worth highlighting though that each mRNA should be seen as a unit the behaviour of which results from the cooperation or competition of its distinct elements throughout the CDS and UTRs. This concept, known as the combinatorial code of mRNAs, states that all the elements in a given mRNA constitute a unique "bar code" that determines mRNA behaviour throughout its life cycle (Piqué et al. 2008).

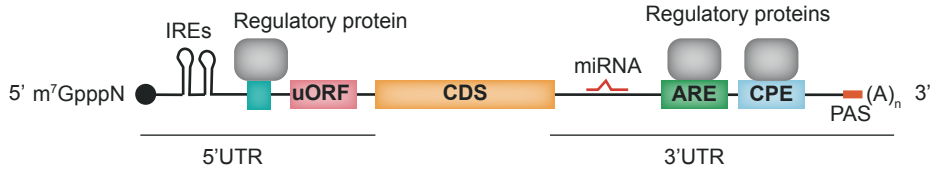

Figure 3. Regulatory elements in mature mRNAs.

The cytoplasmic fate of mRNAs

After nuclear export, the cytoplasmic fates of mature mRNAs can be basically divided into translation, degradation and localization. In the next sections, we will dissect these processes, emphasizing the possible regulatory functions exerted by the previously mentioned mRNA features.

1.3. mRNA translation

The translation of mRNA into proteins is the final step of protein expression. It is a complex energy-consuming process subject to tight regulation. Translation of mRNAs occurs in four phases: initiation, elongation, termination and ribosome recycling.

1.3.1. Translation initiation

Translation initiation represents the most complex and rate-limiting step in translation, involving more than 50 proteins in eukaryotes.

Cap-dependent translation initiation is determined by the eIF4F complex, which is bound to the 5' cap and is responsible for recruiting the 43S pre-initiation complex to the mRNA (Sonenberg & Hinnebusch 2009; Jackson et al. 2010). The eIF4F complex is composed of eIF4E that binds to the cap, the scaffold protein eIF4G that recruits the 43S pre-initiation complex, and the RNA helicase eIF4A that favours 43S binding and scanning. The 43S pre-initiation complex consists of 40S ribosomal subunit to which the ternary complex (TC) has been recruited. The TC is a complex of the eukaryotic initiation factor 2 (eIF2, a heterotrimer of α, β and γ subunits) bound to GTP and a methionine-charged initiator tRNA (Met-tRNAi).

Once the 43S pre-initiation complex binds the mRNA, it scans along the 5' UTR until it recognizes the initiation codon AUG in an appropriate sequence context (Kozak 2002). Upon AUG recognition, it will now form the 48S initiation complex following which, hydrolysis of eIF2-GTP takes place and most initiation factors are released. Subsequently, the large 60S ribosomal subunit joints and the this 80S translationally competent ribosome can start the elongation process (Gebauer & Hentze 2004; Hinnebusch & Lorsch 2012). Importantly, eIF4G also interacts with PABP at the poly(A) tail, bringing both ends of the mRNA together in a closed-loop conformation so that termination and re-initiation of translation are efficiently coupled (Tarun & Sachs 1995).

Alternatively to CAP-dependent translation initiation, some cellular transcripts rely on other elements such as internal ribosomal entry sites (IRES) to initiate their translation. IRES are RNA elements that through their secondary structure or primary sequence, recruit the 40S ribosomal subunit independently of the cap-binding factor eIF4E (Shatsky et al. 2018).

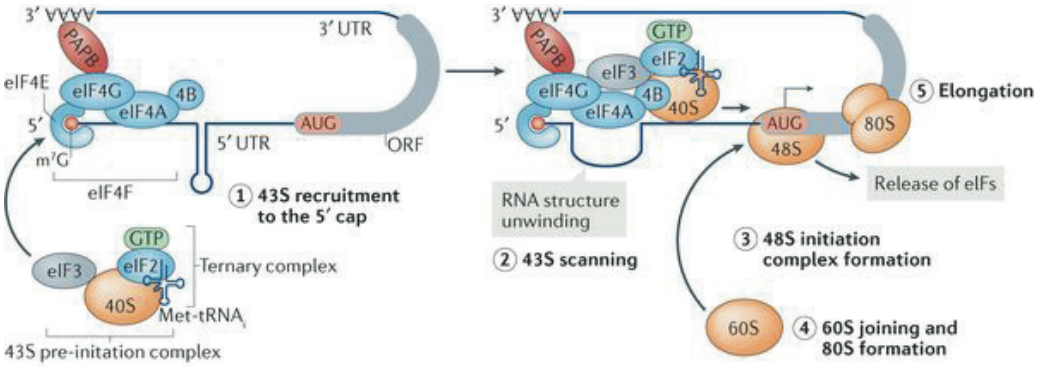

Figure 4. Canonical cap-dependent translation initiation. Scheme of the different steps during cap-dependent translation initiation. Source: Leppek et al. 2018.

1.3.1.1. Regulation of translation initiation

The formation of the TC is the major checkpoint that the cell uses to regulate global protein production. eIF2 is a G-protein that cycles between its active form (GTP-bound) and the inactive one (GDP-bound). After eIF2-bound GTP hydrolysis upon AUG recognition, eIF2-GDP is recycled back to its GTP-bound state, a process mediated by the guanine nucleotide exchange factor eIF2B. Since eIF2-GTP is the limiting factor for the assembly of the ternary complex, this recycling step is crucial for translation initiation. Indeed, eIF2α phosphorylation, which reduces the dissociation rate of eIF2 from eIF2B, leads to a global inhibition of translation initiation. This process has been shown to occur under certain stress conditions, such as viral infection or the accumulation of misfolded proteins in the endoplasmic reticulum (ER) (Pakos-Zebrucka et al. 2016) **(Fig. 5a)**.

As formerly described, some mRNAs contain upstream open reading frames (uORF) in their 5'UTRs. Briefly, uORFs are sequences defined by an initiation codon upstream of the main coding region. In normal conditions, uORFs are translated by ribosomes, which generally initiate translation on the first available AUG codon. As a consequence, uORFs repress the translation of the main protein-coding sequence as fewer ribosomes, if any, reach its initiation codon. However, uORF-containing mRNAs benefit from eIF2α phosphorylation, as low initiation rates favour that ribosomes skip uORFs and get to translate the main coding sequence (Barbosa et al. 2013) **(Fig. 5b)**.

The cap-binding protein eIF4E is another node of protein synthesis regulation. In most cells, eIF4E levels are limiting, and thus the regulation of its activity has a strong impact on the translation efficiency of many mRNAs. For example, eIF4E-binding proteins (4E-BPs) can inhibit translation by competing eIF4E binding to the cap. Extracellular stimuli like mitogens and growth factors can trigger 4E-BPs phosphorylation by the mTOR kinases. Phosphorylated 4E-BPs are not able to bind eIF4E and translation initiation is enhanced (Richter & Sonenberg 2005; Sonenberg & Hinnebusch 2007; Roux & Topisirovic 2018). Alternatively, impairment of eIF4A activity or availability can also lead to translational repression, a strategy that is being explored as a cancer therapy (Chu & Pelletier 2015) **(Fig. 5c)**.

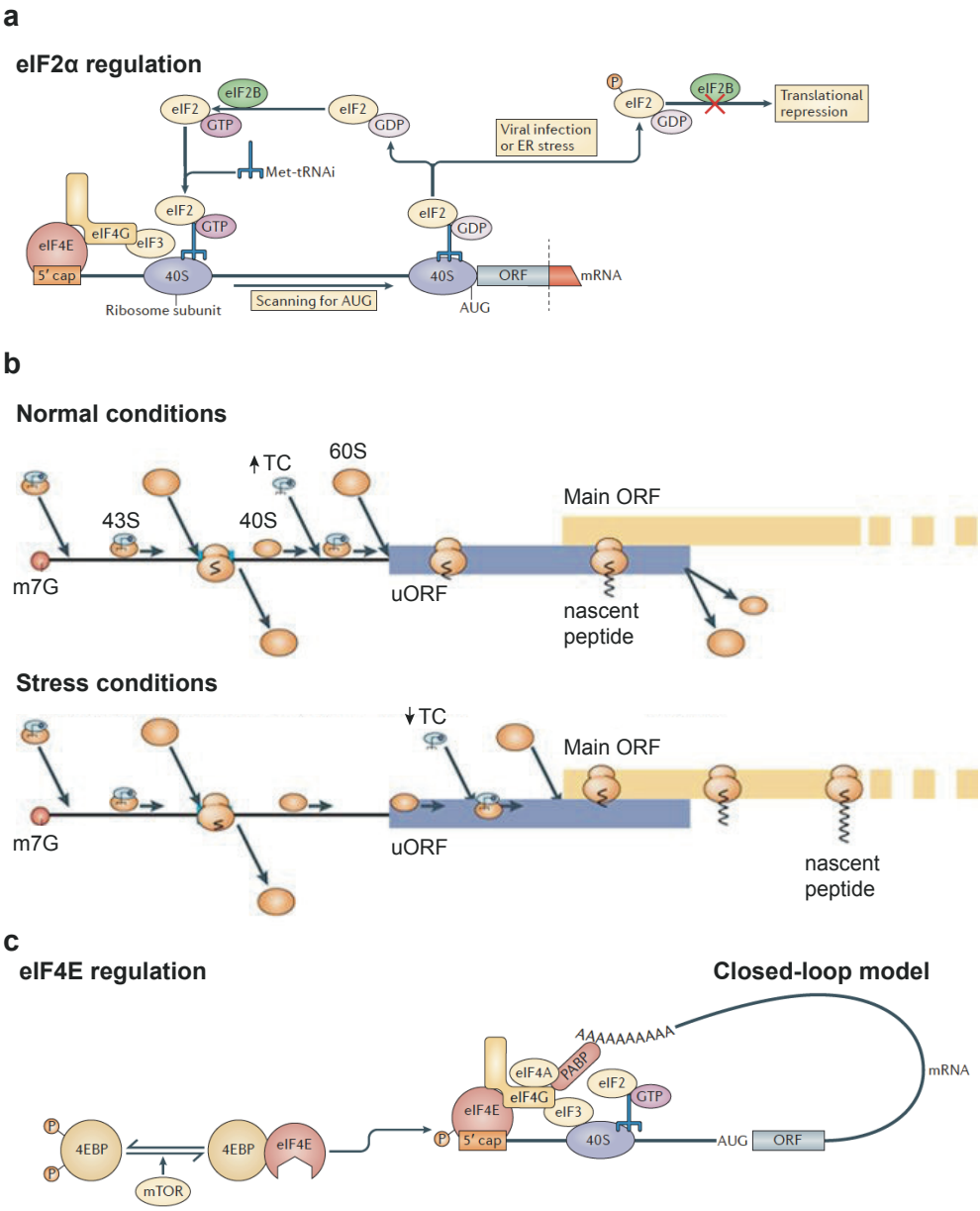

Figure 5. Regulation of translation initiation. (a) Under stress conditions, eIF2a-phosphorylation inhibits eIF2-GDP recycling and represses global translation initiation. **(b)** mTOR phosphorylates 4EBPs, inhibiting its binding to eIF4E that will bind the CAP and promote translation. Closed-loop model: in this scheme it is also shown the circularized mRNA due to the binding of PABP to eIF4G. **(c)** In stress conditions, uORF-containing mRNAs benefit from the low availability of the ternary complex (TC) as ribosomes get to translate the main ORF, and are not sequestered by uORFs as in normal conditions. Source: (a,c) Adapted from Carpenter et al. 2014. (b) Adapted from Jackson et al. 2010.

Finally, another factor modulating translation initiation is the previously mentioned closed-loop model. The simultaneous interaction of eIF4G with eIF4E and the PABP, which are bound to the cap and the poly(A) tail respectively, brings together both ends of the mRNA resulting in mRNA pseudo-circularization (Imataka et al. 1998; Wells et al. 1998). This conformation allows the 5' cap and the 3' poly(A) tail to synergistically favour the recruitment of the small ribosomal subunit to the mRNA. At least in yeast, this conformation is essential for translation initiation and, in other systems, it has also been shown that it can favour ribosome recycling or promote mRNA stability (Tarun & Sachs 1995; Sachs et al. 1997; Kahvejian et al. 2005). Consequently, any regulation that favours or compromises the cap–eIF4E–eIF4G–PABP–poly(A) "bridge", and thus the close-loop structure, can in turn stimulate or inhibit translation of mRNAs **(Fig. 5b)**.

1.3.2. Translation elongation

Translation elongation is the stepwise addition of amino acids in order to produce the codified protein chain. The order of amino acids is specified by the sequence of codons in the mRNA, that tRNAs with the pairing anticodon will recognize bringing with them the needed amino acids in the appropriate order. This process is performed by the 80S ribosome together with the elongation factors eEF1A and eEF2 and, of course, the cellular pool of charged tRNAs. While translation initiation is directly regulated by more than 25 proteins, the elongation and termination processes require a minimum number of them, thereby underscoring the preponderance of the initiation step over the other two (Lackner & Bähler 2008). Nevertheless, translation regulation can also occur at the elongation step. For example, eEF2 phosphorylation by the eukaryotic elongation factor 2 kinase (eEF2K) reduces its affinity for ribosomes and therefore represses translation elongation. Among others, MAPK (mitogen-activated protein kinase) or mTOR signalling pathways can inactivate eEF2K in order to promote eEF2 elongation function (Kaul et al. 2011). Moreover, in recent years, further elongation-related regulatory mechanisms have emerged as new determinants of protein synthesis. Some examples would be acyl-tRNA availability and modifications, ribosome composition and function, and codon optimality (Richter & Coller 2015; Shi et al. 2017; Simsek et al. 2017; Schuller & Green 2018).

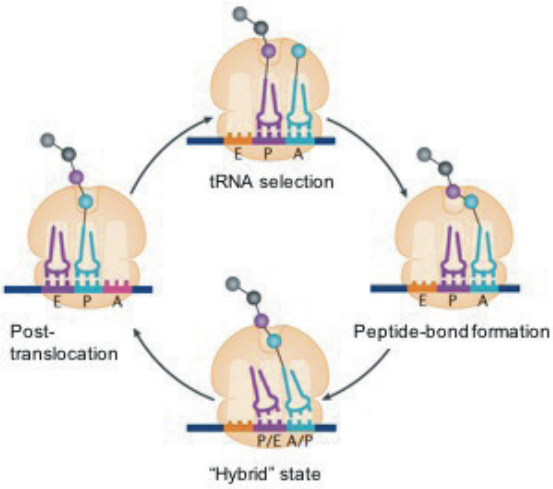

Figure 6. Translation elongation. Ribosomes contain three positions for tRNAs: an acceptor site (A site), where the aminoacyl-tRNA is placed; the peptidyl site (P site), which contains the tRNA with the growing polypeptide; and the exit site (E site), where the empty tRNA exits the ribosome. During translation elongation, aminoacyl-tRNAs are carried to the empty A. Then, a peptide bond is formed between the incoming amino acid and the growing polypeptide, which will be now placed in the A site. After peptide bond formation, tRNAs are translocated, the empty tRNA is positioned in the E site and the peptidyl-tRNA in the P site again. The A site is then empty and available for binding the next aminoacyl-tRNA (Kapp & Lorsch 2004; Dever & Green 2015). Source: Schuller & Green 2018.

1.3.3. Translation termination and ribosome recycling

Translation termination is triggered by the appearance of a stop codon in the A position of the ribosome. In eukaryotes, termination is mediated by two release factors (eRF1 and eRF3), which mediate the release of the synthesized peptide and the establishment of the post-termination complex. This complex, composed of the ribosome and eRF1, will facilitate ribosomal recycling.

Ribosome recycling is the process by which the 80S ribosome splits into its 40S and 60S subunits to prepare for another round of translation. Although eRF1 and eRF3 are sufficient to mediate both translation termination and ribosome recycling, the latter can also be facilitated by ABCE1 (Preis et al. 2014). Ribosome recycling is often described as a key step for the beginning of initiation, as ABCE1 can also associate with several initiation factors. Furthermore, the closed-loop structure of mRNAs can also favour the direct re-entry of ribosomes to the translation initiation point, enhancing mRNAs translation efficiency (Nürenberg & Tampé 2013).

However, ribosome recycling does not only occur after completion of the translation process, but can also happen upon failure of polypeptide synthesis when damaged mRNA is encountered, or following the assembly of empty ribosomes.

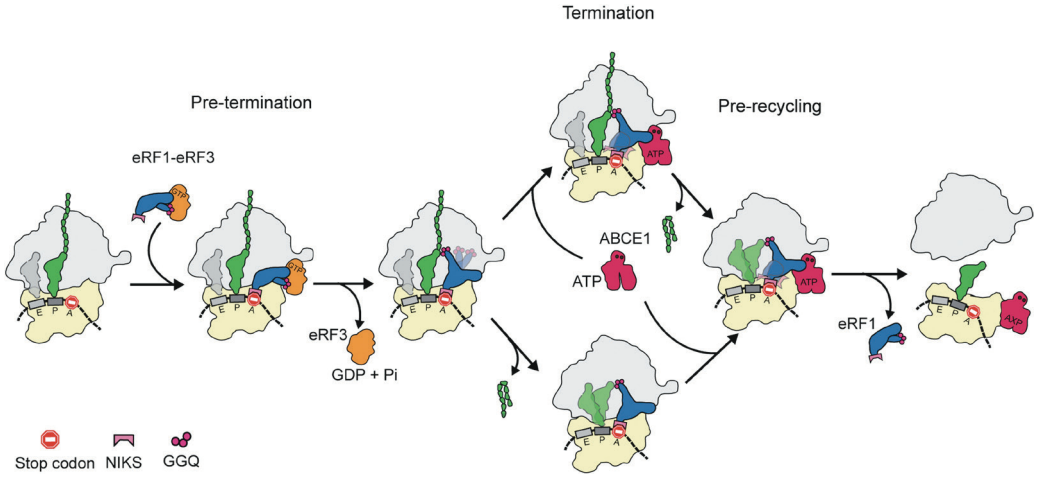

Figure 7. Translation termination and ribosome recycling. The first event in translation termination is eRF1 recognition of the stop codon. Then, eRF1 binds to the ribosome as part of a pre-assembled ternary complex comprising eRF1, eRF3 and GTP. Then, eRF3-mediated GTP-hydrolysis induces eRF1 to mediate the peptidyl-tRNA hydrolysis and peptide release. Following GTP hydrolysis, the RF3-GDP dissociates leaving behind RF1, which remains bound to the ribosome in what is known as the post-termination complex until ribosome dissociation occurs, a process that can be facilitated by ABCE1. Source: Preis et al. 2014.

1.4. mRNA localization

After nuclear export, some mRNAs are not directly translated but instead are first localized at specific subcellular compartments. Depending on the final localization, this process may lead to mRNA storage, degradation or localized translation. For example, to achieve localized protein synthesis, some mRNAs are translationally repressed, assembled into RBP-motor protein complexes and then transported to defined locations such as the endoplasmic reticulum (ER), mitochondria or neuronal dendrites, where they will be derepressed and translated (Chin & Lécuyer 2017).

On the other hand, mRNAs can be also maintained in translationally inactive mRNPs. These mRNPs can assemble into membrane-less cytoplasmic organelles named mRNP granules. Localization of mRNAs to these granules is a way to either store them translationally inactive or to promote their decay. The best characterized mRNP granules in somatic cells are processing bodies (P-bodies) and stress granules (Parker & Sheth 2007; Decker & Parker 2012).

P-bodies are present in non-stressed cells and are characterized by the accumulation of proteins involved in translational repression and mRNA decay. Thus, P-bodies are mainly thought to be centres for mRNA decay. On the other hand, stress granule (SG) formation is enhanced upon cellular stresses, such as ER stress, heat-shock or arsenite treatment. They not only contain proteins involved in translational repression but also translation initiation factors. Consequently, they are thought to be aggregates of mRNPs stalled at translation initiation, where mRNAs are repressed and stabilized during the cellular stress. Noteworthy, P-bodies and SG are dynamic structures with partially overlapping functions. In accordance with this some of their components are shared and both proteins and mRNAs can cycle between P-bodies, stress granules and polysomes (Markmiller et al. 2018; Youn et al. 2018).

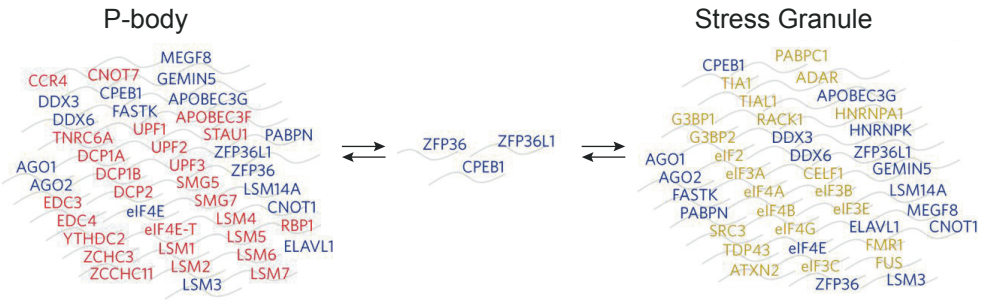

Figure 8. Dynamic composition of P-bodies and Stress Granules. Adapted from Turner & Díaz-Muñoz 2018.

1.5. mRNA decay

Finally, the last step in a mRNA's lifecycle is mRNA decay. Individual mRNA half-lives in a cell vary widely, from more than 24 hours to less than 15 minutes (Kumagai et al. 2016). To achieve this, a large cohort of mechanisms can regulate mRNA stability. Broadly, cellular mRNA decay can be divided into two types of processes: basal mRNA decay and quality control decay.

1.5.1. Basal mRNA decay

Basal mRNA decay consists on the degradation of mRNAs at the end of their translational life, and it occurs mainly through the exonucleolytic cleavage of mRNAs. The previously described 5' cap, 3' poly(A) tail or the process of circularization, physically prevent the access of exonucleases to mRNAs ends and thus are crucial features that promote mRNA stability. Despite being a multi-step process, basal mRNA decay initiates with a gradual shortening of the poly(A) tail. Deadenylation triggers removal of the 7mG-cap by the decapping complex Dcp1/2 and its activators (Halbeisen et al. 2008). These events expose the mRNA to rapid exonucleolytic degradation, primarily from the 5' end by Xrn1, and from the 3' end by the exosome and Dis3L2 (Gallouzi & Wilusz 2013).

1.5.2. Quality control (QC) decay

Cells also need to immediately destroy cytoplasmic mRNAs recognized as aberrant. In such cases, mRNAs are usually first cleaved internally by an endonuclease and then further degraded by components of the basal mRNA decay machinery. The best-characterized cellular mRNA QC pathway is nonsense-mediated decay (NMD), which identifies mRNAs with premature termination codons (PTC) (Popp & Maquat 2013). Other RNA QC pathways recognize aberrant translation events, such as stalled or non-terminating ribosomes, leading again to mRNA inactivation through endonucleolytic cleavage (Inada 2013; Abernathy & Glaunsinger 2015).

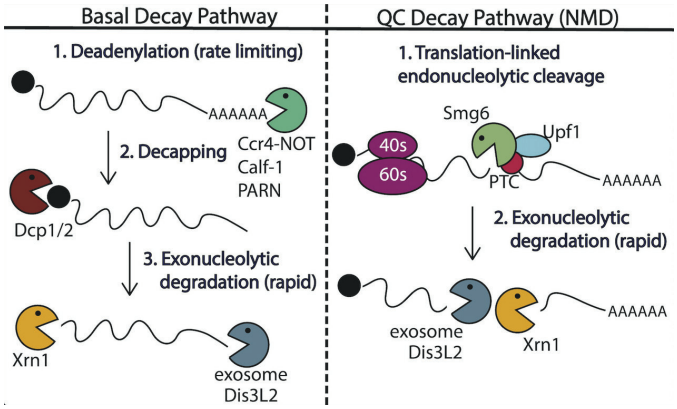

Figure 9. Mechanisms mediating mRNA decay. Source: Abernathy & Glaunsinger 2015.

1.6. mRNA deadenylation

Importantly, reduction of the poly(A) tail length is not only the first determinate for basal mRNA decay but also the rate-limiting step, as the subsequent exonucleolytic decay of the message body is rapid and irreversible. Therefore, shortening of the poly(A) tail is tightly regulated, in some cases in reversible manners, by multiple mechanisms (Schoenberg & Maquat 2009; Eckmann et al. 2011; Weill et al. 2012).

The enzymes responsible for this process are deadenylases. So far, dozens of deadenylases have been described in mammals, however, the number is still expanding and several details about their specificities and redundancies are still unknown. They are usually part of multi-functional complexes, possessing deadenylase, decapping, remodelling and translational repressive activities, and thus controlling globally mRNA fate at multiple levels (Goldstrohm & Wickens 2008). One example of such a complex is the CCR4-Not complex. Besides a role in global mRNA decay, deadenylases can be recruited to specific subsets of mRNAs by cis-acting elements such as AU-rich Elements (AREs), miRNA binding sites or Cytoplasmic Polyadenylation Elements (CPEs), among others (Yan 2014).

AU-rich elements (AREs) consist of various large clusters of overlapping AUUUA pentamers and UUAUUUAUU nonamers. Approximately 5–8% of all human transcripts contain AREs, which are specifically recognized by over 20 different ARE-binding proteins (ARE-BPs) (Beisang & Bohjanen 2012). Among them,

tristetraprolin (TTP), KSRP and AUF1 recruit deadenylases and downstream degradation machinery to their targets, thereby stimulating transcript decay. By contrast, when other ARE-BPs bind ARE-containing mRNAs, they can compete with the binding of destabilizing ARE-BPs and thus lead to mRNA stabilization. Examples of these are the ELAV (family members Hu-antigen R (HuR) and HuD (Beisang & Bohjanen 2012).

In the last decade miRNAs have emerged as one of the major mechanisms mediating specific mRNA decay. More than 1,000 miRNAs have been identified in the human genome and around 50% of all mRNAs are predicted to contain miRNA binding sites (Huntzinger & Izaurralde 2011a; Kozomara & Griffiths-Jones 2011). Briefly, miRNAs are ~21-nucleotide-long non-coding RNAs that are part of an active RNA-induced silencing complex (RISC). At position 2-7 from the miRNA 5'-end, miRNAs contain the "seed sequence", that mediates target mRNA recognition through base-pairing. In mammals, usually this pairing is partially complementary, leading to mRNA deadenylation and destabilization and/or translational repression. Alternatively, few miRNAs can bind to target sites with extensive or perfect sequence complementarity, which results in mRNA endonucleolytic cleavage (Huntzinger & Izaurralde 2011b).

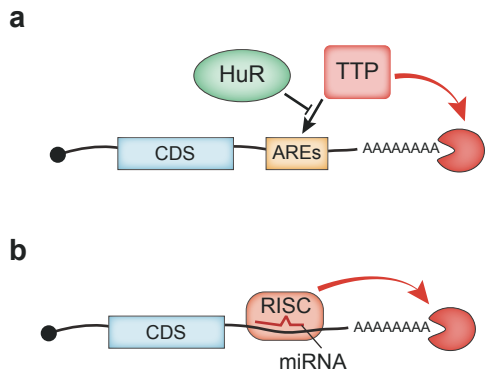

Figure 10. Elements in the 3'UTR regulate mRNA stability. (a) Recognition of AREs by destabilizing ARE-binding proteins, such as tristetraprolin (TTP), stimulates mRNA deadenylation and decay. Conversely, the binding of stabilizing proteins — such as Hu-antigen R (HUR) — that compete with destabilizing factors inhibits ARE-mediated RNA degradation. **(b)** Numerous transcripts contain microRNA (miRNA) binding sites in their 3´ UTRs. Specific recognition of these sites by the RNA-induced silencing complex (RISC) leads to deadenylation of the mRNA and its subsequent degradation.

1.7. Cytoplasmic Polyadenylation

We have seen so far how, after nuclear export, mRNAs can be translated, deadenylated and stored, or deadenylated and degraded. Additionally, some mRNAs can be re-adenylated in the cytoplasm, a process that allows to de-repress deadenylated mRNAs and promote again their translation. This process, named cytoplasmic polyadenylation, allows cells to fine tune the location of protein synthesis. For example, in neurons, repressed mRNAs are localized to synapses, where they are polyadenylated and locally translated (Miller et al. 2002). Moreover, cytoplasmic polyadenylation also contributes to create complex temporal patterns of protein synthesis, like circadian oscillations or the sequential waves of mRNA activation that drive meiosis progression (Kojima et al. 2012; Belloc et al. 2008). Therefore, the dynamic regulation of the poly(A) tail has emerged as another layer to regulate protein expression, not only in abundance, but also in timing and space (Eckmann et al. 2011).

As nuclear polyadenylation, cytoplasmic elongation of the poly(A) tail is mediated by poly(A) polymerases (PAP). Among them, PAPD4 (Gld2) is the best characterized cytoplasmic PAP. Cytoplasmic polyadenylation element (CPE) is the most characterized sequence on mRNAs mediating cytoplasmic polyadenylation. A few other sequences have been also proposed to mediate this process, but their contribution to cytoplasmic polyadenylation is still poorly understood (Charlesworth et al. 2013).

CPEs are sequences in the 3'UTR of mRNAs recognized by the Cytoplasmic Polyadenylation Element Binding (CPEB)-family of proteins. Importantly, CPEBs can promote opposite functions on their target mRNAs. Thus, CPEBs binding to mRNAs can result in mRNA deadenylation and silencing or polyadenylation and translation (Weill et al. 2012; Fernández-Miranda & Méndez 2012). In the next sections, we will summarize what is currently known of CPEBs regulation and function.

1.7.1. Cytoplasmic Polyadenylation Element Binding Proteins (CPEBs)

In mammals, the CPEB-family is comprised of four paralogs that, based on sequence identity, can be clustered into two subfamilies: CPEB1 and CPEB2-4 (Fernández-Miranda & Méndez 2012). The four CPEB proteins share common structural features. They all contain an unstructured N-terminal regulatory domain (NTD), different for each CPEB, and a similar RNA-binding C-terminal domain (CTD) comprised of two RNA recognition motifs (RRMs) and a zinc-binding domain (ZZ domain) (Merkel et al. 2013). The RRMs of CPEB2–4 share 97% sequence identity between them, while the RRMs of CPEB1 shares 48% pairwise sequence identity with those of CPEB2-4 (Hake et al. 1998; Fernández-Miranda & Méndez 2012). Despite that it was suggested that all four CPEB family members target the same population of CPE-containing mRNAs, these differences in their RRMs can confer certain specificities to the two subfamilies. In accordance with this, the structures of the C-terminal domains of hCPEB1 and hCPEB4 C-terminal domain that were recently solved show that the these two proteins interact differently with the fifth position of the CPE motif (Afroz et al. 2014).

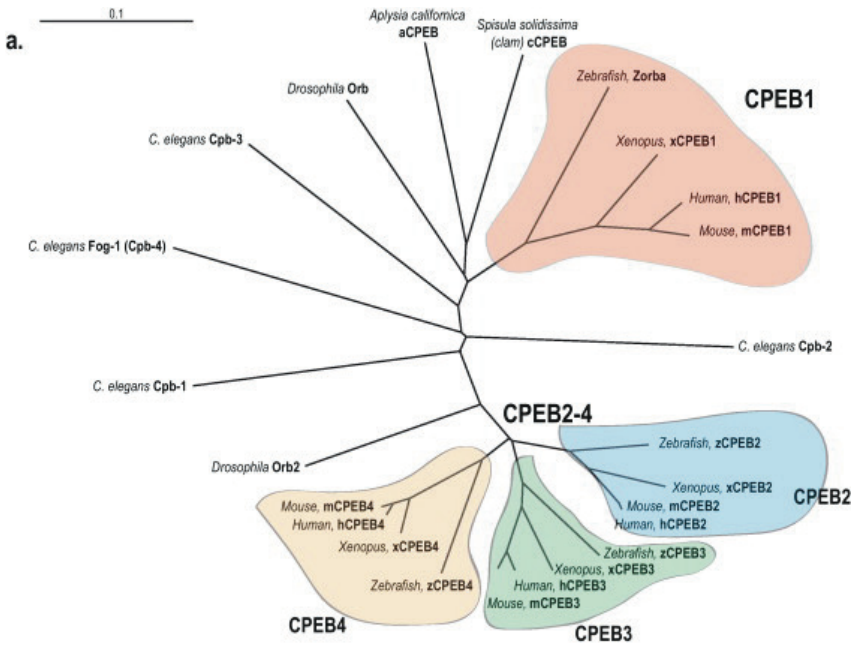

Figure 11. CPEB family of RNA-binding proteins. →

← **Figure 11. CPEB family of RNA-binding proteins.** Unrooted phylogenetic tree of the most representative CPEB proteins based on a multiple sequence alignment using complete protein sequences. Distances between orthologs are significantly closer than those between parologs. CPEB1 vertebrate orthologs (red balloon) are the most distant members of the family; whereas vertebrates CPEB2 (blue), CPEB3 (green) and CPEB4 (yellow) are closely related and placed in the same branch. Source: Fernández-Miranda & Méndez 2012.

1.7.2. Cytoplasmic Polyadenylation Elements (CPEs)

The consensus CPE (CPEc) sequence has been defined as $UUUUA_{1-2}U$ (Richter 2007). However, there is still controversy on how to define a CPE. First, based on *in vitro* selex experiments, it was proposed that CPEB3-4 recognize a U-rich loop motif (Huang et al. 2006). Second, CPE variations such as UUUUACU were also found to be functional and were named non-consesus CPEs (CPEnc) (Piqué et al. 2008). Finally, cross-linking and immunoprecipitation (CLIP) experiments showed different CPE-binding motifs for Orb and Orb2b, the orthologs of the subfamilies CPEB1 and CPEB2-4 in *Drosophila melanogaster* (Stepien et al. 2016). The latter work defined UUUUA and UUUU as the motifs preferentially bound by Orb and Orb2b, respectively. Moreover, they also found an enrichment of UUUUG motifs in targets of Orb2b, but not of Orb (Stepien et al. 2016). Altogether, these data suggests thatCPEBs can bind more elements besides CPEc and that, despite sharing overlapping targets, some mRNAs might be preferentially bound by one CPEB subfamily.

It has been shown that, to be functional, CPEs need to be located at an appropriate distance from the polyadenylation signal (Piqué et al. 2008). Based on functional CPEc and CPEnc, bioinformatic predicts that up to 20% of human genome transcripts are potential CPEBs targets (Belloc & Méndez 2008; Novoa et al. 2010). However, this percentage could be actually higher if other CPE definitions were included. Therefore, CPEB-mediated translational control seems to be a widespread mechanism to regulate protein production in metazoans.

1.7.3. Regulation of CPEBs activity

In contrast to their conserved RNA-binding domain, the N-terminal regulatory domain (NTD) of CPEB proteins is highly variable and subject to specific post-translational modifications (PTMs). Importantly, these PTMs can determine if CPEBs act as translational repressors or translational activators (Mendez, Murthy, et al. 2000; Mendez, Hake, et al. 2000; Drisaldi et al. 2015). It is worth stressing that distinct pathways and mechanisms regulate each CPEB. Therefore, in a given context, even if their targets partially overlap, each CPEB might be performing opposite functions.

CPEB1 activity is modified via phosphorylation by Aurora A, and it undergoes rapid degradation through CDK1- and PLK1-mediated phosphorylation (Mendez, Murthy, et al. 2000; Mendez, Hake, et al. 2000). When unphosphorylated, CPEB1 represses mRNAs by recruiting the deadenylase PARN or inhibiting the formation of the eIF4F complex (Fernández-Miranda & Méndez 2012). On the other hand, upon phosphorylation by Aurora A, CPEB1 binds CPSF, which displaces PARN and allows Gld2 to extend the poly(A) tail of the mRNA (Mendez, Murthy, et al. 2000; Kim & Richter 2006). Importantly, besides Aurora A-mediated phosphorylation, the arrangement and number of CPE-elements within the 3' UTR can also determine the effectiveness of CPEB1 repressor activity (Piqué et al. 2008). Finally, beyond cytoplasmic polyadenylation, CPEB1 is also able to participate in alternative cleavage and polyadenylation of mRNAs in the nucleus (Bava et al. 2013).

For CPEB2, no post-translational modifications have been described so far. However, it has been proposed to repress transcript translation by interacting with eEF2 and inhibiting the elongation phase (Chen & Huang 2012). Alternatively, although the molecular mechanisms are not clear, CPEB2 can also activate the translation of target mRNAs (Hägele et al. 2009; Pascual et al., under review).

CPEB3 has been shown to act as a repressor, but after undergoing modifications like monoubiquitination, N-terminal cleavage or deSUMOylation, it can switch its function and promote the translation of its targets (Pavlopoulos et al. 2011; Wang & Huang 2012; Drisaldi et al. 2015). It has also been described that CPEB3 is regulated by PKA- and CamKII-mediated phosphorylation (Kaczmarczyk et al. 2016). Unlike CPEB1, that changes partners to perform each function, the switch on CPEB3

activity is determined by a change from a soluble to an aggregate state (Drisaldi et al. 2015). Moreover, data on CPEB3 localization suggests that it could have a nuclear function not related to cytoplasmic polyadenylation (Chao et al. 2012).

Finally, CPEB4 activity is regulated via ERK2- and CDK1-mediated hyperphosphorylation of the NTD. These phosphorylation events additively maintain CPEB4 in its monomeric state, promoting mRNA polyadenylation and translation. In contrast, unphosphorylated CPEB4 separates into liquid-like droplets where mRNA is stored but not polyadenylated (Guillén-Boixet et al. 2016). Moreover, it has also been proposed that CPEB4 may act as a repressor of translation during terminal erythroid differentiation through an interaction with eIF3 that represses translation globally (Hu et al. 2014).

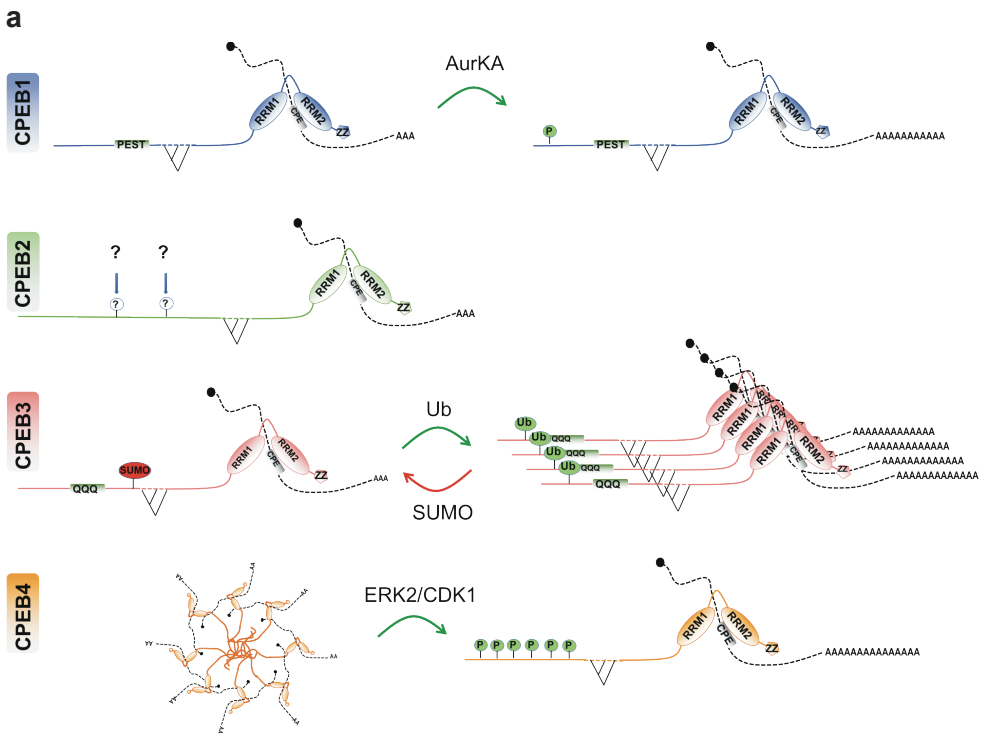

Figure 12. Post-translational modifications modify CPEB activity. (a) Upon AurKA-mediated phosphorylation, CPEB1 interacts with different partners and changes from a repressor to an activating function. For CPEB2, no PTMs have been described so far. CPEB3 polyadenylating function is determined by modifications like monoubiquitination and SUMOylation, which determine its soluble or aggregate state. CPEB4 activity is regulated by ERK2 and Cdk1 kinases. Upon hyperphosphorylation, CPEB4 disassembles the liquid like droplets and its found on its monomeric active state, where it can promote mRNA polyadenylation.

1.7.4. CPEBs biological function

Regarding the biological functions exerted by CPEBs, they have been studied mainly during *Xenopus laevis* oocyte maturation and early developmental stages, in contexts where transcription is absent and post-transcriptional control of gene expression is particularly important. However, in recent years, data unveiling CPEB functions in somatic cells have started to emerge.

Concerning meiotic progression, it has been shown that CPEB1 is required for the repression and storage of maternal mRNAs in arrested oocytes. Upon meiotic resumption, CPEB1 and CPEB4 drive sequential waves of translational activation at different steps of the cell cycle (Igea & Méndez 2010). Interestingly, in this context it was shown how the arrangement of CPEs and AREs on the 3'UTR of mRNAs, leads to opposing polyadenylation and deadenylation activities that determine the precise activation times of mRNAs during meiosis progression (Belloc et al. 2008) **(Figure 13)**.

In somatic cells, CPEB1, 2 and 4 have been also involved in mitotic cell cycle progression (Novoa et al. 2010; Giangarrà et al. 2015). CPEBs repressing and activating function has also been shown to participate in mRNA localization and cell polarity (Xu et al. 2014). Moreover, all four CPEBs are expressed in the brain and especially CPEB3, has been shown to participate in neural functions such as memory establishment or thermosensitivity (Peng et al. 2010; Pavlopoulos et al. 2011; Wang & Huang 2012; Chao et al. 2013; Huang et al. 2014; Fioriti et al. 2015; Fong et al. 2016; Lu et al. 2017). On the other hand, CPEBs are also highly expressed in the liver. It has been reported that CPEB1 and CPEB4 sequentially regulate VEGFa expression in cirrhotic livers and, in homeostasis, CPEB4 maintains ER and mitochondrial homeostasis (Calderone et al. 2016; Maillo et al. 2017). Moreover, CPEBs have been studied in some tumour environments, showing for example a tumour-promoting role of CPEB4 in pancreatic cancer and glioblastoma (Ortiz-Zapater et al. 2012).

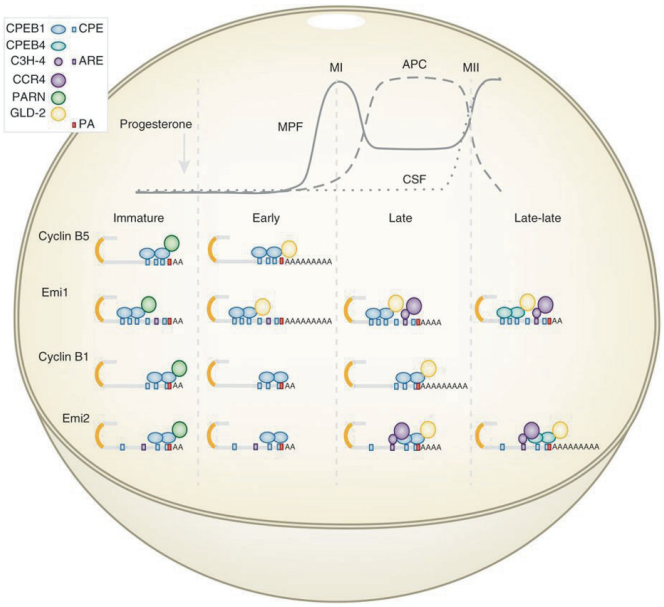

Figure 13. Sequential waves of cytoplasmic polyadenylation activate mRNA translation during meiosis progression. In immature oocytes, CPE-containing mRNAs are deadenylated and stored repressed. Upon progesterone stimulation, CPEBs trigger three sequential waves of cytoplasmic polyadenylation, activating translation of specific mRNAs at the different stages of meiosis progression. The number and relative position of CPEs, AREs and the PAS determines the timing when the mRNA is going to be translated, a model known as the combinatorial code. Source: Weill et al. 2012

1.7.5. Mechanisms regulating CPEBs expression

Little is known about the transcriptional mechanisms that control CPEBs expression. *Cpeb1* gene undergoes epigenetic silencing during gastric cancer progression by heavy methylation of its promoter (Caldeira et al. 2012). Moreover, circadian transcriptomics in mouse liver revealed the rhythmic expression of *Cpeb2* and *Cpeb4* mRNAs (Kojima et al. 2012), which was further confirmed for Cpeb4 (Maillo et al. 2017).

On the other hand, *Cpebs* mRNAs are subject to several mechanisms of translational control. First of all, *Cpeb2-4* 3'UTRs contain CPEs and *Cpeb4* mRNA has been shown to be regulated by CPEB1 and CPEB4 itself (Igea & Méndez 2010). All CPEB mRNAs also contain multiple predicted miRNA binding sites and miR-92 and miR-26 have been shown to regulate *Cpeb2-4* mRNA stability (Morgan et al. 2010) whereas miR-122 controls *Cpeb1* mRNA translation (Burns et al. 2011). Finally, *Cpeb4* translation is also controlled by the unfolded protein response (UPR) through uORFs within the 5'UTR (Maillo et al. 2017). This mechanism was shown to be CPEB4-specific and not shared by the other CPEBs.

Finally, CPEB function can also be altered by alternative splicing or alternative cleavage and polyadenylation of *Cpebs* pre-mRNAs (Wang & Cooper 2009; Wang & Cooper 2010; Parras et al. 2018).

In the second section of the introduction, we will address macrophage biology. We will dissect the molecular mechanisms involved in the development of an inflammatory response and the processes that mediate inflammation resolution. Moreover, we will give an overview of the contribution of posttranscriptional regulatory mechanisms to each phase of the LPS response.

2. The Innate immune system

The immune system is a set of host defence mechanisms against pathogens and diseases. It is classically divided into two categories: the innate immune system and the adaptive. The innate immune system represents our first line of defence against pathogens and it is composed of the skin and mucous membranes that form external barriers, the complement system and immune cell types such as macrophages, dendritic cells, neutrophils or natural killer cells. As a second defence mechanism we have the adaptive immune system, which confers a more specific response adapted to each antigen, and can provide long lasting immunity. T cells, B cells and their produced antibodies are part of the adaptive immune response.

The crosstalk between the innate and the adaptive immune system has been widely studied. Given that adaptive immune cells displayed complex maturation mechanisms to achieve antigen-specific responses, it had long been thought that specific adaptive responses (T and B cells) governed the unspecific behaviour of innate immune cells (Mills 2015). However, now, it is well established that there is an innate control of adaptive immunity that can drive immune responses towards type 1 or type 2 immunity (Iwasaki & Medzhitov 2015). Type 1 immunity consists of inflammatory responses developed against microorganisms such as viruses, bacteria, fungi and possibly protozoa. Recognition of pathogens by the innate immune system is mediated by pattern-recognition receptors (PRRs), which detect conserved pathogen-associated molecular patterns (PAMPs), such as bacterial cell-wall components and viral nucleic acids. Briefly, type 1 immune responses lead to rapid and effective inflammatory responses to eliminate the pathogen. On the other hand, type 2 immune responses are induced by parasitic worms and allergens. In this case, innate immunity activation occurs by sensing functional characteristics indicative of a pathogen's presence, rather than specific structures in those pathogens. The

sensing pathways responsible for this recognition overlap with pathways responsible to sense tissue damage. Therefore, type 2 immunity not only activates pathogen clearance mechanisms, but also tissue repair responses.

In both types of immunities, first the innate immune system recognizes the damage, then it signals to adaptive cells so that they polarize towards type 1 or 2 responses and, finally, adaptive cells activate effector cells to perform the needed response. Importantly, each type of immunity uses cell types in common, however secretion of different cytokines allows that they acquire specific functions adapted to the insult received. However, it should be taken into account that this useful classification to understand immune functions is not always reproduced *in vivo*, as several pathologies damage our organism at multiple levels triggering both types of immune responses at the same time.

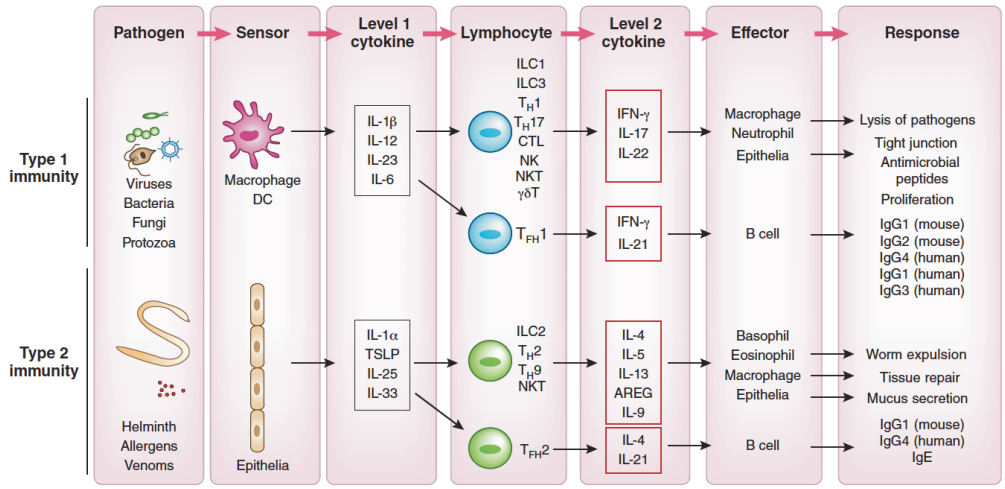

Figure 14. Schematic vision of type 1 and type 2 immunity. Immune responses are orchestrated by three categories of cells. Innate immune cells function as 'sensors' that detect pathogens and secrete 'level 1' cytokines, the tissue-resident lymphocytes that respond to 'level 1' cytokines to secrete 'level 2' cytokines, and the effector cells that respond to 'level 2' cytokines to carry out effector functions to eliminate the pathogen. Type 1 and type 2 immunity use different cytokines in order to trigger the appropiate response to the insult received. Source: Iwasaki&Medzhitov 2015.

2.1. The mononuclear phagocytic system (MPS)

The mononuclear phagocytic system (MPS) (van Furth et al. 1972) comprises monocytes, macrophages and dendritic cells (DCs), as well as their respective committed bone marrow (BM)-resident progenitors (Geissmann et al. 2010; Yona & Gordon 2015). In adult organisms, mature macrophages can be subdivided in monocyte-derived macrophages and tissue-resident macrophages.

Tissue resident macrophages mainly originate from progenitor cells generated in the yolk sac during embryogenesis. In some tissues and conditions, resident macrophages are long lived and have self-renewing capacity, while in others, maintenance of resident macrophages relies on monocyte infiltration (Perdiguero & Geissmann 2016). Tissue-resident macrophages are highly heterogeneous as they participate in functions that are specific of their location, such as bone morphogenesis (osteoclast), ductal branching (macrophages in the mammary gland) or neural networking (microglia) (Pollard 2009).

On the other hand, monocytes are cells circulating in the blood, bone marrow, and spleen that arise from hematopoietic stem cells (HSCs) in the bone marrow. Besides the replenishment of certain populations of resident macrophages and DCs, under inflammatory conditions, monocytes are recruited to the source of infection or damage. Upon tissue infiltration, they differentiate into macrophages and, together with resident macrophages, orchestrate the immune response.

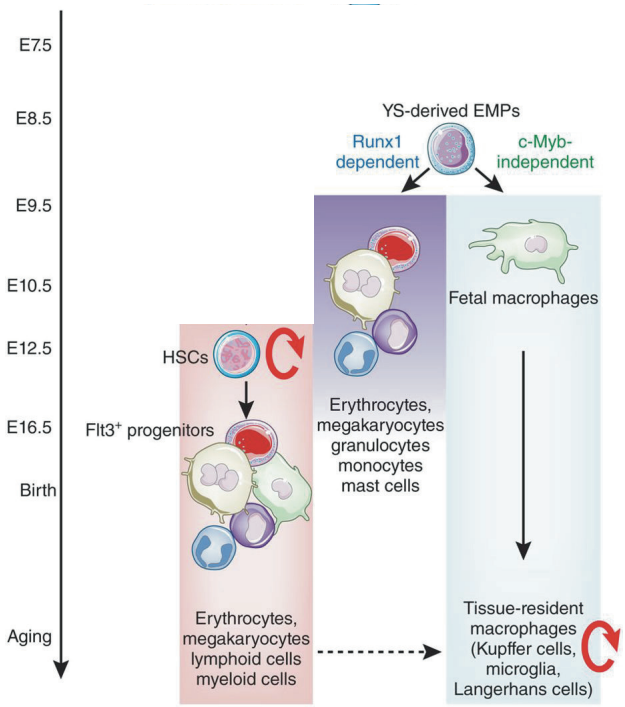

Figure 15. Origin of the mononuclear phagocytic system. EMP-derived hematopoiesis gives rise to erythrocytes and short-lived myeloid cells (monocytes, granulocytes and mast cells) that are replaced by HSC-derived cells late during gestation. EMPs-derived fetal macrophages colonize all tissues during fetal development, where they specialize to their tissue of residency after birth and can persist throughout adult life by local proliferation (circular red arrows indicate self-renewal potential). Depending on the age of the organism and environmental challenges, HSC-derived cells can contribute to adult tissue-resident populations. EMPs: Erythro-myeloid progenitors, HSCs: Hematopoietic Stem Cells. Source: Perdiguero and Geissmann 2016.

2.2. Macrophage function during an inflammatory response

An inflammatory response against a pathogen can be divided into different phases. The first phase is mainly aimed at destroying the pathogen and, as it uses mechanisms that can also damage endogenous tissues, needs to be tightly controlled. Then, a clearance phase follows in which dying cells, damaged extracellular matrix material, and cellular debris are removed. Finally, there is a recovery phase in which the tissue is repaired and restored to a healthy and fully functional condition.

Macrophages play key roles in several of these steps. Following infection or tissue injury, they participate in pathogen recognition and they express proteins that are involved in direct antimicrobial functions, such antimicrobial peptides or inducible nitric oxide synthase (iNOS); or cytokines and chemokines, like TNFα, IL-6, and IL-1b, which lead to increased endothelium permeability and promote early recruitment of other innate immune cells. Moreover, being antigen-presenting cells, they can also contribute to T cell differentiation and activation of the adaptive immune response. Finally, macrophages are also essential in resolving inflammation by the phagocytosis of dead cells, secreting anti-inflammatory cytokines, and facilitating wound-healing and repair mechanisms (Serhan et al. 2008; Murray & Wynn 2011; Lavin & Merad 2013).

2.3. Macrophage activation by LPS

To recognize pathogens, macrophages express several classes of PRRs, including Toll-like receptors (TLRs), RIG-I-like receptors (RLRs), NOD-like receptors (NLRs) and C-type lectin receptors (CLRs) (Arthur & Ley 2013). All PRRs mentioned above activate both MAPK and nuclear factor-κB (NF-κB) pathways, which are crucial to generate immune responses. In addition, certain PRRs can also promote activation of other pathways like the inflammasome or interferon regulatory factors (IRFs) (Kawasaki & Kawai 2014).

TLRs were the first PRRs to be identified and are the best characterized. The TLR family comprises 10 members (TLR1–TLR10) in human and 12 (TLR1–TLR9, TLR11–TLR13) in mouse. TLRs localize to the cell surface or to intracellular compartments such as the ER, endosome or lysosome, and they recognize distinct or overlapping PAMPs and DAMPs (danger-associated molecular patterns, such as HMGB1, endogenous RNA and DNA) **(Figure 16)**. Each TLR is composed of an ectodomain that mediates PAMPs recognition, a transmembrane domain, and a cytoplasmic Toll/IL-1 receptor (TIR) domain that initiates downstream signalling (Kawasaki & Kawai 2014). TLRs are expressed by innate and adaptive immune cells (macrophages, neutrophils, DCs, NK cells, mast cells, T- and B-lymphocytes); as well as by some nonimmune cells, such as epithelial and endothelial cells.

Lipopolysaccharide (LPS) is the major component of the outer membrane of Gram-negative bacteria and one of the most immune-stimulatory glycolipid. Many pathogenic bacteria such as *Pseudomonas aeruginosa*, *Neissera gonorrhoeae*, *Chlamydia trachomatis* or *Yersinia pestis* are gram-negative bacteria. In mammals, LPS recognition is mediated by TLR4.

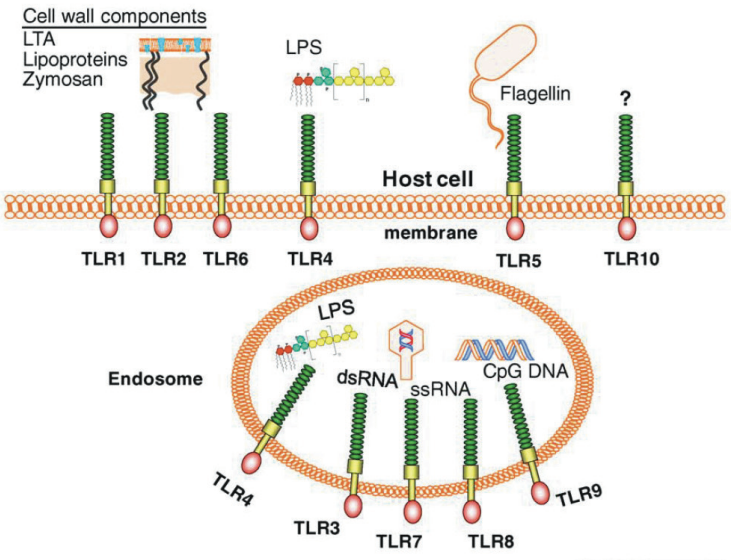

Figure 16. Toll like receptor (TLR) family of pattern-recognition receptors. TLRs plays a central role as sensors of infection. Different TLRs recognize distinct types of conserved microbial structure, thus endowing the innate response with a degree of specificity. Source: Hajishengallis & Lambris 2010.

2.4. TLR4 signalling pathway

LPS recognition by TLR4 does not occur directly. LPS first needs to bind soluble LPS-binding protein (LBP), and then the LPS-LBP complex bind the cell-surface receptor CD14, which associates with TLR4 and the accessory protein MD-2 (Fan & Cook 2004). Then, upon LPS binding, TLR4 triggers an intracellular response. TLR signalling is mediated through their cytoplasmic TIR domains, which interact with adaptor proteins following agonist stimulation. TLR4 signals via two adaptor proteins, MYD88 and TRIF **(Figure 18)**.

BOX 1. MAPK SIGNALLING CASCADES

Mitogen-activated protein kinases (MAPKs) are a superfamily of proline-directed serine/threonine protein kinases that are activated in front of several stimuli such as hormones and growth factors, cytokines, or environmental stresses (Roux & Blenis 2004). MAPKs pathways consist of a series of at least three kinases: a MAPK kinase kinase (MAP3K) that activates a MAPK kinase (MAP2K), which in turn phosphorylates and activates the MAPK. Mammalian cells express 14 MAPKs that, based on their pathways, can be subdivided into different families: the extracellular signal-regulated kinases (ERK1/2), p38 MAPKs (p38α, p38β, p38γ and p38δ), Jun N-terminal kinases (JNK1/2/3) and the ERK5 MAPK. The remaining MAPKs are ERK3/4/7/8 and Nemo-like Kinase (NLK), although their function and regulation have been less characterized. In figure 17, it can be seen how each MAPK can be activated by several MAP2K and MAP3K, depending on the stimuli and cell type. Downstream each MAPK pathway, several kinases, transcription factors or RNA-Binding proteins are regulated. Moreover, it is worth mentioning that the different MAPK can also cross-regulate each other's function.

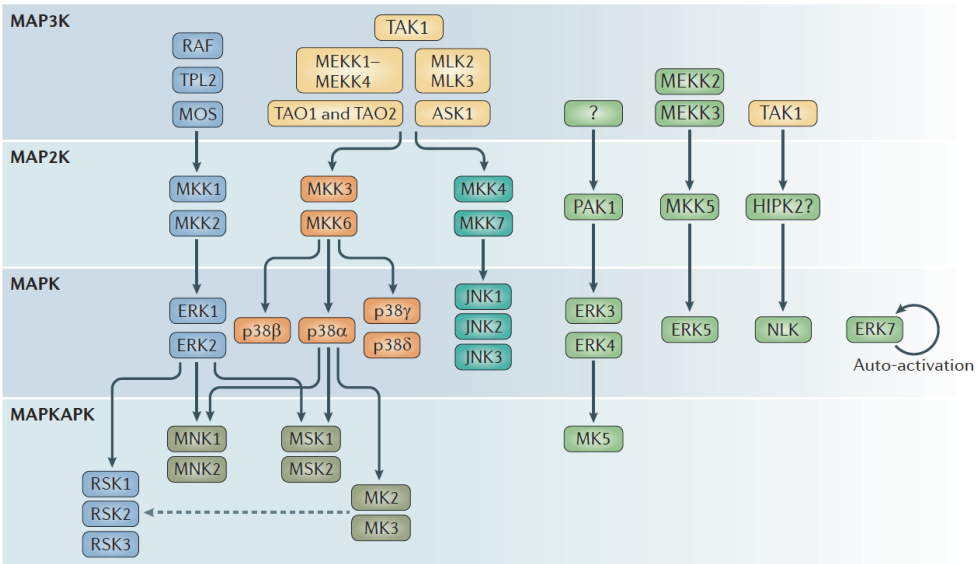

Figure 17. MAPKs signalling cascade. Source: Arthur & Ley 2013.

2.4.1. MyD88-dependent signal transduction

Following ligand binding to TLRs, MYD88 adaptor-like protein (MAL) mediates MYD88 recruitment to TLR4 TIR domains. Then, MYD88 interacts with and activates the kinases IRAK1/2 and IRAK4, which in turn activate the E3 ubiquitin ligase TRAF6. TRAF6, along with ubiquitin-conjugating enzyme UBC13 and UEV1A, promotes K63-linked polyubiquitination of TRAF6 itself and the MAP3K TAK1, inducing TAK1 activation and the subsequent activation of both p38 and JNK pathways.

The IKK complex is composed of the catalytic subunits IKKα and IKKβ and the regulatory subunit NEMO (also called IKKγ). Once ubiquitinated, through its K63-Ub chains, TAK1 also binds to the IKK complex, promoting that the IKK complex phosphorylates the NF-κB inhibitory protein IκBα. Unphosphorylated IκBα masks the nuclear localization signal of NF-κB retaining it in the cytoplasm. Upon phosphorylation, IκBα undergoes proteasome degradation, allowing NF-κB nuclear translocation to induce pro-inflammatory gene expression. IκBα degradation also releases the inhibition of TPL2 , a MAP3K that will activate the ERK1/2 pathway (Arthur & Ley 2013; Kawasaki & Kawai 2014).

2.4.2. TRIF-dependent signal transduction

In addition to the early MyD88-dependent signals, TLR4 triggers a delayed signal cascade through the adaptor TRIF. For this to happen, TLR4 is internalized into endosomes and, via TRIF-Related Adaptor Molecule (TRAM), activates TRIF-dependent pathways. In this case, TRIF activates the kinase TBK1 to promote phosphorylation of the interferon regulatory factors IRF3 and IRF7, which induce the expression of type I interferons (IFNα and IFNβ).

Moreover, TRIF also interacts with the previously mentioned TRAF6. In this case, TRAF6 recruits the kinase RIP-1, which in turn activates again TAK1, leading to second wave of NF-κB and MAPKs activation (Liu et al. 2016; Bode et al. 2012; Wang et al. 2014; Kawasaki & Kawai 2014).

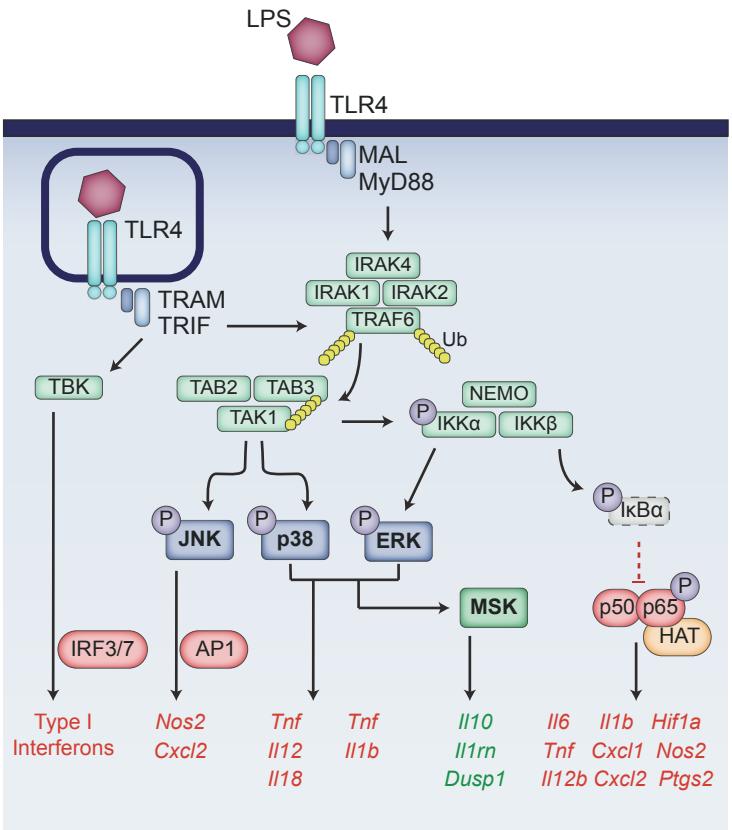

Figure 18. TLR4 signalling pathway. Upon LPS binding, TLR4 triggers an intracellular responses, which are mediated via two adaptor proteins, MYD88 and TRIF. Both pathways lead to the activation of the NF-κB and MAPKs pathway.

2.4.3. Role of MAPK in LPS response: p38, ERK, JNK

Once activated, the three main MAPKs families can mediate both pro- and/or anti-inflammatory functions during LPS-driven macrophage activation (Arthur & Ley 2013; Bode et al. 2012). The JNK family has mainly a pro-inflammatory function, via c-Jun/c-Fos heterodimers (which form AP-1) that activate the transcription of pro-inflammatory genes such as iNOS or CXCL2, some of which are also regulated by NF-κB.

On the other hand, p38αα and ERK1/2 pathways can mediate both pro- and anti-inflammatory functions. For example, ERK1/2 participate in TNFα and IL-1β expression, but negatively regulate the production of IL-12, IFNβ and iNOS. Via MK2, p38α also promotes the expression of inflammatory cytokines, such as TNFα, IL-12 and IL-18. One mechanism is by regulating their mRNA stability, but it can additionally regulate cytokine expression via transcription factors such as C/EBPβ, among others.

However, as previously mentioned, ERK1/2 and p38α also activate anti-inflammatory pathways, mainly by phosphorylating and activating MSKs. In macrophages, the predominant role of MSKs is the transcriptional induction of genes involved in inflammation inhibition such as IL-10, IL-1 receptor antagonist protein (IL-1RA), or DUSP1. This process is mediated by phosphorylation of the transcription factor CREB1, among others.

2.4.4. NF- κB

NF-κB is a dimeric transcription factor generated from combinations of Rel, p65, RelB, p50/NFκB1 and NFκB2 (Hayden & Ghosh 2011; Tugal et al. 2013). The prototypic NF-κB consists of a heterodimer of p50 and p65 and is classically held in an inhibitory IKK complex. As previously mentioned, downstream TLR4 activation, IκBα degradation allows that NF-κB translocates to the nucleus and activates the transcription of genes containing a DNA-binding motif known as a κB-binding site (Hoffmann & Baltimore 2006).

NF-κB regulates the expression of a large number of inflammatory genes including the cytokines TNFα, IL-1β, IL-6 and IL-12p40; the chemokines CXCL1 and CXCL2; or other inflammatory mediators such as cyclooxygenase 2 (COX2), hypoxia-inducible factor 1α (HIF1α) and iNOS. Mechanistically, NF-κB transcriptional activation has been linked to chromatin modification. During macrophage activation, p65 is phosphorylated, enabling the recruitment of histone acetyl transferases (HATs) such as CBP/p300. The subsequent histone acetylation induces chromatin relaxation and activation of gene expression (Bhatt & Ghosh 2014).

2.4.5. Autocrine loops in LPS response

TLR4 signalling triggers the expression of cytokines that, once secreted, can signal in an autocrine manner on macrophages, initiating new signalling cascades that will also contribute to the inflammatory response **(Figure 19)**.

Secreted type I interferons α and β bind to the type I interferon receptor (IFNAR) with consequent activation of the kinase JAK1, which phosphorylates the transcription factors STAT1 and STAT2. P-STAT1/2 proteins dimerize and translocate to the nucleus, activating the expression of interferon-responsive genes, such as the chemokines CXCL9 and CXCL10 (Moynagh 2005; Hu et al. 2008; Wang et al. 2014).

IL-10 induces an anti-inflammatory response via IL-10 receptor (IL-10R)-JAK1-mediated activation of STAT3. P-STAT3 homodimers translocate to the nucleus and activate the expression of anti-inflammatory genes such as IL-10 itself, SOCS3, DUSP1 or TTP. These molecules inhibit NF-κB and other inflammatory pathways through different mechanisms (Saraiva & O'Garra 2010; Hutchins et al. 2013). Interestingly, IL-6 also activates STAT3 through the IL-6 receptor (IL-6R), in this case to mediate a pro-inflammatory response. However, IL-6-dependent STAT3 activation is more transient than the one mediated by IL-10, explaining the different functions of STAT3 in response to each cytokine (Bode et al. 2012).

Macrophages also respond to TNFα, which promotes an inflammatory positive-feedback loop by stimulating JNK activation and AP-1 activity (Tugal et al. 2013). Finally, other LPS-induced proteins also signal back to macrophages in a more indirect manner. For example, COX2 expression leads to the production of prostaglandins (PG), which have pro-inflammatory effects but also induce negative feedback loop that favours the expression of anti-inflammatory molecules such as DUSP1 (Tugal et al. 2013; Tang et al. 2017). Alternatively, iNOS-mediated production of reactive oxygen species (ROS) can activate ASK1 MAP3K leading again to p38 and JNK activation (Arthur & Ley 2013).

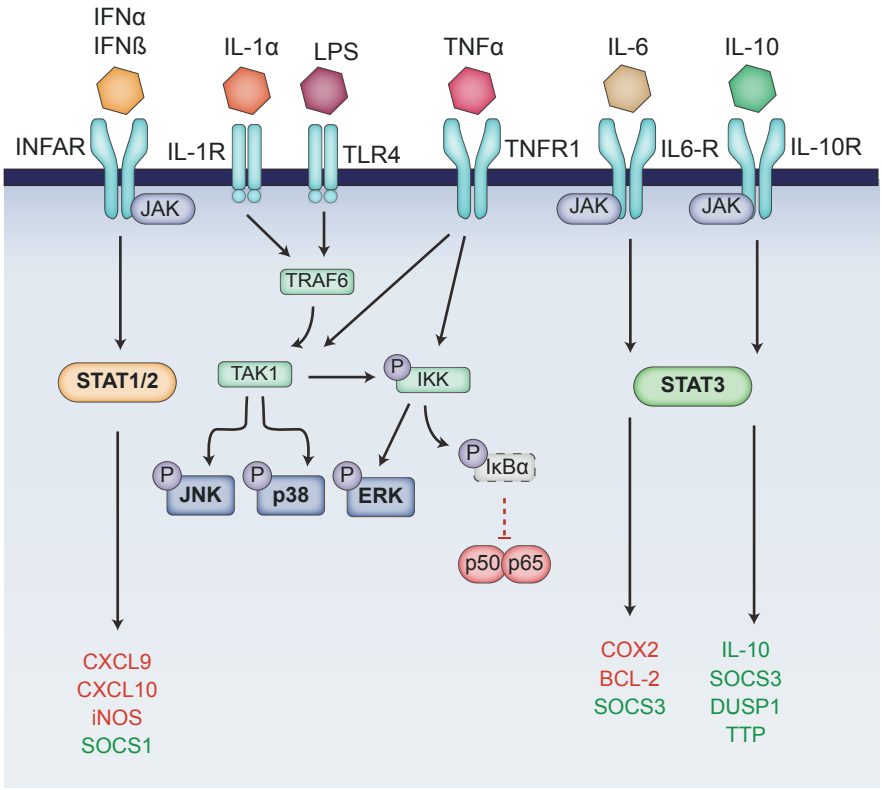

Figure 19. Autocrine loops during inflammatory responses. During the LPS response, macrophage synthesize and secrete cytokines like type I IFNs, IL-1, TNFα IL-6 and IL-10. Once secreted, they can be recognized by their receptors activating again different signalling cascades.

2.5. Inflammation resolution: TLR4 and NF-κB negative regulators

TLR4 activation also induces the expression of inhibitors of the inflammatory signalling cascades (Bode et al. 2012). This negative feedback mechanisms use different strategies to inhibit inflammatory pathways: dephosphorylation, protein degradation or physical blockage, among others. Some examples are listed below.

Dual-specificity protein phosphatases (DUSPs, also known as MKPs) are enzymes that can dephosphorylate threonine and tyrosine residues in the activation loop of MAPKs, thus inactivating them. DUSP1 and DUSP2 are the main DUSPs upregulated following TLR4 activation. DUSP1 predominantly targets p38α and JNKs, while DUSP2 targets only JNKs. DUSP4 and DUSP5 function is still unclear, although they have been suggested to dephosphorylate ERK1 and ERK2 (Arthur & Ley 2013). Other protein-tyrosine phosphatases (PTPs, such as SHP-1, SHP-2, CD45, PIP1B) dephosphorylate receptors at the plasma membrane and thereby block TLR signalling (Lawrence & Fong 2010).

Suppressors of cytokine signalling (SOCS) proteins are also inhibitors of inflammatory pathways. Through their SOCS domain they function as E3 ubiquitin ligases and mediate protein degradation. For example, SOCS1 facilitates the ubiquitylation and degradation of the p65 subunit of NF-κB and the adaptor MAL (Wilson 2014). Besides mediating protein degradation, SOCS1 and SOCS3 also inhibit JAK1 by working as pseudosubstrates (Yoshimura et al. 2007). Through this mechanism, SOCS1 directly inhibits JAK1, IFNAR and the IFNγ receptor (IFNGR) (Schneider et al. 2014; McCormick & Heller 2015). Moreover, SOCS1 might also inactivate JNK and p38 MAPK pathways by binding to ASK1 MAP3K (Yoshimura et al. 2007). On the other hand, SOCS3-mediated inhibition of JAK1 strongly inhibits IL-6R but not IL-10R, explaining STAT3 transient activation in response to IL-6, but sustained in response to IL-10. Moreover, SOCS3 can also inhibit the activation of TRAF6 and TAK1 (Yoshimura et al. 2007; Tugal et al. 2013).

A20/TNFAIP3 is a ubiquitin ligase and deubiquitin enzyme (DUB) that can inhibit TLR signalling in several manners. On the one hand, it adds K48-polyubiquitin chains to the mediators RIP1 and UBC13, leading to their degradation. On the other hand, it removes K63–polyubiquitin chains to disrupt the interactions created during early TLR activation between IRAK1/4, RIP1, TAK1 and the IKK complex. Importantly, other ubiquitin ligases and DUBs are also involved in inflammation resolution (Wertz & Dixit 2010; Das et al. 2018).

Other proteins have been shown to use different mechanisms to inhibit the TLR cascade, such as blocking receptors or interactions. In this category we can find MyD88s, an alternative spliced form of MyD88 that blocks the TLR receptor; Interleukin-1 receptor antagonist (IL-1RA), that blocks IL-1 receptors without inducing any intracellular response; or IRAK-M, which blocks the dissociation of IRAK1-4 from MyD88 (Lawrence & Fong 2010; Wertz & Dixit 2010).

Finally, some mechanisms specifically limit NF-κB function. On the one hand, NF-κB triggers the synthesis of its inhibitor IκBα, which retains NF-κB again in the cytoplasm (Hoffmann & Baltimore 2006). Moreover, different combinations of NF-κB subunits can also disrupt its inflammatory activity. For example, homodimers of the p50 subunit, heterodimers containing RelB or containing unphosphorylated p65, bind to repressive histone deacetylases (HDACs) suppressing transcription of NF-κB target genes (Oakley et al. 2005).

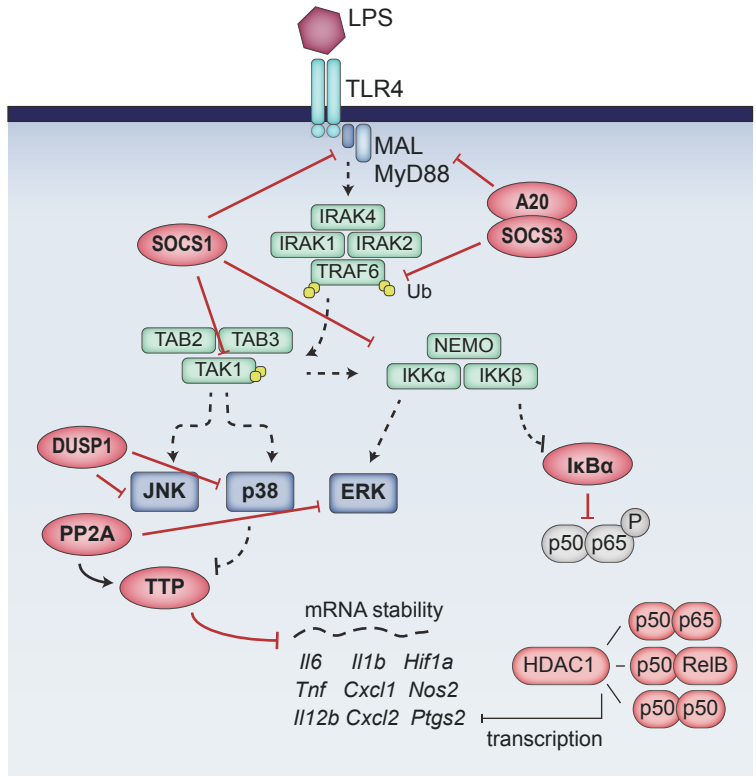

Figure 20. Negative inhibitors of the inflammatory pathways mediate inflammation resolution. Suppression of the TLR4 pathways by multiple inihbitory molecules, shown in red. These negative regulators can also inhibit IL-6, Type I IFN, or IL-1α pathways.

2.6. Post-transcriptional control during the LPS response

The TLR signalling pathway is also subjected to extensive translational regulation. Here, we will give a brief overview of the translational landscape during the LPS response.

2.6.1. mRNA decay during the LPS response

One piece of data showing the relevance of translational control in immune responses comes from the analysis of transcription and mRNA decay dynamics during the LPS response. After LPS stimulation, the increase in RNA levels are mainly due to changes in transcription rates. However, the duration of these responses. particularly those that are rapid and transient, is mainly determined by RNA decay (Carpenter et al. 2014).

As previously mentioned, AU-rich elements (AREs) in mRNAs are highly involved in the regulation of its stability. Numerous inflammatory factors undergo ARE-mediated regulation, including IL-6, TNFα, IL-1β, GM-CSF, iNOS and IL-10. Tristetraprolin (TTP) is an AREs binding protein whose function during the LPS response in macrophages has been widely characterized. Importantly, TTP destabilizing activity is crucial to limit the expression of inflammatory cytokines.

In unstimulated macrophages, unphosphorylated TTP interacts with the CCR4-NOT deadenylase complex promoting the destabilization of its target mRNAs (Fabian et al. 2013). In this context, TTP also destabilizes its own mRNA and it is subjected to proteasomal degradation, therefore TTP mRNA and protein levels are maintained low. Upon LPS stimulation, MK2 downstream p38α phosphorylates TTP triggering several effects. On the one hand, it promotes the assembly of TTP:14-3-3 complexes, which prevent the interaction between TTP and the deadenylase complex (Stoecklin et al. 2004; Clement et al. 2011). Moreover, TTP phosphorylation also prevents its proteasomal degradation leading to an accumulation of TTP protein (Hitti et al. 2006; Brook et al. 2006). Finally, TTP phosphorylation reduces its ARE-binding affinity (Hitti et al. 2006). In the case of TNFα mRNA, this reduction in TTP affinity shifts the competitive AREs-binding equilibrium towards HuR, another ARE-binding protein that contributes to the stabilization and expression of TNFα (Tiedje et al. 2012). Altogether, these processes inhibit TTP-mediated

deadenylation of mRNAs, promoting the stabilization of TTP targets. Moreover, this mechanism contributes to the rapid expression of inflammatory cytokines upon macrophage activation. However, during the resolutive phase of the LPS response, p38 activity its inhibited, favouring Protein Phosphatase 2A (PP2A)-mediated removal of phosphate groups from TTP (Sun et al. 2007; Smallie et al. 2015). Thus, unphosphorylated TTP destabilizes again cytokine mRNAs, favouring the reduction in cytokine expression during inflammation resolution **(Figure 21)**.

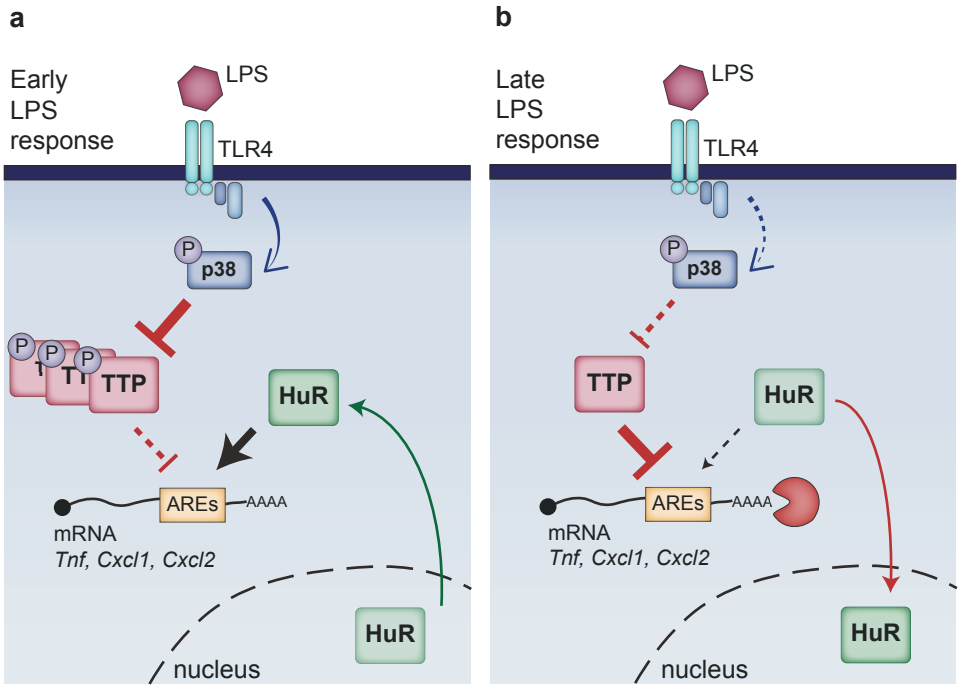

Figure 21. HuR and TTP sequentially regulate the stability of ARE-containing mRNAs.

Despite the extended characterization of this mechanism, there are still pieces that are poorly understood. For example, genome-wide studies have shown that not all TTP targets are destabilized in the same way during the LPS response, nor are they all regulated by the competition between TTP and HuR as is *Tnf* (Sedlyarov et al. 2016). Moreover, HuR depletion leads to exacerbated inflammatory conditions (Yiakouvaki et al. 2012), which undermines its function as a translational activator of inflammatory cytokines, and suggests it also has anti-inflammatory roles, either as a translational activator of anti-inflammatory molecules or as a transcriptional repressor due to its nuclear functions. In this line, HuR nucleo-cytoplasmic shuttling is controlled by several pathways, including the p38-MK2 axis. In this manner, HuR function might be modified along the different phases of the LPS response (Doller et al. 2008)

Finally, other ARE-BPs are also expressed during the LPS response, such as AUF1 and TIA1. These two proteins also target *Tnf* mRNA; AUF1 destabilizes it while TIA1 represses its translation. The competition between these proteins and HuR and TTP could also account for the differential behaviour between ARE-containing mRNAs.

It is worth mentioning that transcript stability can be also affected by non-ARE regulatory elements. Among others, EDEN-like sequences, constitutive decay elements (CDEs) or other stem loop structures can promote mRNA decay, while for example UC-rich sequences can mediate mRNA stabilization (Bode et al. 2012; Carpenter et al. 2014; Mino et al. 2015; Fu & Blackshear 2017). Additionally, abundant evidence has revealed the importance of miRNAs in the initiation and termination of inflammation, as they can target crucial molecules and thus participate in macrophage polarization into pro- or anti-inflammatory functions (Kawasaki & Kawai 2014; Lu et al. 2014; Essandoh et al. 2016).

The interplay between all these regulatory elements that control mRNA decay will determine the duration of mRNA expression during the LPS response.

2.6.2. Translational regulation during the LPS response

Upon LPS stimulation, several translational regulatory mechanisms are also activated affecting the development of the inflammatory response.

As previously mentioned, eIF2α phosphorylation leads to global translational repression of most mRNAs and, moreover, prolonged eIF2α phosphorylation can lead to apoptosis. LPS response triggers eIF2α phosphorylation, however it is compensated by the dephosphorylation of eIF2B via TRIF, which stimulates eIF2B-mediated recycling of eIF2. This mechanism allows the maintenance of efficient mRNA translation and cell survival, even if eIF2α remains phosphorylated (Woo et al. 2009; Woo et al. 2012; Cláudio et al. 2013; Carpenter et al. 2014).

In addition, eIF4E activity and availability is also regulated during the LPS response. For example, TLR-triggered eIF4E phosphorylation has been shown to enhance the translation of mRNAs such IκBα (Herdy et al. 2012). LPS activates mTOR (Lopez-Pelaez et al. 2012), which via 4E-BP phosphorylation favours eIF4E availability. This process mainly enhances translation of 5'TOP (terminal oligopyrimidine) mRNAs and mRNAs with highly structured 5´UTR, some of which are key inflammatory genes such as IRF7, TNFα, IL6 or CXCL1. Although this would point towards mTOR having a pro-inflammatory function, mTOR inhibition can lead to increased expression of inflammatory markers. As the mTOR pathway is involved in multiple other functions such as metabolism regulation, further studies are needed to understand mTOR contribution to both pro- and anti-inflammatory processes (Weichhart et al. 2015; Turner & Díaz-Muñoz 2018).

Alternative mechanisms of regulating translation upon LPS stimulation have been also described: inhibition of eIF4A activity, mRNA localization to stress granules and/or P-bodies or regulation of translation elongation. Furthermore, long non-coding RNAs are an emerging field that may potentially regulate macrophage activation both at the transcription and post-transcriptional levels (Carpenter et al. 2014; Turner & Díaz-Muñoz 2018).

2.6.3. CPEBs in LPS response

The contribution of CPEBs to macrophage activation by LPS remains largely unexplored. For CPEB1, it has been described that KO MEFs and macrophages show enhanced NF-κB activation and cytokine expression, indicating that CPEB1 has a repressor function on cytokine mRNAs such as *Il6*, *Il12*, or the upstream NF-κB activator *Tak1* (Ivshina et al. 2014; Groppo & Richter 2011). For the CPEB2-4 subfamily, their function in macrophages is unknown, although it has been shown in other contexts that they can regulate the mRNAs of inflammatory mediators such as *Hif1a*, *tPA* or *Vegf* (Hägele et al. 2009; Chen & Huang 2012; Ortiz-Zapater et al. 2012; Calderone et al. 2016).

OBJECTIVES

Objectives

The aim of this project is to unveil the contribution of Cytoplasmic Polyadenylation Element Binding Proteins (CPEBs) to macrophage physiology.

Particularly, we focused on the contribution of CPEB4-mediated translational control to the development and resolution of inflammatory processes in response to LPS stimulation.

The specific goals that we have pursued are the following:

- Characterization of the regulatory mechanisms that control CPEB4 expression and activity upon LPS stimulation in macrophages.
- Definition of CPEB4 target mRNAs in quiescent macrophages and during the late phase of the LPS response.
- Understanding the relevance of CPEB4 function in quiescent macrophages and during the LPS response.
- Understanding the relevance of CPEB4 expression in myeloid cells *in vivo*, both in homeostatic conditions and upon LPS challenge.

RESULTS

Results

1. CPEB4 is upregulated upon LPS stimulation in macrophages

Macrophages are immune cells that belong to the innate immune system. Thus, they need to rapidly respond to a great variety of challenges and activate the appropriate gene expression program in order to orchestrate effective immune responses. For example, macrophages develop antimicrobial functions upon encounter with bacteria, while upon sensing of immunomodulatory cytokines like IL4 they acquire properties to promote tissue repair (Martinez & Gordon 2014). Multiple transcriptional and translational mechanisms are involved in the regulation of the duration, extent and resolution of inflammatory responses. Importantly, both positive and negative inputs are needed in order to create transient oscillatory responses. CPEBs have the unique property of being able to repress as well as activate translation through the regulation of the poly(A) tail of mRNAs. Thus, multiple studies have shown CPEBs contribution to rapid responses in response to stimuli, such as neuronal activation after synaptic stimulation or the resumption of meiotic progression upon progesterone sensing. However, whether CPEBs contribute to the development of inflammatory responses remains unexplored.

Therefore, we decided to study if CPEBs are involved in inflammatory responses. For this, we obtained Bone Marrow Derived Macrophages (BMDMs) and characterized CPEBs expression in different situations. First, we observed that under basal conditions, *Cpeb2* mRNA was the most abundant one, followed by *Cpeb4* **(Fig. 22a)**.

Next, we stimulated macrophages with LPS, the main membrane component of gram negative bacteria, or with IL-4, an immunomodulatory cytokine. As expected, these two stimuli triggered opposite polarizations in macrophages, which also involved dramatic changes in CPEBs expression. During the LPS response, *Cpeb4* mRNA was strongly upregulated, *Cpeb3* showed a smaller peak, but the other members of the CPEB family were virtually unaffected **(Fig. 22b)**. On the contrary, after IL4 stimulation, *Cpeb1* levels increased, *Cpeb2* and *Cpeb3* remained stable, and *Cpeb4* was slightly downregulated **(Fig. 22b)**. These results suggested that the expression of *Cpebs* in BMDMs is regulated by independent mechanisms and that each CPEB might be involved in distinct functions, as they are expressed at different stages of macrophage polarization.

Of these observations, we decided to further study the upregulation of *Cpeb4* mRNA after LPS stimulation by assessing the expression of CPEB4 protein. As shown in **figure 22c**, CPEB4 protein was also upregulated upon LPS stimulation. Again, the increase in CPEB4 levels was LPS-specific, as IL-4 or IFNγ did not cause a similar effect **(Fig. 22c)**. Finally, we also confirmed that the alterations in CPEB3 levels after LPS treatment were much weaker **(Fig. 22c)**.

Altogether, these results encouraged us to further study the role of CPEB4 during the LPS response. Specifically, we decided to characterize its regulation and function in this context.

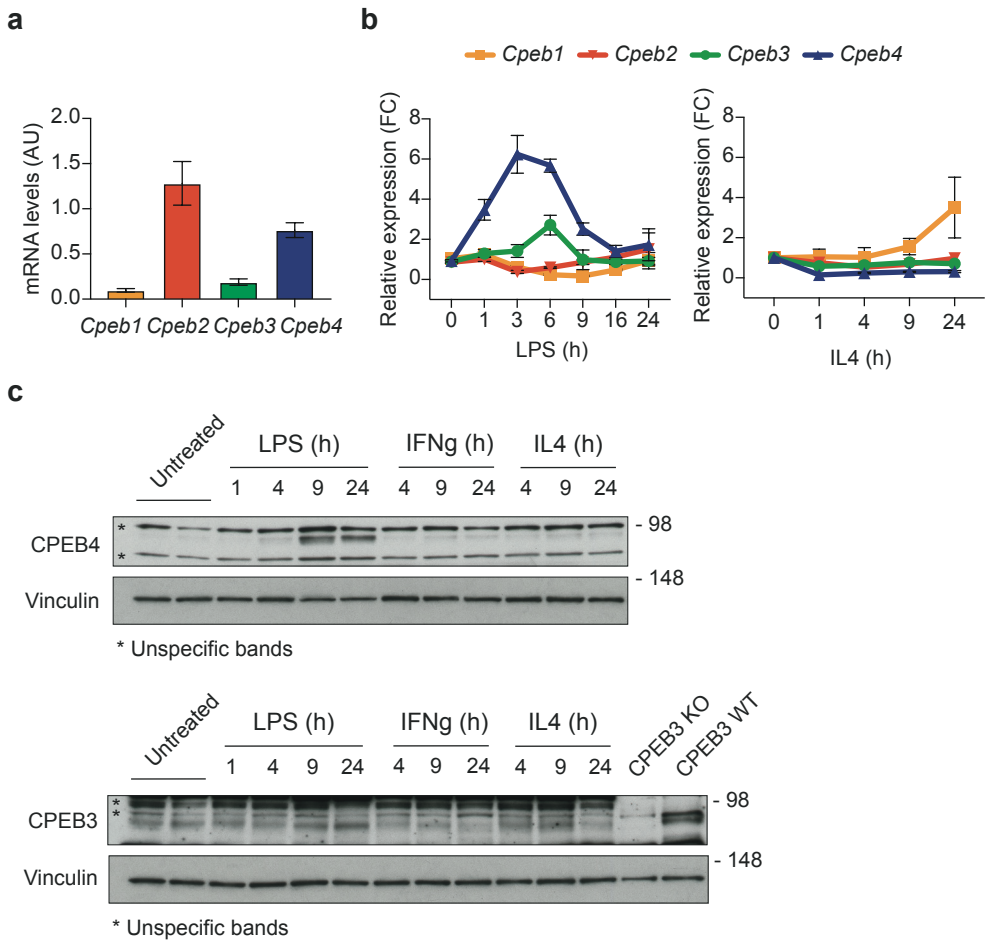

Figure 22. CPEB4 is upregulated upon LPS stimulation in Macrophages. →

← **Figure 22. CPEB4 is upregulated upon LPS stimulation in Macrophages.** **(a)** *Cpeb1-4* mRNA expression in untreated BMDM, normalized to *Tbp*. **(b)** BMDMs were stimulated with LPS or IL4 (10ng/ml) for the indicated times and *Cpeb1-4* mRNA was measured. After normalization to *Tbp*, relative levels were calculated by setting expression of untreated samples as 1 for each gene. **(c)** Immunoblot analysis of CPEB4 and CPEB3 in BMDMs stimulated with LPS, IFNγ or IL-4 (10ng/ml) for the indicated times. Retina protein extracts from wild type and *Cpeb3*KO mice were used as control for CPEB3 antibody. Vinculin served as loading control. **(a,b)** Data are shown as mean ± s.e.m. Untreated and LPS: data show at least three independent experiments. IL4: data show at least two replicates/timepoint for *Cpeb1* and *Cpeb4*. N=1 for *Cpeb2* and *Cpeb3*.

2. CPEB4 mRNA stability is regulated during the LPS response via p38a-HuR-TTP[1]

One of the main features of macrophage response to inflammatory stimuli is that, in very short periods of time, they are able to increase dramatically the expression of inflammatory genes, but in a transient manner. Thus, the expression of these molecules is usually restricted to defined temporal windows. One of the most characterized systems to limit cytokine expression during the LPS response involves the MAPK p38α and two ARE-binding proteins, HuR and TTP, which regulate the stability of ARE-containing mRNAs.

Briefly, LPS stimulation activates p38α, which promotes TTP phosphorylation, and therefore inhibits TTP-mediated mRNA destabilization (Hitti et al. 2006; Brook et al. 2006). This process favours that ARE-containing mRNAs are bound by HuR, which mediates their stabilization and upregulation (Tiedje et al. 2012; Ke et al. 2017). However, this state is transient as, during the late LPS response, TTP recovers its activity, favouring again mRNA decay and driving the downregulation of ARE-containing mRNAs (Sun et al. 2007). Among others, cytokines like *Tnf* and *Il10* harbour AREs in their 3'UTR and have been shown to be regulated by this system.

We observed that *Cpeb4* expression during the LPS response followed this pattern of transient up- and downregulation **(Fig. 22b)**. Moreover, *Cpeb4* contains multiple AREs in its 3'UTR **(Fig. 23a)**. Therefore, we decided to study if *Cpeb4* expression was also regulated by this system.

[1]These results were mainly obtained by the Dr. Annarita Sibilio.

First, we assessed p38α contribution to *Cpeb4* expression. For that, we obtained BMDMs from myeloid-specific p38α Knock-Out mice (*p38*αMKO) (Youssif et al. 2018) and stimulated them with LPS. Interestingly, we observed that *Cpeb4* upregulation was reduced in *p38*αMKO macrophages **(Fig. 23b)**. Moreover, wild type macrophages treated with the p38 inhibitor PH797804 showed the same phenotype **(Fig. 23c)**, indicating that p38α kinase activity mediates the increase in *Cpeb4* levels during the LPS response. To assess whether p38α-mediated control of *Cpeb4* occurred through mRNA stability, we performed an Actinomycin D chase assay after 1 hour of LPS treatment. As shown in **figure 23d**, *Cpeb4* mRNA decay was significantly faster in *p38*αMKO BMDMs, indicating that p38α indeed stabilizes *Cpeb4* mRNA during the early LPS response. Finally, we also examined how p38α-mediated regulation of *Cpeb4* mRNA affected CPEB4 protein levels. As for *Cpeb4* mRNA, we observed that after 3 hours of LPS treatment CPEB4 protein levels were significantly lower in the absence of p38α **(Fig. 23e)**.

It is worth mentioning, though, that after 9 hours of LPS stimulation, both the mRNA and protein levels of CPEB4 were comparable between wild type and *p38*αMKO macrophages **(Fig. 23b-c, e)**. Therefore, these results suggest that, during the late LPS response, CPEB4 expression was regulated by a p38α-independent mechanism. Given that *Cpeb4* mRNA levels are already downregulated at 9 hours, when CPEB4 protein peak, we hypothesize that this second mechanism regulating CPEB4 expression probably involved translational control. According to published data, one possibility could be that CPEB4 itself, once it has been partially upregulated, mediates an autoregulatory loop where it promotes the translation of its own mRNA and, thus, progressively upregulates its own levels (Igea & Méndez 2010; Calderone et al. 2016; Maillo et al. 2017).

Having seen that *Cpeb4* mRNA stability was regulated by p38α, we next wanted to assess whether HuR and TTP were mediating this process. First, we stimulated BMDMs with LPS for 3 hours and performed HuR RNA immunoprecipitation and qPCR (RIP-qPCR, **Fig. 24a**). As for *Tnf* mRNA, we observed that HuR binding to *Cpeb4* mRNA binding to HuR was strongly enriched upon LPS treatment **(Fig. 24b)**. Furthermore, in *p38*αMKO macrophages this process was reduced **(Fig. 24b)**, suggesting that HuR mediates *Cpeb4* mRNA stabilization downstream p38α, during the early LPS response.

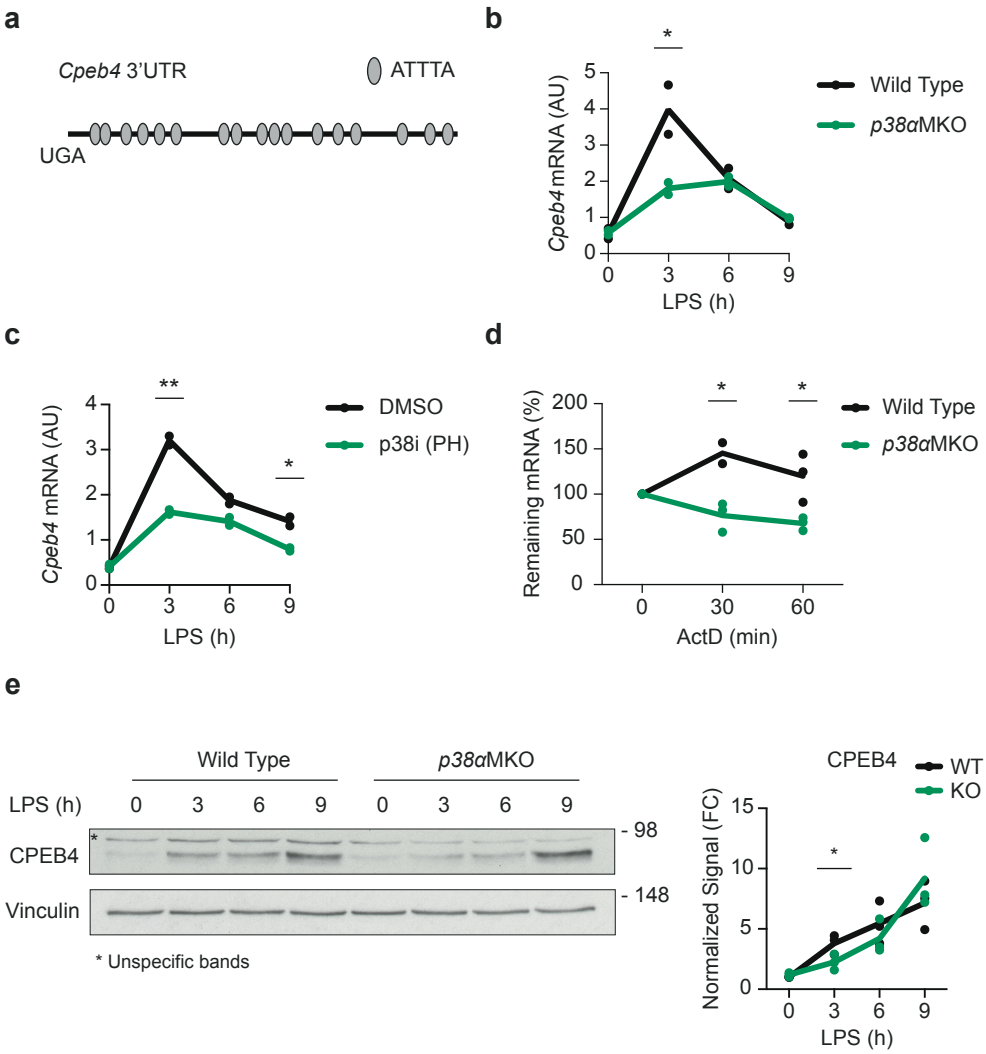

Figure 23. *Cpeb4* mRNA stability is regulated during the LPS response via p38α. (a) Schematic representation of *Cpeb4* 3'UTR showing its AREs domains. **(b)** BMDMs obtained from wild type or *p38α*MKO mice were stimulated with LPS (10ng/ml) for the indicated times and gene expression was analysed by RT-qPCR. **(c)** BMDMs were treated with the p38 inhibitor PH797804 (1uM) and LPS (10ng/ml). After the indicated times, gene expression was analysed by RT-qPCR. **(d)** BMDMs obtained from wild type or *p38α*MKO mice were stimulated with LPS (10ng/ml) for 1h and then treated with Actinomycin D (10ug/ml). At the indicated times, gene expression was analysed by RT-qPCR. **(e)** Immunoblot analysis of CPEB4 in Wild type or *p38α*MKO BMDMs stimulated with LPS (10ng/ml) for the indicated times. Vinculin served as loading control. Quantification of triplicate experiments is shown. Ratio paired t-test pv *pv<0,05. **(b-d)** Data are shown as mean and s.e.m. of duplicate experiments. mRNA expression is normalized relative to *Gapdh* (b,c) or *18S* (d). Statistics Two-way ANOVA *pv<0.05 **<0.01.

Finally, to study whether *Cpeb4* mRNA is regulated by TTP during the late LPS response, we took advantage of a recent publication that studied TTP function in LPS-stimulated BMDMs from wild type and TTP myeloid-KO mice (TTPMKO) (Sedlyarov et al. 2016). Remarkably, *Cpeb4* mRNA followed again the same pattern as *Tnf*. First, analysis of their iCLIP data showed that TTP binds both *Tnf* and *Cpeb4* mRNA after 6 hours of LPS treatment **(Fig. 24c**, *Tnf* not shown**)**. Second, the decay rate of both mRNAs was significantly slower in TTPMKO macrophages, suggesting that TTP is indeed promoting their destabilization **(Fig. 24d)**. Finally, consistent with a reduced *Cpeb4* destabilization, after 9 hours of LPS treatment, TTPMKO macrophages presented increased levels of *Cpeb4*. This difference, though, was much weaker for *Cpeb4* than for *Tnf* **(Fig. 24e)**. These results indicate that TTP mediates *Cpeb4* mRNA destabilization during the late LPS response.

Altogether, we have shown that the MAPK p38α regulates *Cpeb4* mRNA stability during the LPS response. Downstream of p38α, HuR and TTP regulate *Cpeb4* through the AREs in its 3'UTR. At early timepoints, HuR mediates *Cpeb4* stabilization and upregulation, and during the late LPS response, TTP mediates its downregulation by destabilization.

→ Figure 24. *Cpeb4* mRNA is regulated by HuR and TTP during the LPS response. (a-b) BMDMs obtained from wild type or *p38α*MKO mice were stimulated with LPS (10ng/ml) for 3h, and immunoprecipitation (IP) with anti-HuR antibody or IgGs was performed. **(a)** Immunoblot analysis of HuR IP. **(b)** RNA was extracted and analysed by RT-qPCR. Data are shown as mean and s.e.m. of duplicate experiments. mRNA expression is normalized relative to *Gapdh*. **(c)** BMDMs were treated with LPS for 6h and TTP PAR-iCLIP was performed. Coverage plots represent the number of crosslink sites detected in each position of *Cpeb4*. Binding sites to *Cpeb4* Transcription Start Site (TSS) and their scores are indicated in the table. **(d)** *Cpeb4* and *Tnf* decay rates in wild type and TTPMKO BMDMs stimulated for 6 h with LPS. **(e)** *Cpeb4* and *Tnf* expression profile in wild type and TTPMKO BMDMs treated with LPS for the indicated times. Differential expression analysis was performed using DESeq2 software. **qvalue= 0.00891 **(c-e)** LPS treatment 10ng/ml. Data was obtained from Sedlyarov *et al*. 2016.

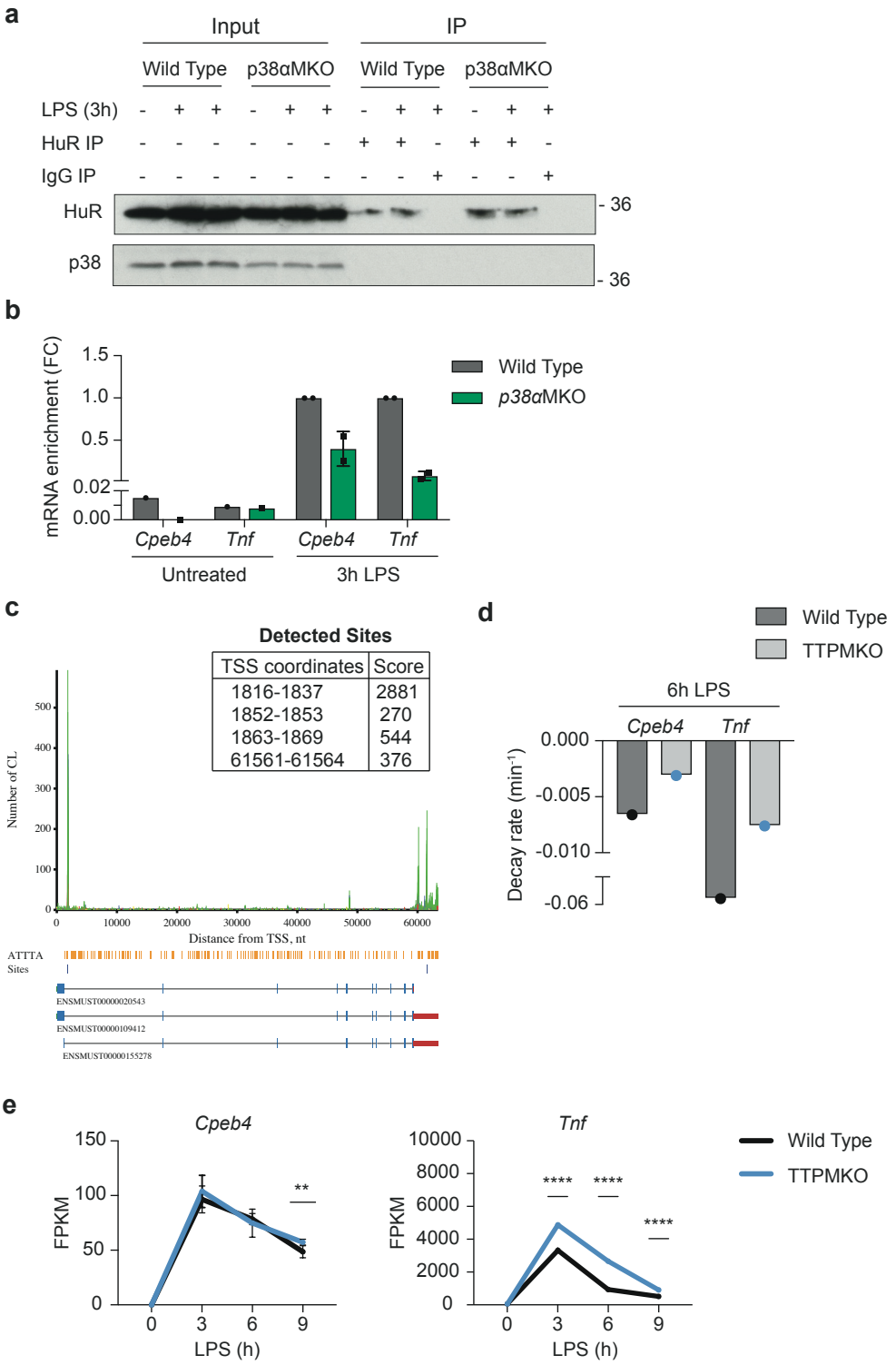

← Figure 24. CPEB4 mRNA is regulated by HuR and TTP during the LPS response.

3. CPEB4 is phosphorylated during the LPS response

While studying the increase in CPEB4 protein levels upon LPS exposure, we observed that CPEB4 migrated as a doublet **(Fig. 25a)**, suggesting that CPEB4 was post-translationally modified. Indeed, we confirmed by lambda phosphatase treatment that the upper band in this doublet was phosphorylated CPEB4 (P-CPEB4) **(Fig. 25b)**.

In *Xenopus laevis* oocytes, CPEB4 hyperphosphorylation is mediated by ERK1/2 and CDK1 kinases, a process that regulates CPEB4 activity (Guillén-Boixet et al. 2016). When unphosphorylated, CPEB4 assembles phase-separated structures, where its target mRNAs are stored. However, upon hyperphosphorylation, these structures are disassembled and CPEB4 is able to promote the polyadenylation and translation of its target mRNAs (Guillén-Boixet et al. 2016).

In macrophages, ERK1/2 MAPKs are known to be activated after LPS stimulation (Weinstein et al. 1992). Importantly, ERK1/2 kinetics of activation were compatible with ERK1/2 being responsible for CPEB4 phosphorylation **(Fig. 25b)**. On the other hand, the main function of CDK1 is to control cell cycle progression during M phase (Malumbres & Barbacid 2009). LPS stimulation, though, induces cell cycle arrest at early G1 (Vairo et al. 1992; Xaus et al. 1999), as we could confirm based on Cyclin D1 expression **(Fig. 25c)**. Consequently, CDK1 is expected to be inactive during the LPS response. Therefore, we predict that ERK1/2 MAPKs mediate CPEB4 phosphorylation in LPS-activated BMDMs.

So far, we have seen how multiple mechanisms regulate CPEB4 expression and activity upon LPS stimulation. Consequently, during the later timepoints of the LPS response, CPEB4 reaches its highest levels and is mainly found phosphorylated, thus being able to promote the polyadenylation and translation of its target mRNAs. Hence, we next decided to investigate which mRNAs are associated with CPEB4 in this context.

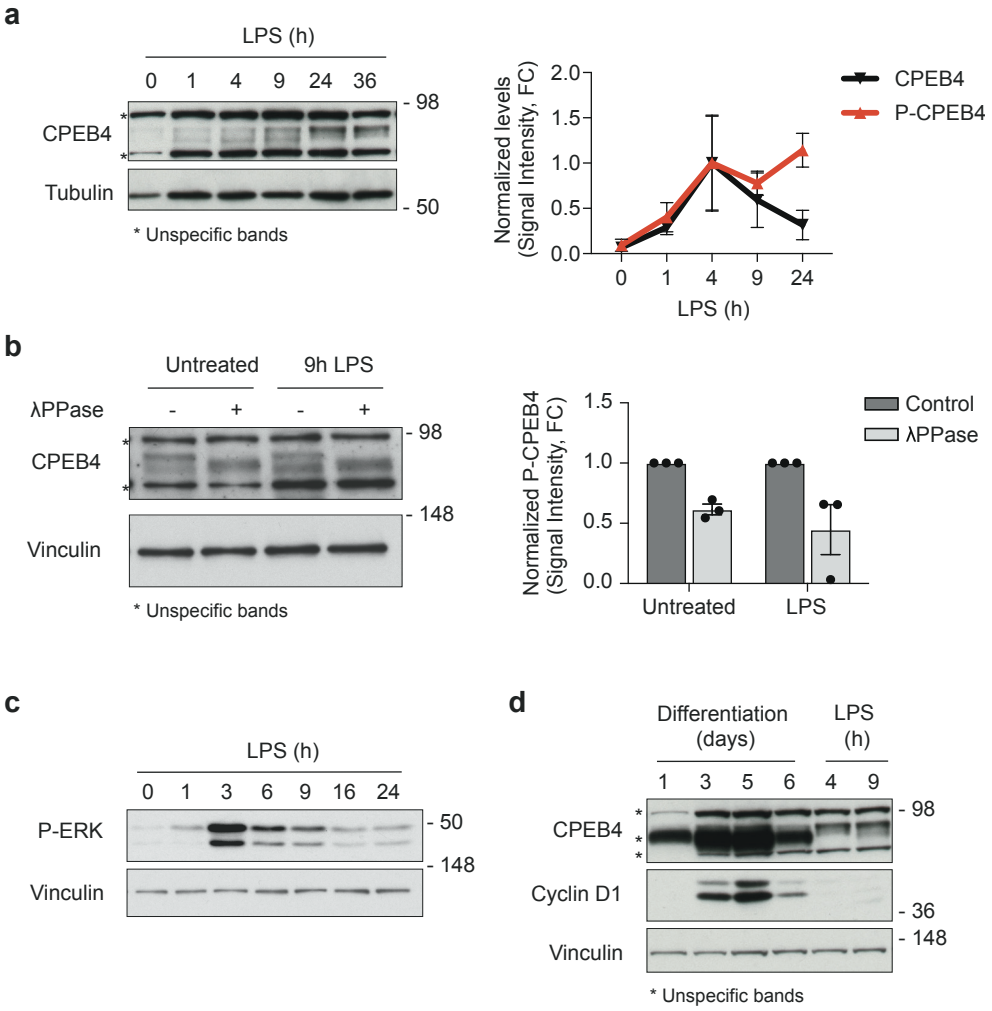

Figure 25. CPEB4 is phosphorylated during the LPS-response. (a) Immunoblot analysis of CPEB4 in control or LPS-treated macrophages. α-Tubulin served as loading control. Quantification of normalized CPEB4 and P-CPEB4 signal is shown. **(b)** Immunoblot analysis of CPEB4 in control and LPS–primed BMDMs. Protein extracts were treated with λPhosphatase when indicated. Quantification of normalized P-CPEB4 signal is shown. **(c)** Immunoblot analysis of Phospho-ERK1/2 in control or LPS-treated BMDMs. **(d)** Immunoblot analysis of CPEB4 and CyclinD1. Lanes 1-4 are samples obtained during the differentiation of Bone Marrow Progenitor cells to BMDMs in the presence of M-CSF (time indicated in days). Lanes 5-6 are samples stimulated with LPS (10ng/ml for the indicated hours). **(b-d)** Vinculin served as loading control.

4. Defining CPEB4 function during the late LPS response in BMDMs

4.1. CPEB4 regulates negative feedback inhibitors of the LPS response[2]

To define CPEB4 target mRNAs, we applied CPEB4 RNA-immunoprecipitation and sequencing (RIP-seq) to wild type BMDMs, in untreated conditions and at 9 hours after LPS stimulation. BMDMs from *Cpeb4*KO mice (Maillo et al. 2017) were used as controls **(Fig. 26a, b)**. CPEB4 targets were defined as those significantly enriched in wild type CPEB4 IP compared to the corresponding IP in *Cpeb4*KO BMDMs (Peak calling analysis, pvalue<0,02 or peak score>500). Hence, we identified 1079 and 1782 mRNAs associated with CPEB4 in untreated and LPS conditions, respectively **(Appendix I, II)**. We defined as the "BMDMs transcriptome" those transcripts detected in our input wild type samples in untreated or LPS conditions. As shown in **figure 26c**, CPEB4 targets represented the 10-15% of the BMDMs transcriptome and 797 genes were identified as targets in both conditions. As a quality control, we observed that the 3'UTRs of the identified mRNAs were enriched in CPE motifs as expected of CPEB4 targets (Chi Square test pv<0,0001; Piqué et al. 2008) **(Fig. 26d, see Box 2)**. Moreover, previously described CPEB4 targets such as *Txnip* or *Vegfa* were identified, while negative controls such as *Gapdh* were not **(Fig. 26e)**.

→ Figure 26. Identification of CPEB4 targets in LPS-primed BMDMs. (a) Immunoblot for CPEB4 from inputs and immunoprecipitated fractions with anti-CPEB4 antibody in BMDMs obtained from Wild type or *Cpeb4*KO mice (n=1); Vinculin served as a loading control. **(b)** RNA integrity was evaluated with an Agilent 2100 BioAnalyzer with the RNA 6000 Pico kit. **(c)** Percentage of CPE-containing transcripts in RIP-seq defined CPEB4 targets and *Mus musculus*/BMDMs transcriptome. Statistics with Fisher's exact test.****pv<0.0001. **(d)** Read coverage of *Vegfa*, *Txnip* and *Gapdh* mRNAs in RNAseq (Input) or RIP-seq samples (IP). Detected peak enrichments in wild type (WT) versus *Cpeb4*KO (KO) IP are shown. Image obtained using integrated genomic viewer (IGV) with a minimum range of 0-20 arbitrary units (AU).

[2]Bioinformatic analysis of the RIP-seq data was done in collaboration with Dr. Oscar Reina.

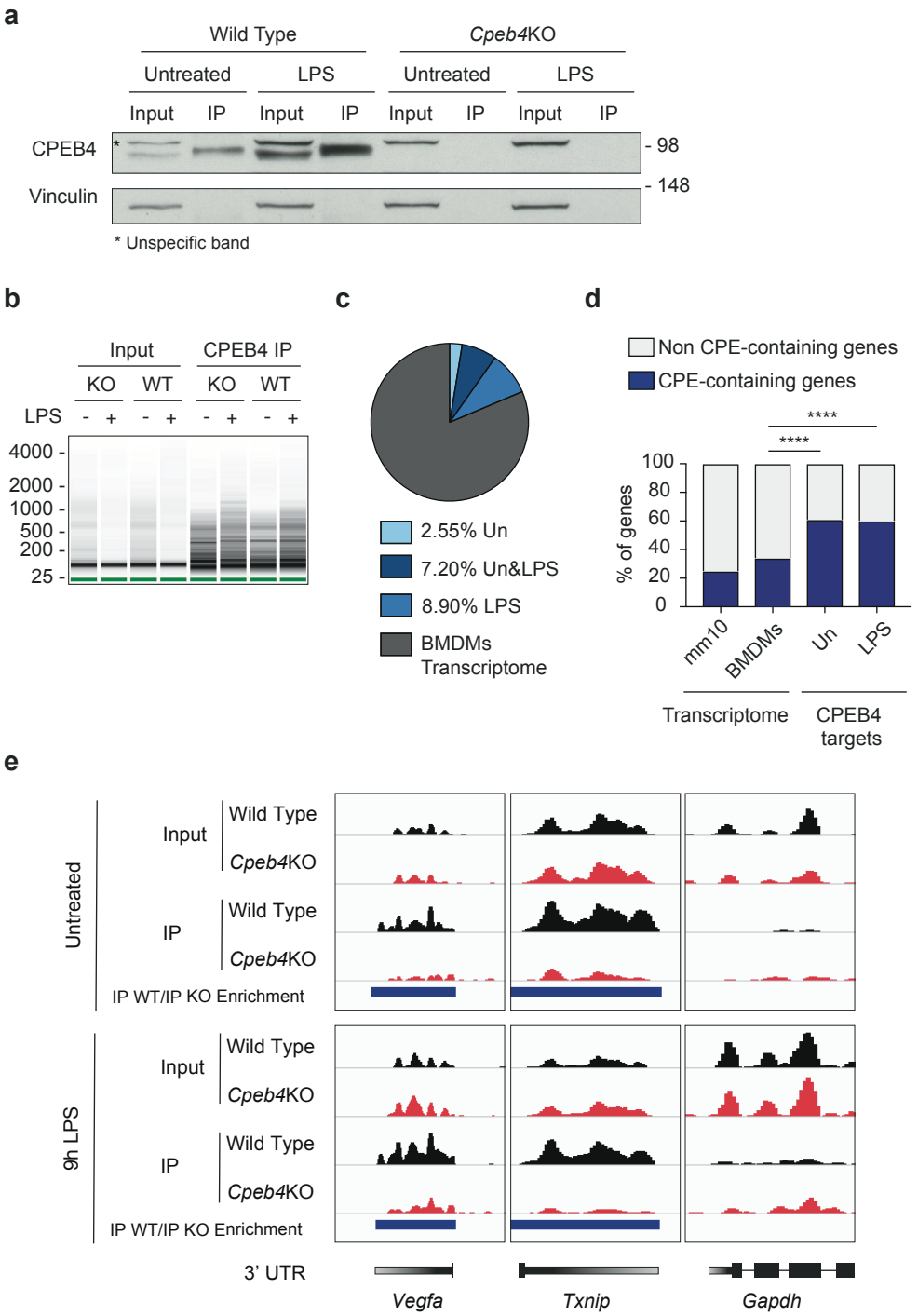

← Figure 26. Identification of CPEB4 targets in LPS-primed BMDMs.

BOX 2. REVISITING CPEs DEFINITION

As shown in **figure 26d**, according to the CPE motif defined by Piqué and colleagues (which we will refer as CPE-As), 60% of CPEB4 targets contained functional CPE-As in their 3'UTRs (Piqué et al. 2008). Recent publications though, suggest that CPEB4 could bind other CPE motifs that were not included in Piqué's analysis. For example, a CPE-G motif (UUUUG) was found to be bound by Orb2, the Drosophila ortholog of CPEB2-4 (Stepien et al. 2016; Afroz et al. 2014). Therefore, we decided to explore if CPEB4 targets were enriched in CPE-G motifs in their 3'UTRs that could explain CPEB4 binding.

First, we defined the CPE-G-containing mRNAs as those with UUUUGU sequences in their 3'UTR within the same functional distances from the PAS established in Piqué's script (<100bp). We found that around 20% of the mRNAs in the mouse transcriptome contained CPE-Gs, a similar proportion as mRNAs containing CPE-As **(Fig. 27a)**. Therefore, considering both CPE-A- and CPE-G-containing mRNAs, the total percentage of potential CPEBs targets increased to 36%.

Next, we evaluated whether CPE-G containing mRNAs were enriched in different sets of CPEB4 targets: two published sets in erythroblast and hepatocytes (Hu et al. 2014; Maillo et al. 2017) and our sets in untreated or LPS-stimulated macrophages. Interestingly, all lists of CPEB4 targets displayed a significant increase in the proportion of CPE-G containing mRNAs **(Fig. 27b)**. Indeed, after combining the CPE-A and CPE-G definition, the proportion of CPE-containing targets in macrophages increased to almost 80% **(Fig. 27c)**.

Based on these results, we decided to consider both CPE-G- and CPE-A-containing mRNAs as putative CPEBs targets.

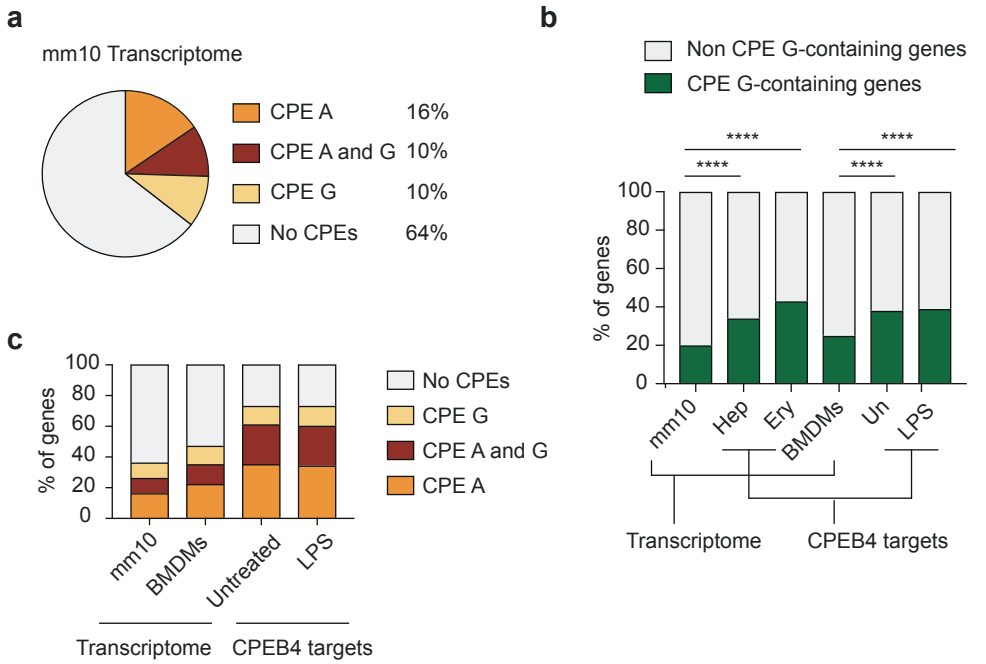

Figure 27. Analysis of CPE-G presence in CPEB4 targets. →

← **Figure 27. Analysis of CPE-G presence in CPEB4 targets. (a)** Percentage of CPE-A, CPE-G and CPE-A&G containing transcripts in *Mus musculus* transcriptome. **(b)** Percentage of CPE-G-containing transcripts in RIP-seq defined CPEB4 targets (Hep=Hepatocytes, Ery=Erythroblast, Un=Untreated) and *Mus musculus*/BMDMs transcriptome. Statistics with Chi-Square with Yates' correction.****pv<0.0001.**(c)** Percentage of CPE-A, CPE-G and CPE-A&G-containing transcripts in RIP-seq defined CPEB4 targets in macrophages and *Mus musculus*/BMDMs transcriptome.

To gain more insight into the targets that were bound by CPEB4 in untreated and LPS conditions, we performed gene ontology analysis using DAVID Bioinformatic Database (Huang et al. 2009b; Huang et al. 2009a). Interestingly, both sets of targets were enriched in MAPK signalling pathways genes **(Fig. 28a)**. Having seen that the MAPKs p38α and ERK1/2 regulate CPEB4 expression and function in this context, these results indicate that CPEB4-mediated translational control signals back to its own regulators generating a feedback regulatory circuit **(Fig. 28b)**. Inflammatory responses typically follow oscillatory patterns (Ferrell & Ha 2014b; Turner & Díaz-Muñoz 2018). For that to occur it is necessary to generate circuits where multiple positive and negative feedback loops cross-regulate each other. Therefore, it is highly relevant that CPEB4 regulates multiple of its regulators, as it will contribute to the oscillatory behaviour of gene expression during the LPS response.

Among CPEB4-regulated mRNAs, we also identified several inhibitors of the inflammatory signalling cascades, such as *Socs1*, *Socs3*, *Dusp1*, *Tnfaip3, Il1rn, Ppp2ca* or *Zfp36* (TTP mRNA) **(Fig. 28c)**. We have previously seen how CPEB4 expression and polyadenylating activity peak during the late phase of the LPS response, when inflammation resolution occurs. Therefore, these results suggest that CPEB4 could participate in inflammation resolution by promoting the expression of these anti-inflammatory molecules. Importantly, decreased expression of these proteins can lead to hyperinflammatory conditions, which have been linked to multiple diseases.

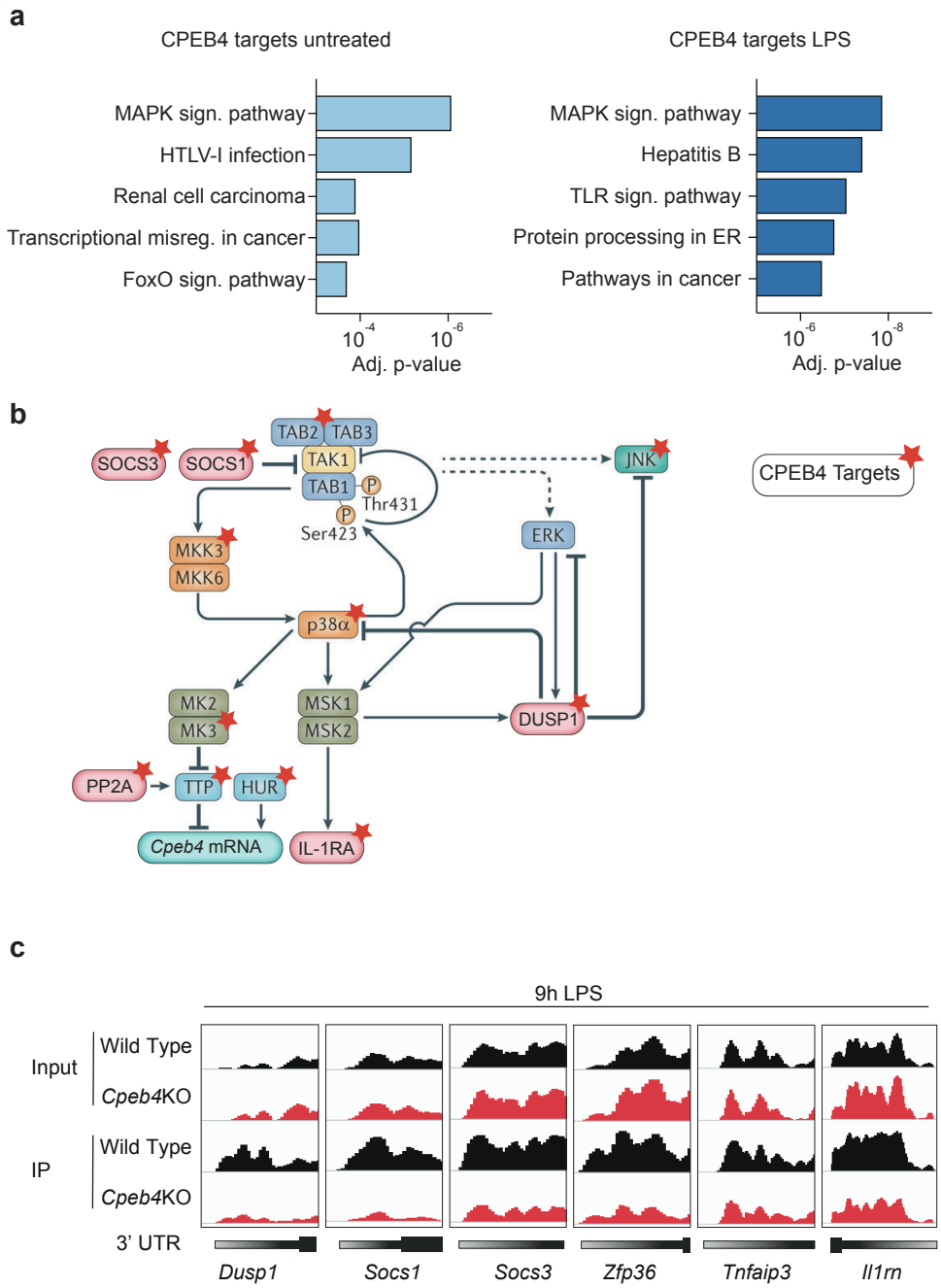

Figure 28. Inflammation feedback inhibitors are regulated by CPEB4 during the late LPS response. (**a**) Top 5 Gene Ontology KEGG categories enriched in CPEB4 targets in BMDMs (Untreated/9h LPS). Statistics with Benjamini adjusted p-value. **(b)** Schematic representation of CPEB4 targets involved in MAPK pathway. Modified from Arthur & Ley 2013. **(c)** Read coverage in Inputs and IPs of selected CPEB4 targets. Image obtained using IGV with a minimum range of 0-50 AU.

4.2. Assessing CPEB4 function in BMDMs by ribosome profiling[3]

Previous studies on CPEB4 have described how its polyadenylating function increases the translation efficiency of its target mRNAs (Ortiz-Zapater et al. 2012; Calderone et al. 2016; Maillo et al. 2017). However, not all CPEB4 targets are affected by CPEB4 function to the same extent. To describe in a genome wide manner which target mRNAs showed decreased translation efficiency rates in the absence of CPEB4 we performed ribosome profiling. As in our RIP-seq experiment, we compared wild type and *Cpeb4*KO BMDMs, in untreated conditions and after 9 hours of LPS stimulation. Ribosome profiling experiments calculate translation efficiency (TE) differences by measuring ribosome density on mRNAs. For that, ribosome-protected fragments (RPF) are isolated and ribosome abundance is corrected by the corresponding mRNA levels. Importantly, before calculating TE rates, it is necessary that the RPF libraries meet certain quality standards to ensure that the RPF isolation was successful.

With this aim, we first measured the proportion of reads aligned to the CDS and UTRs of transcripts. As expected, RPF had a much higher proportion of CDS-aligned reads than their corresponding RNAseq datasets **(Fig. 29a)**. Next, we calculated RPF length, expecting ribosomes to protect fragments between 28 and 33 nucleotides. In our case, we observed that most RPF had between 32 and 34 nucleotides, suggesting that the RNA digestion had been incomplete **(Fig. 29b)**. Finally, we measured RPF read position relative to the CDS start **(Fig. 29c)**. As expected, an increase in RPF density was found around twelve nucleotides upstream the start site, and the RPF profile was not flat but followed a three-nucleotide periodicity **(Fig. 29d)**.

[3]Ribosome profiling was performed in collaboration with dr. Vittorio Calderone. Bioinformatic analysis was perfomed in collaboration with Dr. Oscar Reina (Quality control) and Dr. Ivan Dotu (Replicates, DiffExp, DT, TE).

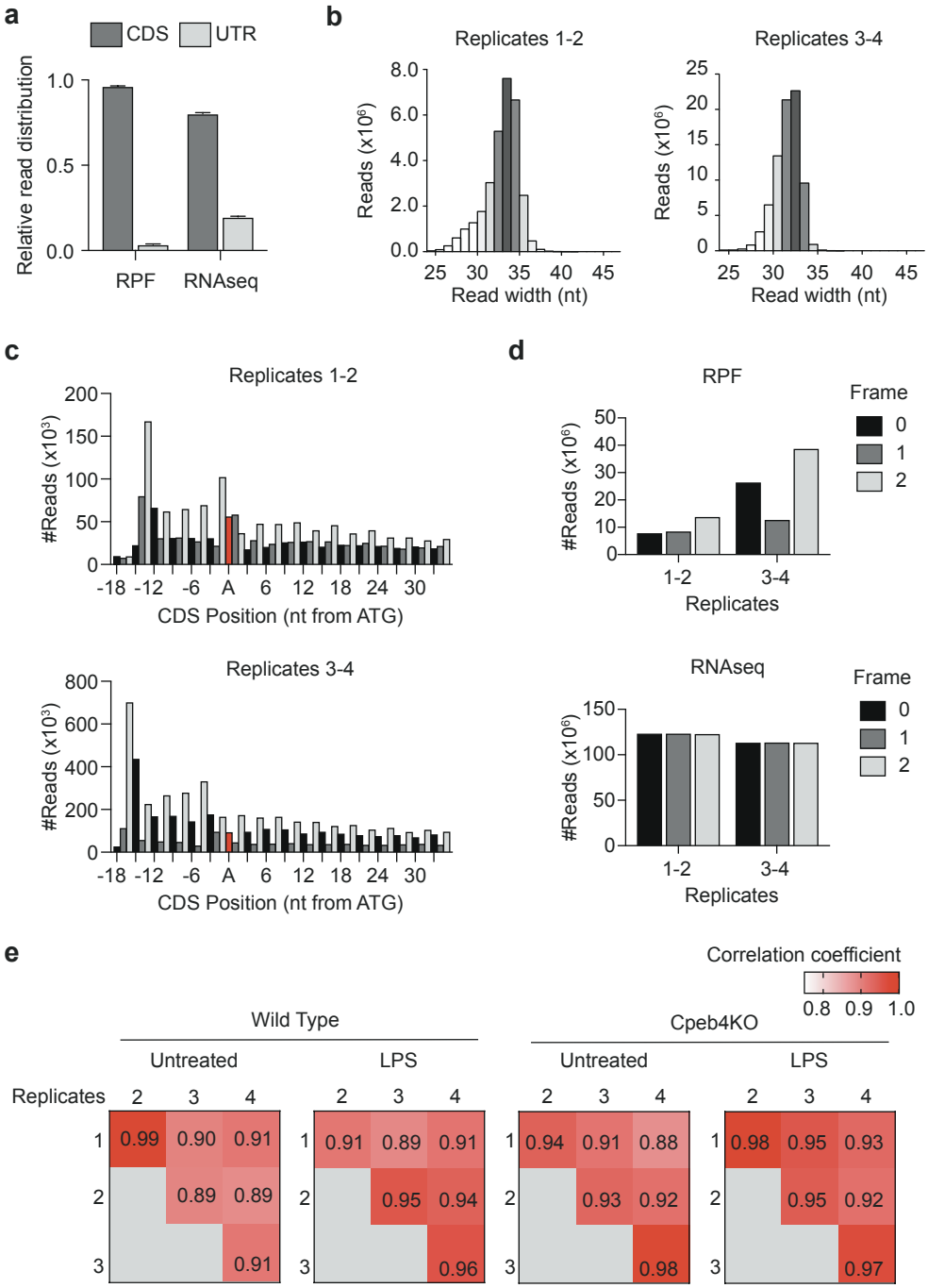

Figure 29. Ribosome profiling quality control. (a) Relative distribution of the reads obtained between the CDS and UTRs of the reads obtained by Ribosome Profiling (RPF) or RNA sequencing (RNAseq). **(b)** Size distribution of RPF reads. **(c)** Coverage around start AUG codon (A/red) of RPF data. **(d)** In-frame RPF/RNAseq read abundance. **(e)** Correlation coefficient between the different RPF replicates.

This periodicity should peak at nucleotides in codon position 0, as ribosomes stay for longer times in this position until the appropriate tRNA is charged. In our case, though, periodicity peaked at position +2, probably due to the inefficient RNA digestion. Finally, as the last quality control, we observed that the four RPF biological replicates had a good correlation coefficient **(Fig. 29e)**. Overall, these results suggest that we efficiently isolated RPF, even if some unprotected nucleotides remained undigested. Therefore, we decided to continue with the analysis and calculate the mRNA TE, as well as compare mRNA expression (RNAseq) and translation (RPF) levels between wild type and *Cpeb4*KO conditions.

Unexpectedly, in untreated conditions, only *Stard13* mRNA showed a significant decrease in TE in the absence of CPEB4 **(Fig. 30a)**. Moreover, few genes showed differential expression or translation levels between wild type and *Cpeb4*KO macrophages. As a positive control, we could find *Cpeb4* mRNA as one of the genes with significantly decreased RPF. In the same line, in LPS conditions, no mRNAs had significant TE differences and few genes displayed different expression or translation levels **(Fig. 30b).** Among those, we observed increased *Cpeb2* translation in *Cpeb4*KO macrophages, suggesting a compensatory mechanism between these two CPEBs. Crossing this data with our previously defined CPEB4 targets, we could not find any CPEB4 target that presented reduced translation efficiency rates in the absence of CPEB4 **(Fig. 30a, b)**.

On the one hand, these results suggest that CPEB4 absence does not alter substantially the macrophage gene expression landscape in untreated conditions or after 9 hours of LPS stimulation. However, considering the data we had obtained by RT-qPCR and immunoblots, these ribosome profiling results contained multiple false negatives. Thus, to further test the sensitivity of our experiment, we compared the two wild type samples, untreated and with LPS, knowing that LPS has a dramatic effect on macrophage transcriptome. Indeed, by doing this comparison, we were able to detect thousands of significant changes, both at the mRNA and RPF level **(Fig. 31a)**.

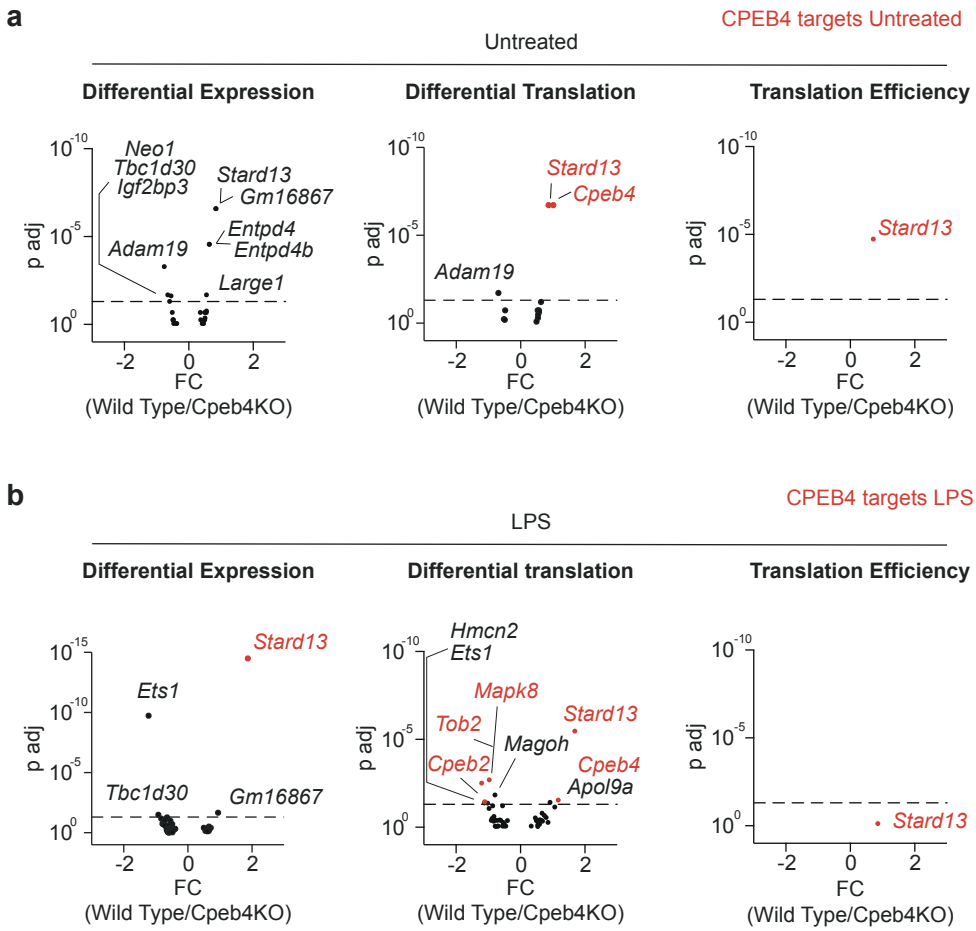

Figure 30. Few differences between wild type and *Cpeb4*KO macrophages by ribosome profiling. (a-b) Differential expression and translation analysis comparing RNAseq and RPF data from wild type and Cpeb4KO BMDMs untreated **(a)** or stimulated with LPS (10ng/ml) for 9h **(b)**. Corresponding translation efficiency data is also shown. Dashed line indicates pvalue=0.05.

As expected, *Il1rn* and *Socs3* were among the most strongly induced with LPS, as they are highly upregulated during the late LPS response to mediate inflammation resolution. Despite these major changes in expression or translation, only 6 genes showed increased translation efficiency after 9h of LPS stimulation and none of these was included in our sets of CPEB4 targets. It was remarkable though, how the TE of multiple histone mRNAs decreased upon LPS treatment, probably as part of the cell cycle arrest induced by LPS.

Next, we took advantage of this comparison to check how the expression and translation of CPEB4 targets was affected by LPS stimulation **(Fig. 31b)**. For this, we divided the mRNAs into four categories: those associated with CPEB4 only in LPS or untreated conditions, those associated in both situations and the rest of mRNAs, which are not considered CPEB4 targets. Interestingly, mRNAs associated with CPEB4 after LPS stimulation were mostly upregulated during the LPS response, both at the expression and translation level.

Altogether, these results suggested that the function of CPEB4 in macrophages, at least after 9h of LPS treatment, was most likely not related to increasing the translation efficiency of its target mRNAs. Nevertheless, we hypothesize that CPEB4 could be involved in the upregulation of its target mRNAs during the LPS response.

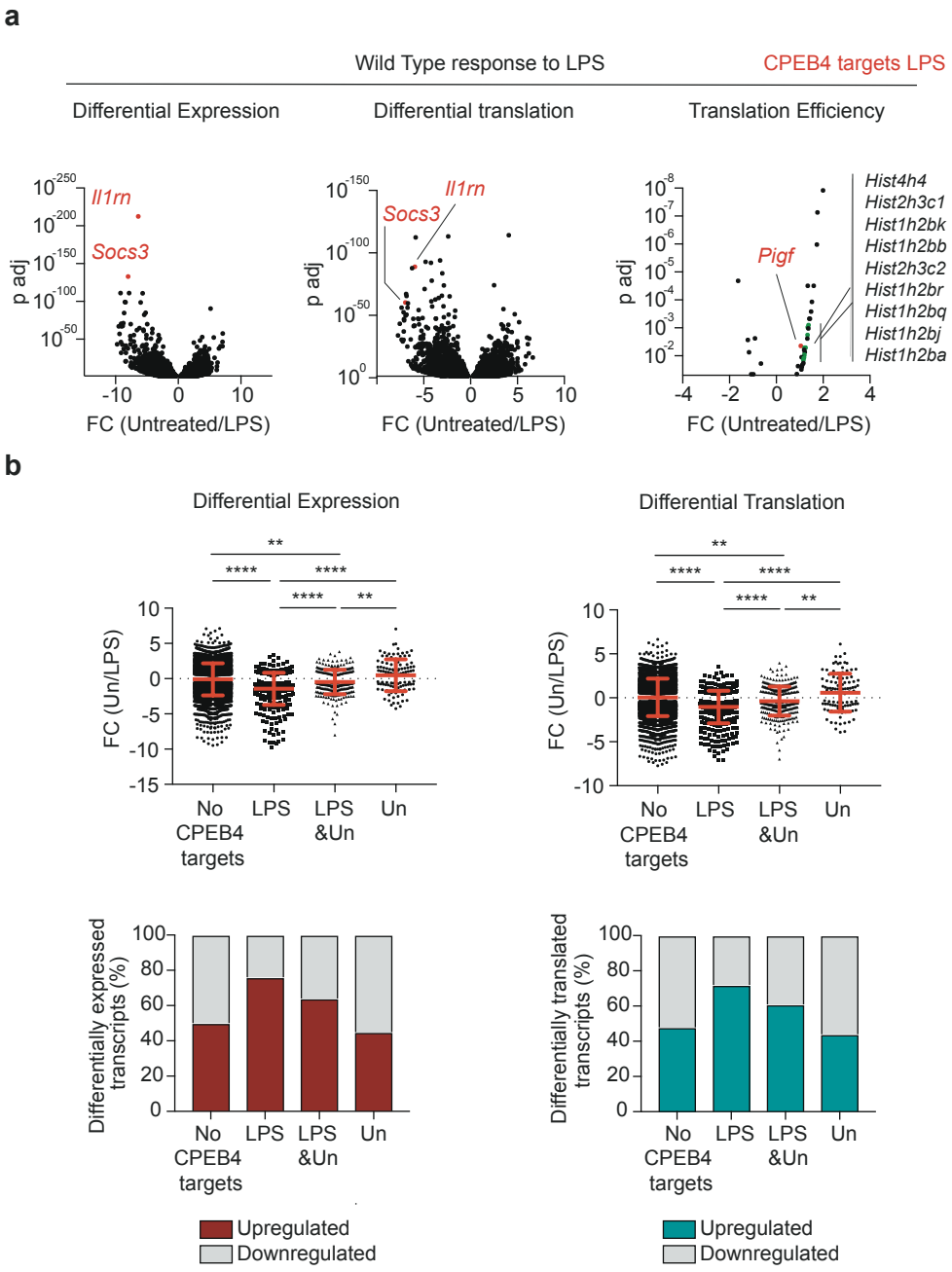

Figure 31. Main changes during the LPS response occur at the expression level. (a) Differential expression and translation analysis comparing RNAseq, RPF and TE data from wild type untreated or stimulated with LPS (10ng/ml) for 9h. Only differences with pvalue<0.05 are shown. In differential expression and translation plots, only two "CPEB4 targets LPS" are shown in red. **(b)** mRNAs in (a) were separated in four categories according to their association to CPEB4 (Un=untreated). Percentage of up/downregulated transcripts upon LPS treatment is shown.

4.3. Distinct behaviours of CPEB4 targets in Cpeb4KO BMDMs

Ribosome profiling analysis did not detect strong differences between wild type and *Cpeb4*KO macrophages. However, being aware that we had false negatives, we selected some high confidence CPEB4 targets and assessed their expression during the LPS response by RT-qPCR and immunoblot analysis. Interestingly, we observed that the expression of some of these genes was indeed affected in the *Cpeb4*KO conditions.

First, we detected a dramatic reduction in the levels of the anti-inflammatory protein SOCS1 **(Fig. 32a)**. These results were in accordance with the hypothesis that CPEB4 favours the expression of negative feedback inhibitors of the inflammatory pathways. Then, we observed a strong upregulation of the HIF1α protein, also during the later timepoints of the LPS response **(Fig. 32a)**. As HIF1α has been linked to pro-inflammatory functions, we speculated that in *Cpeb4*KO BMDMs the resolution of inflammation was impaired, causing increased levels of inflammatory markers like HIF1α. In the same line, after 9 hours of LPS we detected a reduction of TTP levels together with an increase of COX2 expression **(Fig. 32b)**. Even if these alterations were weaker, these results supported our hypothesis, since TTP and COX2 have anti- and pro-inflammatory functions, respectively. Finally, despite its anti-inflammatory function, the levels of the NF-κB inhibitor IκBα were also increased in *Cpeb4*KO macrophages **(Fig. 32b)**.

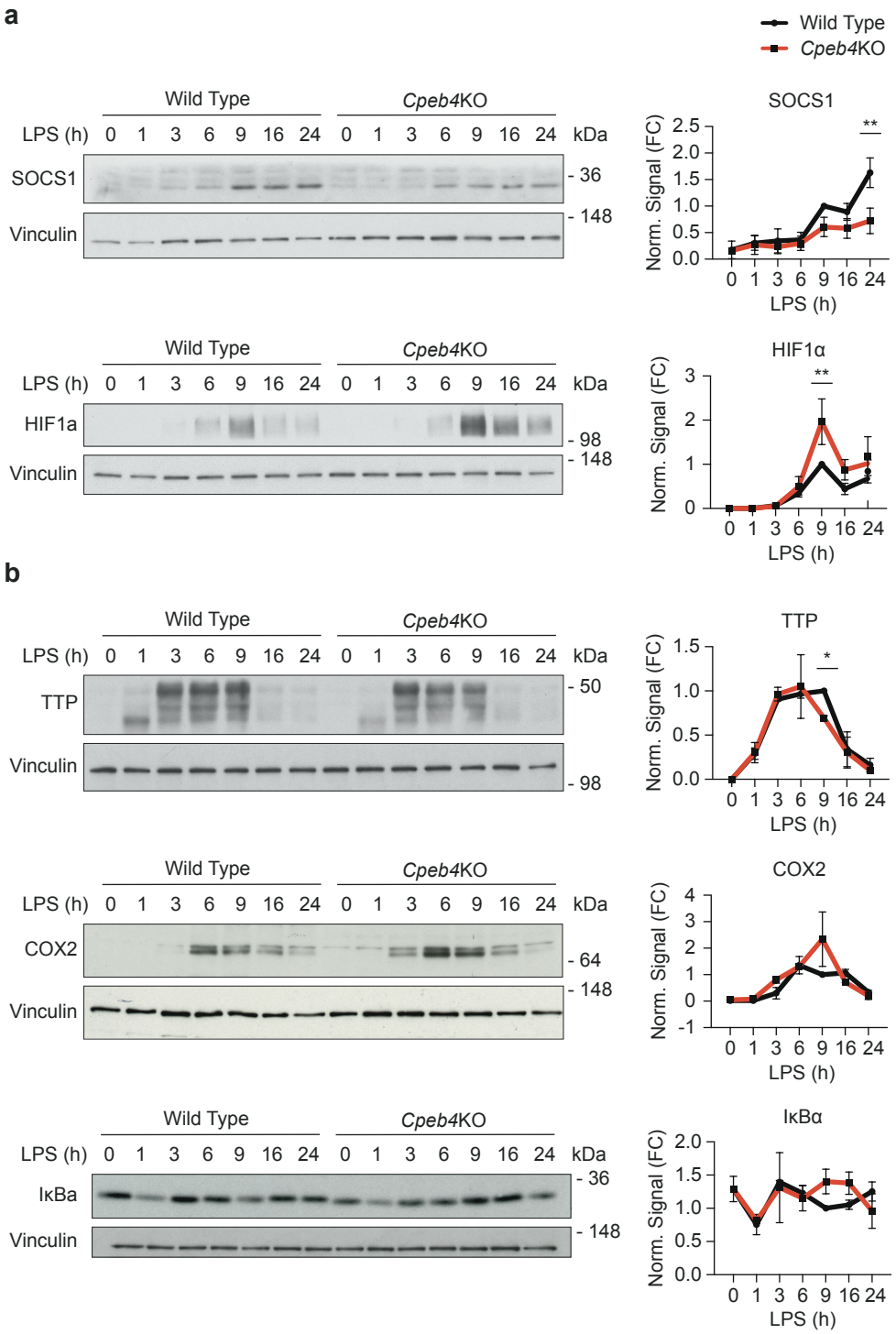

Figure 32. Altered expression of CPEB4 targets in *Cpeb4*KO BMDMs at the protein level. →

← Figure 32. Altered expression of CPEB4 targets in *Cpeb4*KO BMDMs at the protein level. (**a-c**) Immunoblot analysis of the indicated proteins in wild type or *Cpeb4*KO BMDMs treated with LPS for 0-24h. Vinculin served as loading control. Signal intensity was normalized to wild type 9h LPS. Data from duplicate (TTP, IκBα, COX2; Statistics: multiple t-test) and triplicate (SOCS1, HIF1α; Statistics: Two way ANOVA) experiments. *pv<0.05; ** pv<0.01.

Next, we measured the expression of the corresponding mRNAs, to understand if these changes were occurring at the mRNA level or resulted from translation efficiency rates. As shown in **figure 33a**, alterations in mRNA of *Socs1* and *Hif1a* could explain their altered protein expression. On the contrary, levels of TTP, COX2 and IκBα mRNAs (*Zfp36*, *Ptgs2* and *Nfkbia*, respectively) were overall comparable between wild type and *Cpeb4*KO macrophages **(Fig. 33b)**. Thus, these results suggest that the expression of SOCS1 and HIF1α was dysregulated at the mRNA level, while for TTP, COX2 and IκBα this process occurred at their TE rates. Importantly, as we had seen in the ribosome profiling data, differences were much stronger in mRNA expression than in translation rates.

Consequently, we decided to focus on how CPEB4 polyadenylating function regulated the expression of mRNAs like *Socs1* or *Hif1a*. First we considered that, to explain the dual behaviour of these targets, other proteins need to be involved in their alterations. These could be for instance transcription factors or regulators of the mRNA stability.

As previously mentioned, TTP is one of the major regulators of mRNA stability during the LPS response. Moreover, both *Socs1* and *Hif1a* mRNAs were considered TTP targets in Sedlyarov datasets (Sedlyarov et al. 2016). Having seen that TTP and CPEB4 cross regulate each other mRNAs, we hypothesized that the phenotypes we were observing in *Cpeb4*KO macrophages could be caused by a disruption in the interplay between these two proteins, which could affect the stability and levels of mRNAs like *Socs1* and *Hif1a*.

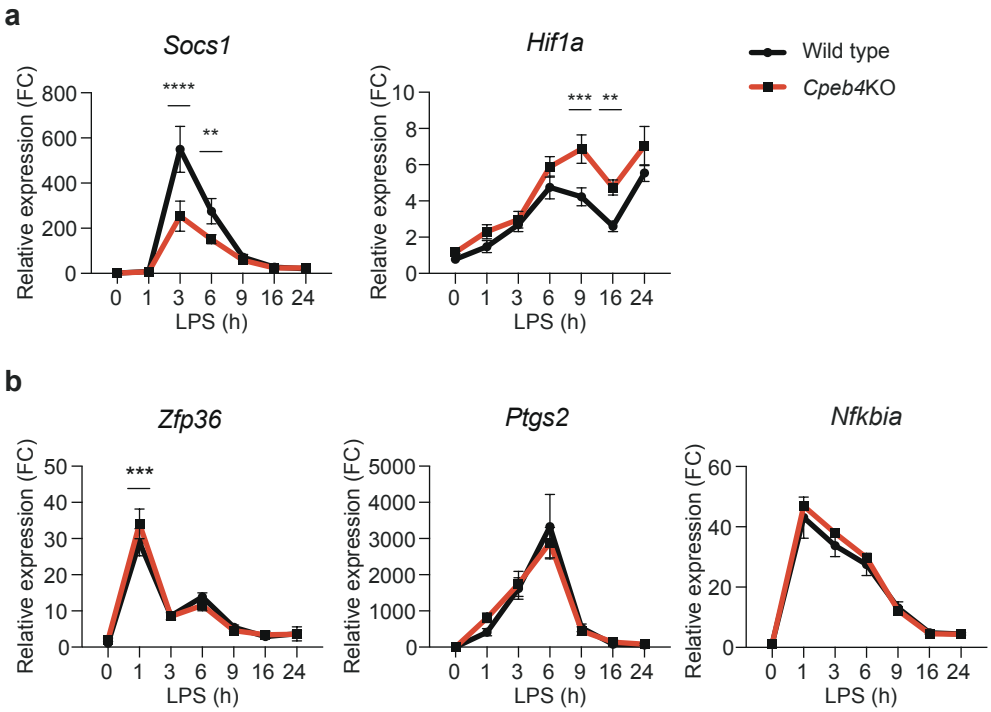

Figure 33. Altered mRNAs levels of CPEB4 targets in *Cpeb4*KO BMDMs. (a-b) Wild type or *Cpeb4*KO BMDMs were stimulated with LPS (10ng/ml) for 0-24h and mRNA was measured. *Tbp* was used to normalize and relative levels to untreated wild type were calculated. Data are shown as mean and s.e.m.; n=6. Statistics: Two-way ANOVA **pv<0.01; *** pv<0.001; ****pv<0.0001.

4.4. Interplay between CPEB4 and TTP during the LPS response

At this moment, it is worth recapitulating the information we have seen so far. We have shown that CPEB4 is upregulated and phosphorylated during the late LPS response **(Fig. 25)**, which has been shown to promote its polyadenylating function (Guillén-Boixet et al. 2016). Moreover, we have seen how TTP-mediated mRNA destabilization is recovered during the late phase of inflammation. Mechanistically, TTP recruits the CCR4-NOT complex to its target mRNAs, promoting their deadenylation and consequent destabilization (Lykke-Andersen & Wagner 2005). Additionally, our ribosome profiling data suggests that, between untreated and 9 hours of LPS stimulation, gene expression changes mostly occur at the mRNA level but not at translation efficiwency. And finally, most CPEB4 targets are upregulated during this timing of the LPS response.

Taking all these observations together, we hypothesized that, as opposed to TTP action, CPEB4 polyadenylating function could be favouring mRNA stability instead of mRNA TE in this context. If true, it seemed also possible that during the late LPS response, when both TTP and CPEB4 are active, their opposite deadenylating and polyadenylating functions could compete to regulate target mRNAs that they have in common.

It is important to mention that during meiosis progression a similar situation was described for CPEB1 and C3H4, another ARE-BP that recruits the CCR4-NOT complex. In this case, their opposite polyadenylating and deadenylating functions determined the kinetics of translational activation of mRNAs upon progesterone stimulation (Belloc et al. 2008; Belloc & Méndez 2008). Moreover, it was recently shown how in LPS-stimulated macrophages, TTP binding to mRNAs was not always related to mRNA destabilization. In some cases, the competition with HuR for these mRNAs could explain this behaviour, but other factors were needed to explain mRNA kinetics during the LPS response (Sedlyarov et al. 2016).

4.4.1. Key genes of the inflammatory response are regulated by TTP and CPEB4

To study the possible interplay between TTP and CPEB4, the first question we addressed was if these two RNA binding proteins shared common target mRNAs during the late LPS response. Thus, we compared our set of CPEB4 targets in the presence of LPS with the iCLIP-defined TTP targets defined by Sedlyarov and colleagues **(Fig. 34a)** (**Appendix III,** Sedlyarov et al. 2016). Interestingly, we found that CPEB4 was associated with 50% of TTP targets **(Fig. 34b)**. Among the common regulated genes, we found crucial inflammatory mediators, like *Il6*, *Il1a*, *Cxcl1* or *Nos2*, but also multiple of the previously mentioned negative feedback inhibitors, like *Socs3*, *Dusp1* or *Il1rn*. Remarkably, not only *Socs1* and *Hif1a*, but also *Zfp36*, *Ptgs2* and *Nfkbia* were targets of both CPEB4 and TTP. Thus, this was a common feature of all the mRNAs whose proteins were altered in *Cpeb4*KO macrophages.

a

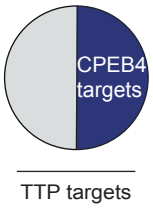

b

Abcc1	*Cflar*	*Fam49b*	*Mapk6*	*Peli1*	*Slfn5*	*9530068E07Rik*
Anxa5	*Cmtm6*	*Fos*	*Marcks*	*Pim3*	*Socs1*	*D1Ertd622e*
Arf4	*Cpd*	*Gch1*	*Mcl1*	*Plaur*	*Socs3*	
Arl8a	*Cpne3*	*Golga7*	*Mdm2*	*Plek*	*Spred1*	
Bcl10	*Csf3*	*H2-T24*	*Mmp13*	*Ppp3r1*	*Stx7*	
Ccdc50	*Csrnp1*	*Hif1a*	*Mxd1*	*Ptgs2*	*Tiparp*	
Ccl2	*Cxcl1*	*Ifit2*	*Myadm*	*Pvr*	*Tmem2*	
Ccl3	*Cxcl10*	*Il12b*	*Myl12a*	*Rab18*	*Tnfaip3*	
Ccl7	*Cxcl2*	*Il1a*	*Myl12b*	*Rbm33*	*Tns3*	
Ccng2	*Dusp1*	*Il1rn*	*Nos2*	*Rhob*	*Tor1aip1*	
Ccrl2	*Dusp11*	*Il6*	*Notch1*	*Serpine1*	*Tpm4*	
Cd274	*Edn1*	*Ldlr*	*Nt5c3*	*Sfmbt1*	*Txnrd1*	
Cd44	*Ets2*	*Lpl*	*Papd7*	*Sgk3*	*Ywhaz*	
Cd69	*Etv6*	*Maf*	*Pcgf3*	*Slc16a10*	*Zfp36*	
Cdkn1a	*Evl*	*Mafk*	*Pde4b*	*Slc4a7*	*Zfp36l2*	

Figure 34. Overlap between CPEB4 and TTP target mRNAs during late LPS response. (a-b) TTP targets (184 mRNAs) were defined by iCLIP in BMDMs treated for 6h with LPS (10ng/ml) (Sedlyarov et al. 2016). CPEB4 targets (1782 mRNAs) were defined by RIP-seq after 9h of LPS treatment. LPS (10ng/ml). Pie chart shows the % of TTP targets that are also considered CPEB4 targets. **(b)** List of common TTP and CPEB4 regulated mRNAs.

Next, to further study TTP and CPEB4 interplay, we selected some of these common target mRNAs and assessed their expression during the LPS response in TTPMKO and *Cpeb4*KO conditions **(Fig. 35a-d)**. Although there were some exceptions, we could observe consistent trends in their behaviours. The expression of a first group of genes, including *Cxcl1*, *Cxcl2* and *Il1a*, showed significant alterations in TTPMKO macrophages but not in *Cpeb4*KO **(Fig. 35a)**. Genes in the second group were affected in both KOs, but we could distinguish two patterns. While *Ccl2* and *Il6* were affected at overlapping timepoints **(Fig. 35b)**, *Socs3* and *Nos2* presented alterations at different moments in each KO **(Fig. 35c)**. Finally, the third group included *Hif1a* and *Socs1*, which showed a surprising behaviour in TTPMKO BMDMs. Instead of being upregulated, as one would expect in the absence of TTP-destabilizing activity, they were downregulated or unaffected **(Fig. 35d)**. Interestingly, these were the genes that were more altered in *Cpeb4*KO conditions **(Fig. 33a)**. On the one hand, these observations suggest that not all common mRNAs are subjected to the same extent to TTP- and/or CPEB4-mediated control. On the other hand, the observed inverse correlation between the alterations in each KO suggested that the mRNAs that are highly regulated by one of these proteins are not subjected anymore to control by the other. Thus, these results strengthen the hypothesis that TTP and CPEB4 compete to regulate their common mRNA targets.

Additionally, it also drew our attention to the fact the peak of expression after LPS also tended to correlate with the alterations we observed. While early expressed genes tended to be more affected by TTP absence, intermediate and late genes were generally altered in both TTP- and CPEB4-KO conditions. Interestingly, this pattern mirrored CPEB4 regulation as CPEB4 protein levels and activity peak during the late LPS response.

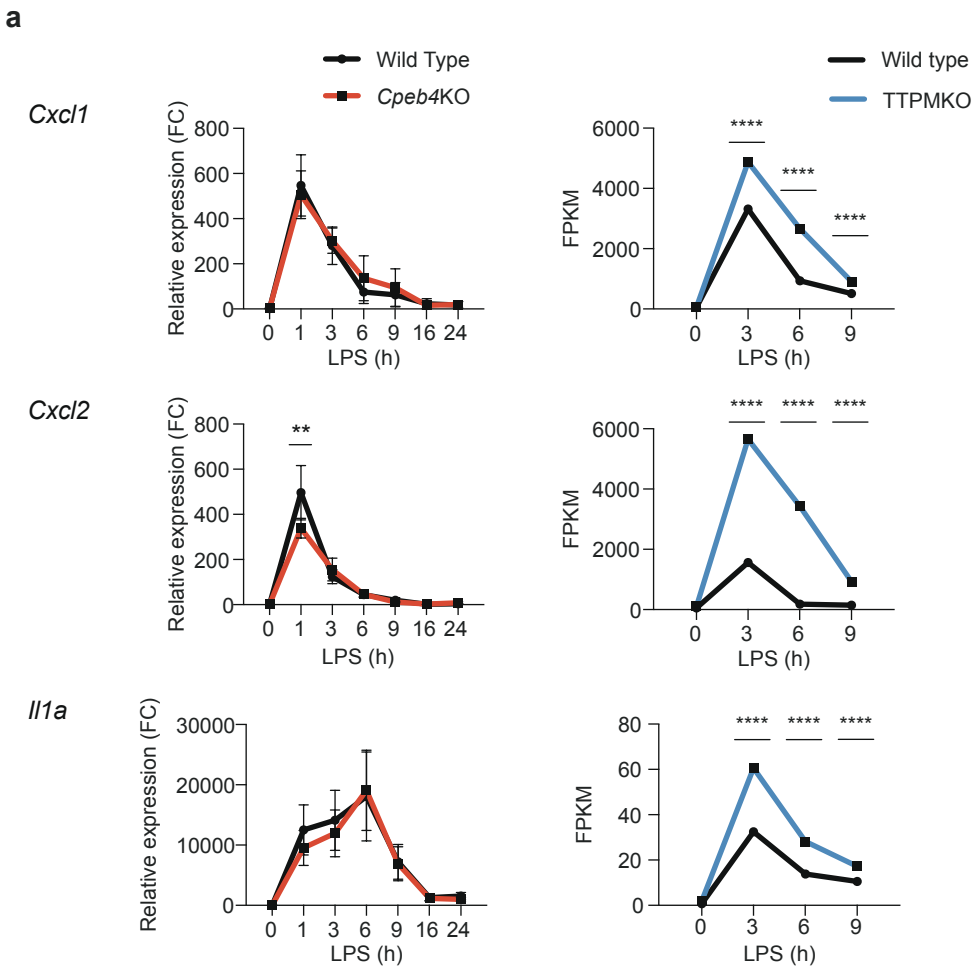

Figure 35. Opposite alterations in LPS response in TTPMKO and *Cpeb4*KO BMDMs. (a) Overlap between TTP target and CPEB4 target mRNAs in BMDMs after 6h or 9h of LPS stimulation, respectively. **(b-e)** Wild type or *Cpeb4*KO BMDMs were stimulated with LPS (10ng/ml) for 0-24h and mRNA was measured by RT-qPCR. *Tbp* was used to normalize and relative levels to untreated wild type were calculated. Data are shown as mean and s.e.m.; n=6. Statistics: Two-way ANOVA *pv<0.05; **pv<0.01; *** pv<0.001; ****pv<0.0001. Wild type or TTPMKO BMDMs were stimulated with LPS (10ng/ml) for 0-9h, mRNA was isolated and sequenced. Expression is shown as mean FPKM. Statistics: *qv<0.05; **qv<0.01; *** qv<0.001; ****qv<0.0001. Source TTPMKO expression and statistics: Sedlyarov et al. 2016. →

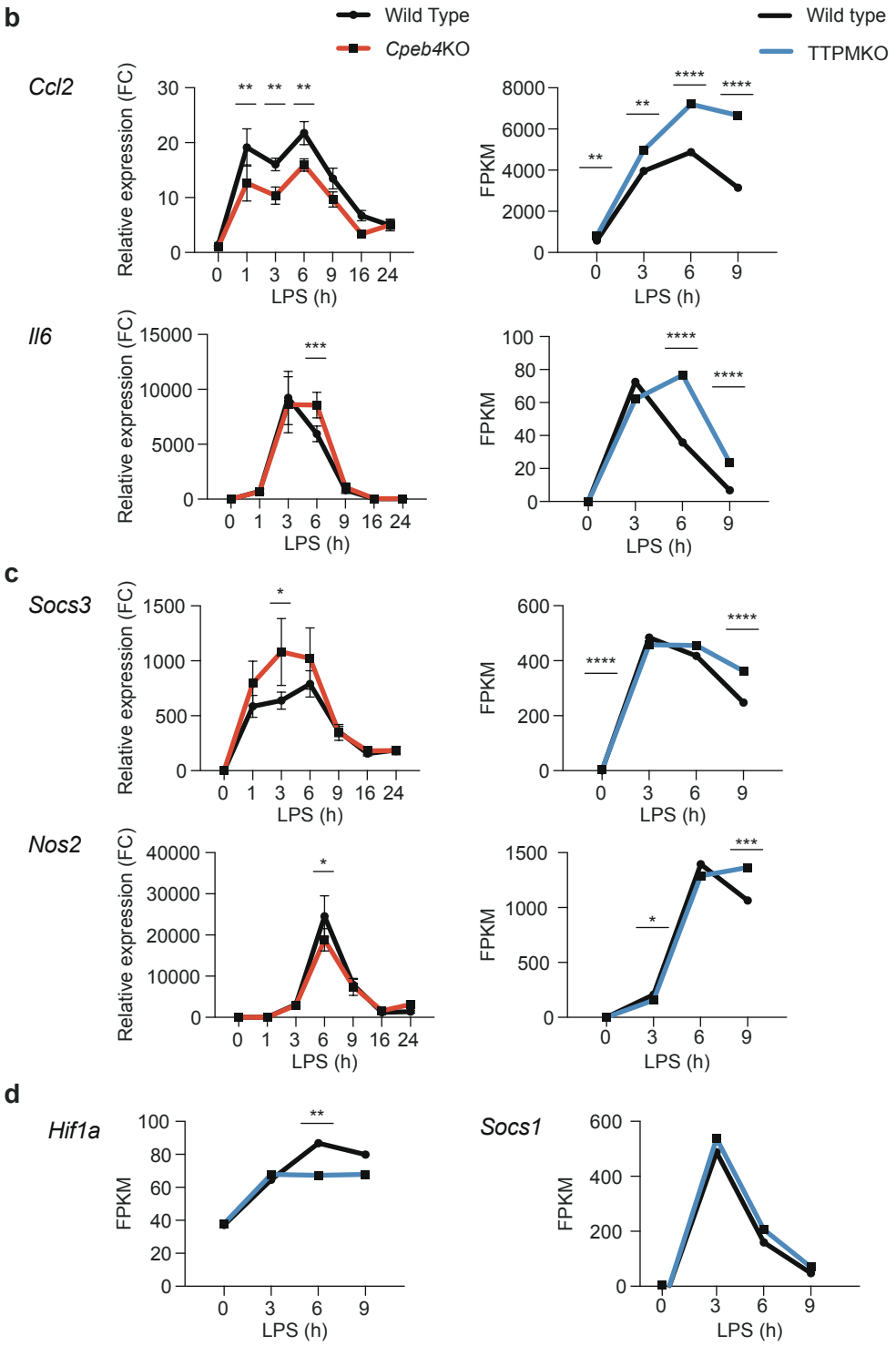

Figure 35. Opposite alterations in LPS response in TTPMKO and *Cpeb4*KO BMDMs. ←

4.4.2. An ARE/CPE score predicts mRNA behaviour during the LPS response

In section 2, we have seen how the competition of HuR and TTP for ARE-containing mRNAs regulates *Tnf* and *Cpeb4* expression upon LPS stimulation. Moreover, results in section 4.4.1. suggest that during the late LPS response, CPEB4 and TTP also compete for their target mRNAs. These two processes lead us to hypothesize that the combined regulation of these three RNA binding proteins, and their corresponding effects on mRNA stability, could be key to determine the expression profiles of multiple mRNAs during the LPS response.

To test this idea we decided not to use our RIP-seq data of CPEB4 targets or the published sets of TTP- and HuR-targets, as they were restricted to certain timepoints, and also subjected to experimental limitations. Alternatively, we thought that the strength and number of AREs and CPEs present in a given mRNA could be key to determine if this mRNA is more susceptible of being regulated by HuR and TTP, by CPEB4 or by all three of them. Therefore, as a first approach, we decided to calculate an ARE/CPE score for multiple mRNAs and check if mRNAs with similar scores clustered in similar expression patterns.

Thus, we selected 62 mRNAs known to be upregulated during the LPS response and calculated their ARE/CPE score. Briefly, this ARE/CPE score was based on the total number of AREs and CPEs in the 3'UTR of each mRNA, considering the transcript with longest 3'UTR for each gene **(Fig. 36a)**. Of the 61 mRNAs, 13 were considered to be CPE-dominant (score<-1) and 14 ARE-dominant (score>0.8), leaving 34 mRNAs in the intermediate category **(Fig. 36b, Appendix IV)**. Taking advantage again of the publication of Sedlyarov *et al.*, we looked for the expression levels of these mRNAs in wild type BMDMs after 0, 3, 6 and 9 hours of LPS treatment. After normalizing each gene to its peak of expression, we calculated the expression pattern of each category as the mean of all the included genes. Interestingly, as seen in **figure 36c**, each mRNA category presented a significantly different expression pattern, which was consistent with the expression and regulation of HuR, TTP and CPEB4 during the LPS response. For example, the expression of ARE-dominant genes like *Cxcl1*, *Tnf* and *Il10*, peaked at 3h and was rapidly downregulated, a process that was probably mediated by the action of HuR and

TTP, respectively. Alternatively, CPE-dominant mRNAs like *Cpeb4*, *Nfkbia* or *Il1rn*, presented a later upregulation and a more sustained expression during the late LPS response, resembling CPEB4 activity. Finally, intermediate genes showed features of both groups, as they were upregulated at early timepoints but also showed sustained expression at 9 hours. Examples of this category are *Il6*, *Hif1a* or *Socs3* mRNAs. Altogether, these results show how the combination of CPEs and AREs is key to define the expression pattern of crucial players of the LPS response.

Additionally, the categories obtained with the ARE/CPE score helped us to explain why some CPEB4 or TTP targets are not altered in the expected direction upon the depletion of these proteins. For example, we have seen previously that *Cxcl1* and *Cxcl2* are highly upregulated in TTPMKO macrophages but unaltered in *Cpeb4*KO **(Fig. 35a)**. These two mRNAs belong to the ARE-dominant category and, consequently, they are not altered in CPEB4 absence because they are mainly regulated by TTP. Accordingly, *Tnf* and *Il10* also follow the same pattern **(Fig. 23e, 37a)**. On the contrary, the CPE-dominant category included the two mRNAs that were more dramatically downregulated in *Cpeb4*KO conditions, *Ccl2* and *Socs1* **(Fig. 34a, 36c)**. Finally, although the data in *Cpeb4*KO conditions is not available yet, we confirmed that other ARE- or CPE-dominant mRNAs behaved as expected in TTPMKO conditions **(Fig. 37b)**.

Importantly, this result suggest that CPEB4 polyadenylating function could be responsible for the stabilization and expression of CPE-dominant mRNAs, a function that has never shown for CPEB4. Moreover, all these observations establish a link between the ARE/CPE score and the specific functions of TTP and CPEB4. Thus, they support that these proteins are indeed responsible for defining the different expression waves of the LPS response **(Fig. 36c)**.

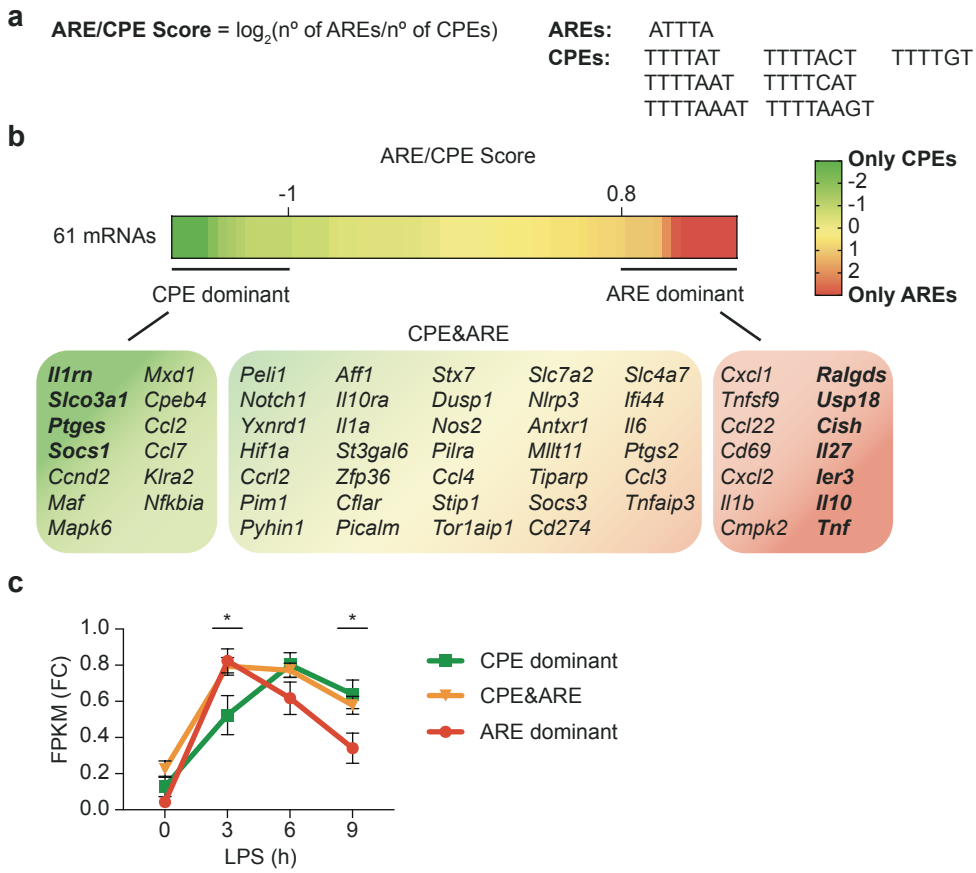

Figure 36. An ARE/CPE score can predict mRNA expression pattern during the LPS response. **(a)** Formula to calculate the ARE/CPE score. The number of AREs/CPEs was assessed on the transcript with the longest 3'UTR. **(b)** 61 mRNAs were divided in three categories based on the ARE/CPE score. mRNAs in bold only had CPEs or AREs in their 3'UTRs. **(c)** Wild type BMDMs were stimulated with LPS (10ng/ml) for 0-9h, mRNA was isolated and sequenced. Expression data was normalized to each peak of expression and the of the 62 mRNAs were clustered as shown in (b). Data are shown as mean and s.e.m. Statistics: Two-way ANOVA *pv<0.05; **pv<0.01. Statistics in graph compare CPE dominant Vs ARE dominant. Additional significant comparisons: 3h pv** (CPE dominant Vs CPE&ARE); 9h pv* (ARE dominant Vs CPE&ARE). Source expression data: Sedlyarov et al. 2016.

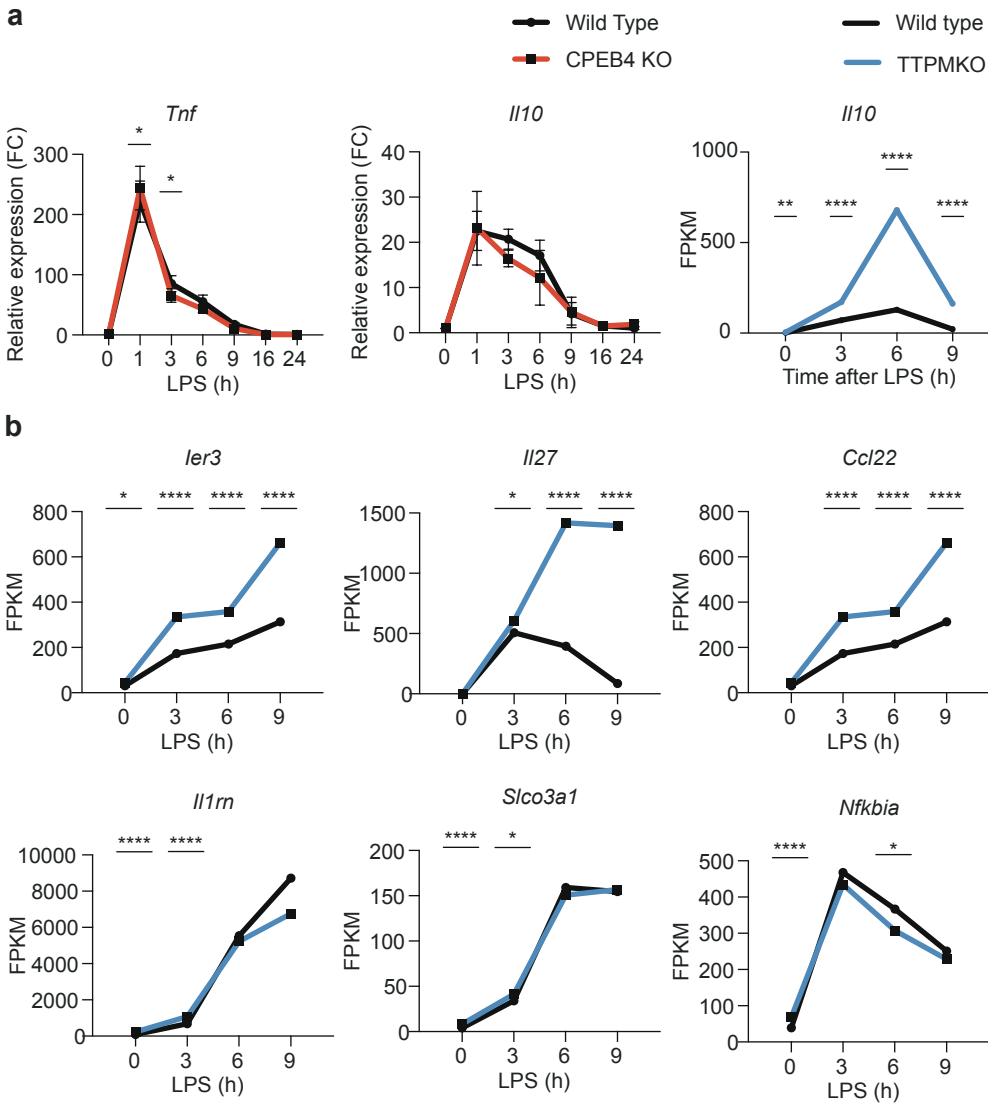

Figure 37. ARE-dominant mRNAs showed increased dependency on TTP-mediated decay. (a) Wild type or *Cpeb4*KO BMDMs were stimulated with LPS (10ng/ml) for 0-24h and mRNA was measured by RT-qPCR. *Tbp* was used to normalize and relative levels to untreated wild type were calculated. Data are shown as mean and s.e.m.; n=6. Statistics: Two-way ANOVA *pv<0.05. **(a-b)** Wild type or TTPMKO BMDMs were stimulated with LPS (10ng/ml) for 0-9h, mRNA was isolated and sequenced. Expression is shown as mean FPKM. Statistics: *qv<0.05; **qv<0.01; *** qv<0.001; ****qv<0.0001. Source TTPMKO expression and statistics: Sedlyarov et al. 2016.

4.5. Transcriptional control of the LPS response in *Cpeb4*KO BMDMs

As previously mentioned, the observed alterations at the mRNAs level in *Cpeb4*KO macrophages could also have been caused by alterations in transcriptional rates. Thus, we assessed the activity of NF-κB and STAT1, the main factors regulating *Hif1a* and *Socs1* transcription, respectively.

To assess NF-κB activity, we performed immunofluorescence against the p65 subunit and evaluated its nuclear localisation. In untreated conditions, NF-κB is retained in the cytoplasm by its inhibitor IκBα. LPS stimulation triggers IκBα degradation, allowing NF-κB nuclear shuttling. However, once in the nucleus, NF-κB limits its own activity by promoting the transcription of *Nfkbia* (IκBα mRNA). In this way, IκBα levels are restored and NF-κB is retained again in the cytoplasm (Kawasaki & Kawai 2014). As expected, 1h after LPS treatment p65 nuclear levels increased, and this was partially reverted at 9h **(Fig. 38a)**. Even if this process occurred in a similar manner in wild type and *Cpeb4*KO conditions, we observed a slight but significant reduction of p65 nuclear levels in *Cpeb4*KO BMDMs 1h after LPS exposure, and a similar tendency at 9h. We had seen previously how *Cpeb4*KO macrophages expressed increased levels of IκBα protein after 9-16h of LPS treatment **(Fig. 32b)**. Therefore, the reduction in NF-κB nuclear localization could be explained by an increased cytoplasmic retention mediated by IκBα.

To assess STAT1 activation, we measured P-STAT1 levels and detected that *Cpeb4*KO BMDMs presented decreased levels during the late LPS response, especially after 9 hours of LPS treatment **(Fig. 36b)**.

These results suggest that *Cpeb4* absence in macrophages may also affect their transcriptional landscape. However, we had not observed a global decrease in the mRNA levels of their controlled genes. Therefore, further experiments are needed to define the functional relevance of these two reductions.

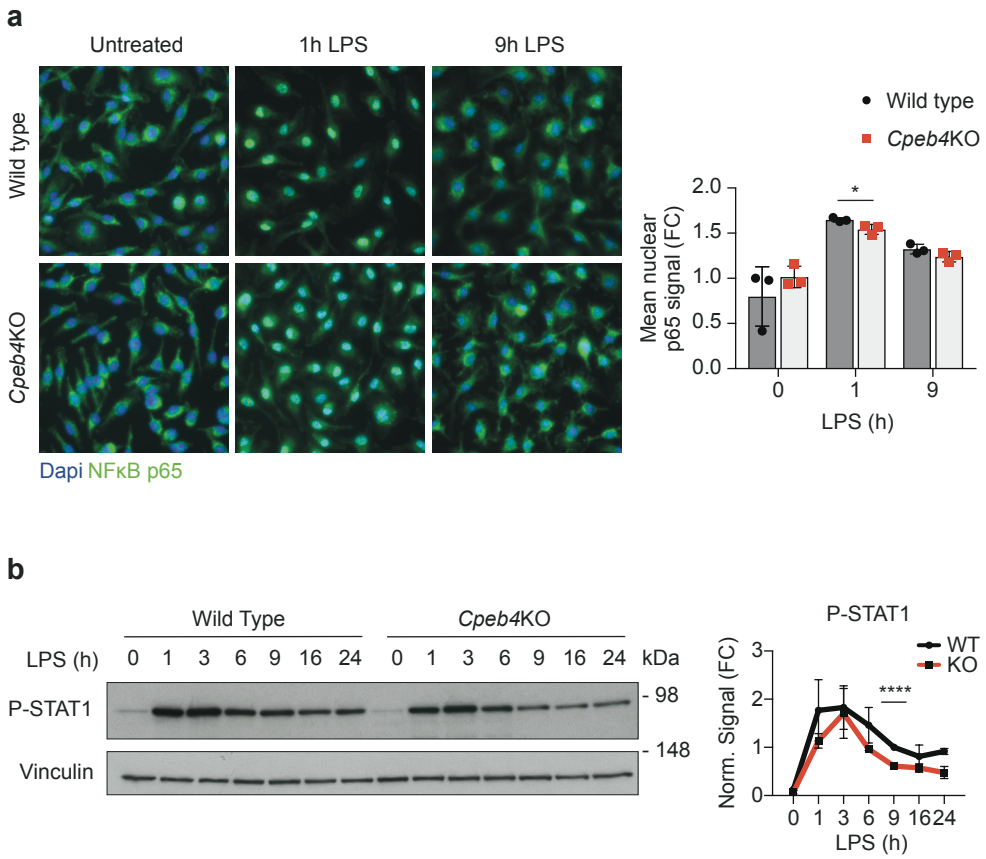

Figure 38. Transcriptional alterations in *Cpeb4*KO BMDMs. (a) p65 NF-kB immunofluorescence (green) of wild type or *Cpeb4*KO BMDMs stimulated with LPS (10ng/ml) for 0-1-9h. Nuclear localization was assessed by comparing with DAPI (blue). Mean nuclear intensity signal for each animal is shown, >100cells/animal/condition. Statistics: Welch's t test *pvalue<0,05 **(b)** Immunoblot analysis of P-STAT1 in wild type or *Cpeb4*KO BMDMs treated with LPS for 0-24h. Vinculin served as loading control. Normalized signal intensity is shown as FC to untreated wild type. Data are shown as mean and s.e.m. of duplicate experiments. Statistics: Multiple t-test **** pv<0.0001.

5. CPEB4 function in quiescent BMDMs

In addition to study CPEB4 function during the LPS response, we also characterized whether CPEB4 contributed to macrophage basal homeostasis. As previously mentioned, to obtain BMDMs we culture bone marrow hematopoietic progenitors in media containing M-CSF. This factor not only induces progenitors cells to differentiate into macrophages but also stimulates their proliferation. As shown in **figure 39a**, during this process CPEB4 was also transiently upregulated. In this context, CPEB4 upregulation occurred when macrophages were highly proliferative, according to CyclinD1 expression **(Fig. 39a)**. Thus, we hypothesized that CPEB4 expression was linked to its function during mitotic cell-cycle progression (Novoa et al. 2010). However, we did not observe differences in the number of cells obtained from wild type or *Cpeb4*KO progenitors (data not shown).

Next, we decided to assess if CPEB4 contributed to macrophage differentiation. For this, we analysed the expression of different myeloid markers by flow cytometry. Interestingly, *Cpeb4*KO BMDMs tended to express higher levels of the major histocompatibility complex class II (MHC class II) **(Fig. 39b)**. MHC class II expression in macrophages is mainly driven by the transcription factor CIITA (Ting & Trowsdale 2002; LeibundGut-Landmann et al. 2004). Hence, we measured *Ciita* mRNA levels as well as the mRNAs of the MHC class II subunits I-A and I-E. Again, all of these were upregulated in *Cpeb4*KO conditions **(Fig. 39c)**, suggesting that the increase in MHC class II levels in *Cpeb4*KO BMDMs was caused by an increase in CIITA-mediated transcription.

Neither *Ciita* nor MHC class II mRNAs were CPEB4 targets according to our RIP-seq experiment **(Appendix I)**, suggesting that CPEB4 depletion affected the expression of these proteins in an indirect manner. Therefore, we looked in the literature which mechanisms had been described to regulate *Ciita* expression. Out of these mechanisms, Histone Deacetylase 1 (HDAC1) seemed a good candidate to explain our phenotype. HDAC1 is an enzyme that catalyses the removal of acetyl groups. Among other functions, it can trigger histone deacetylation, an epigenetic mark that has been linked to chromatin repression (Shakespear et al. 2011).

Through this mechanism, HDAC1 has been shown to inhibit *Ciita* expression, consequently affecting MHC class II levels (Zika et al. 2003; Cycon et al. 2013). Interestingly, we found that *Hdac1* mRNA is associated with CPEB4 in untreated conditions **(Fig. 39d)**. Thus, we hypothesize that by polyadenylating *Hdac*1, CPEB4 could favour HDAC1 expression, which limits *Ciita* and MHC class II levels.

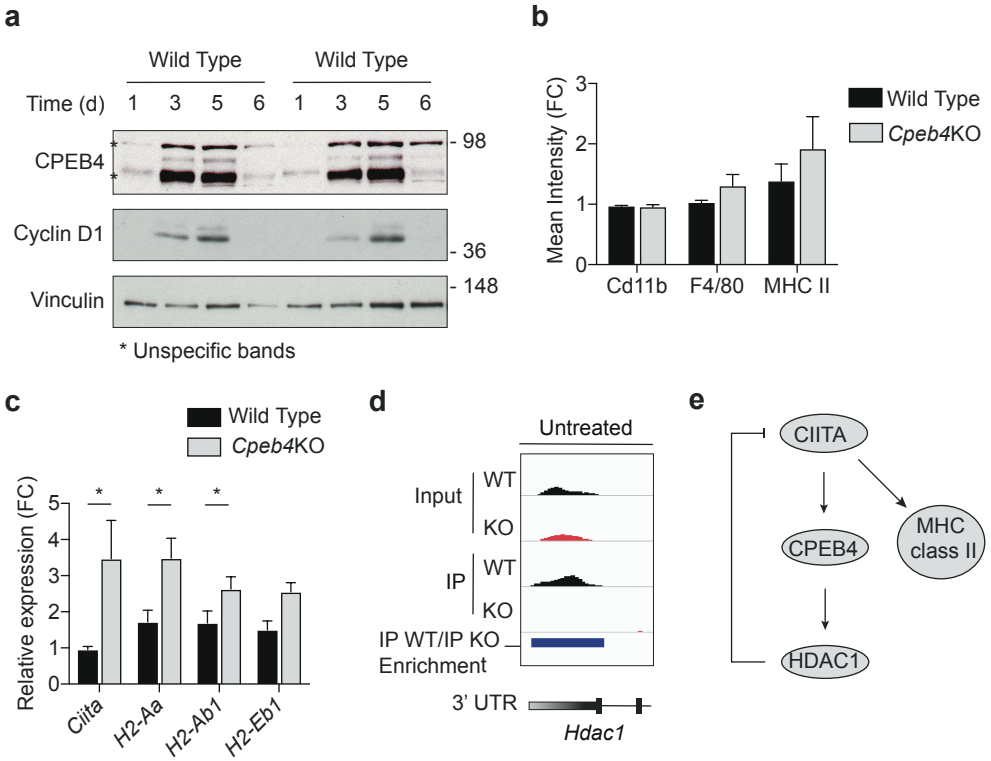

Figure 39. Increased MHC class II expression in *Cpeb4*KO BMDM. (a) Immunoblot analysis of CPEB4 and CyclinD1 during the differentiation of Bone Marrow Progenitor cells to BMDMs in the presence of M-CSF (time is indicated in days). Two biological replicates are shown. Vinculin was used as a loading control. **(b)** Mean expression of myeloid markers was analysed by flow cytometry. Mann-Whitney t-test. **(c)** Gene expression of unstimulated BMDMs obtained from Wild type or *Cpeb4*KO was analysed by RT-qPCR. *Tbp* was used to normalize and relative levels to untreated wild type were calculated. Data are shown as mean and s.e.m.; n=6. Statistics: Wilcoxon match-pairs signed rank test *pv<0.05 **(d)** Read coverage of *Hdac1* mRNAs in RNAseq (Input) or RIP-seq samples (IP). Peak enrichment in wild type (WT) versus *Cpeb4*KO (KO) IP is shown. Image obtained using integrated genomic viewer (IGV) with a range of 0-30 arbitrary units (AU). **(e)** Diagram representing a possible model for CPEB4 regulation of MHC class II expression in unstimulated BMDMs.

Additionally, while studying this mechanism, we found that in a lymphoblast cell line, it had been described that CIITA was associated to Cpeb4 promoter, possibly regulating its expression (Scharer et al. 2015; Kuleshov et al. 2016). Thus, we could establish a regulatory circuit between CIITA, HDAC1 and CPEB4. In this case, CIITA would induce the expression of CPEB4, which by promoting the upregulation of the feedback inhibitor HDAC1 would limit the expression of CIITA and the MHC class II complex **(Fig. 39e)**. Interestingly, increased levels of MHC class II have been linked to macrophages having a more pro-inflammatory phenotype (Van Overmeire et al. 2014). Also, high MHC class II expression has been associated to autoimmune disorders (Reith et al. 2005). Thus, this potential CPEB4 function could also contribute to limit inflammatory responses.

Finally, given that HDAC1 function had been also involved in inflammation resolution (Gupta et al., 2016), we wondered whether CPEB4 also regulated HDAC1 expression during LPS response. However, this was not the case, as *Hdac1* was not included among our sets of CPEB4 targets in LPS-stimulated BMDMs **(Appendix II)**. Morever, *Cpeb4*KO macrophages presented a normal HDAC1 upregulation after LPS stimulation, which was also accompanied of the consequent downregulation on *Ciita* and MHC class II mRNAs **(Fig. 40a, b)**. Thus, HDAC1 upregulation during LPS response occurred in a CPEB4-independent manner.

Overall, these results suggest that, in unstimulated macrophages, CPEB4 could regulate MHC class II expression by promoting HDAC1 expression. As seen in **figure 40a**, unstimulated *Cpeb4*KO macrophages showed a trend to have reduced HDAC1 levels. However, further experiments are needed to validate the interplay between these proteins.

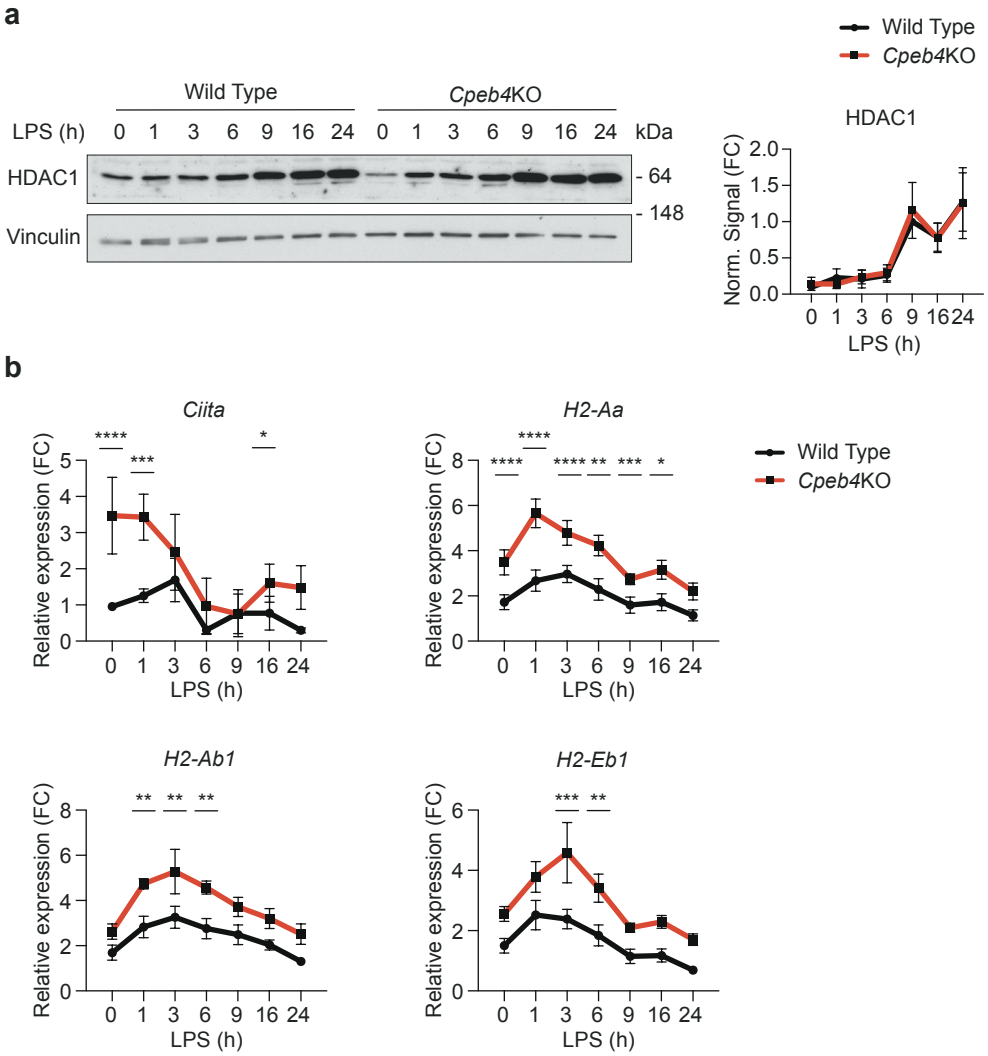

Figure 40. CPEB4-independent upregulation of HDAC1 during the LPS response. (a) Immunoblot analysis of HDAC1 in wild type or *Cpeb4*KO BMDMs treated with LPS for 0-24h. Vinculin served as loading control. Signal intensity was normalized to wild type 9h LPS. Data from triplicate experiments is shown. **(b)** Wild type or *Cpeb4*KO BMDMs were stimulated with LPS (10ng/ml) for 0-24h and mRNA was measured by RT-qPCR. *Tbp* was used to normalize and relative levels to untreated wild type were calculated. Data are shown as mean and s.e.m.; n=6. Statistics: Two-way ANOVA *pv<0.05; **pv<0.01; *** pv<0.001; ****pv<0.0001.

6. CPEB4 function in macrophages in vivo

Finally, we wanted to assess the relevance of CPEB4 expression in macrophages *in vivo*. With this aim, we generated a myeloid-specific *Cpeb4*KO mouse model (*Cpeb4*MKO); crossing Cpeb4$^{lox/lox}$ mice (Maillo et al, 2017) with transgenic mice expressing Cre-recombinase under Lyz2 promoter (Clausen et al. 1999) **(Fig. 41a)**. For their characterization, wild type Cpeb4$^{+/+}$ Cre$^{T/+}$ were used as controls.

We took advantage of the reporter cassette Tomato-GFP (Muzumdar et al. 2007) to have a read-out of Cre recombination activity. As shown in **figure 41b**, GFP was effectively expressed in tissues such as spleen, lung, liver or kidney following the pattern of the myeloid compartment. Moreover, we also obtained BMDMs from *Cpeb4*MKO mice and confirmed that CPEB4 depletion was effective, both during the differentiation process and after LPS stimulation **(Fig. 41c, d)**.

→ **Figure 41. Generation of a myeloid-specific CPEB4 KO mouse model (*Cpeb4*MKO). (a)** Scheme of the alleles used to create *Cpeb4*MKO mouse model. **(b)** GFP Immunohistochemistry of tissues obtained from *Cpeb4*MKO mice. Scale bar 250 µm. **(c-d)** BMDMs obtained from wild type or *Cpeb4*MKO mice. Immunoblot analysis of CPEB4 at different days of differentiation **(c)** or during LPS stimulation **(d)** is shown. Vinculin served as loading control.

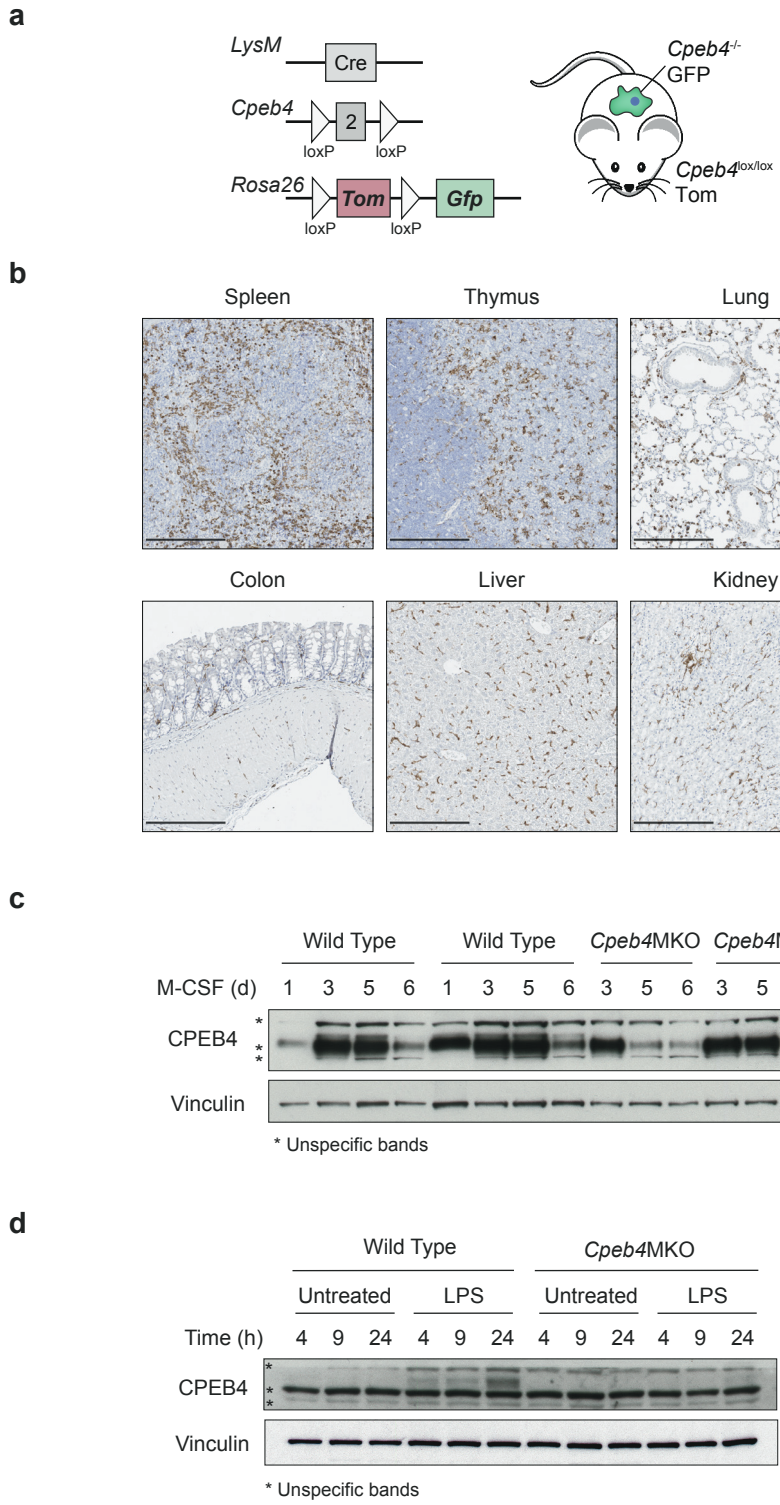

Figure 41. Generation of a myeloid-specific CPEB4 KO mouse model (*Cpeb4*MKO). ←

6.1. Myeloid-specific *Cpeb4*KO mice in homeostasis

When maintained in a specific pathogen-free (SPF) facility, *Cpeb4*MKO mice were born at the expected Mendelian male/female ratios **(Fig. 42a)** and young adult mice (10-18weeks) had normal body weight and did not display any obvious pathology regarding growth, fertility or mobility **(Fig. 42b)**. Moreover, no visible change in the major organs (e.g., liver, spleen, lung, thymus, heart, kidney) was noted, neither at their normalized weight **(Fig. 42c,d)** nor during their histological analysis (data not shown).

Chronic inflammation is a common pathological basis for age-associated diseases. Thus, we let a group of mice age until 80 weeks of age. We observed a certain tendency among *Cpeb4*MKO males to have greater body weight (pv=0,0571), but overall the parameters we evaluated (organ weight and appearance) were comparable between wild type and *Cpeb4*MKO mice **(Fig. 42e-g)**.

In order to challenge their immune system, a group of *Cpeb4*MKO adult mice was transferred for three months to a non-SPF animal house until they were 30 weeks of age. Again, no major differences in their weight or major organs were found between non-SPF wild type and *Cpeb4*MKO mice **(Fig. 42h-j)** (histological analysis not shown).

Finally, we also performed complete blood counts for the previously mentioned groups of mice: adults (in this case 30 weeks old), aged (80 weeks) and non-SPF (30 weeks). As shown in **figure 43a**, we observed significant alterations between adult and aged wild type mice that did not occur in aged *Cpeb4*MKO mice. Nevertheless, we did not find any differences between *Cpeb4*MKO mice and their corresponding controls.

Overall, these results indicate that, under homeostatic conditions, CPEB4 depletion in myeloid cells leads to no obvious defects in adult and aged mice.

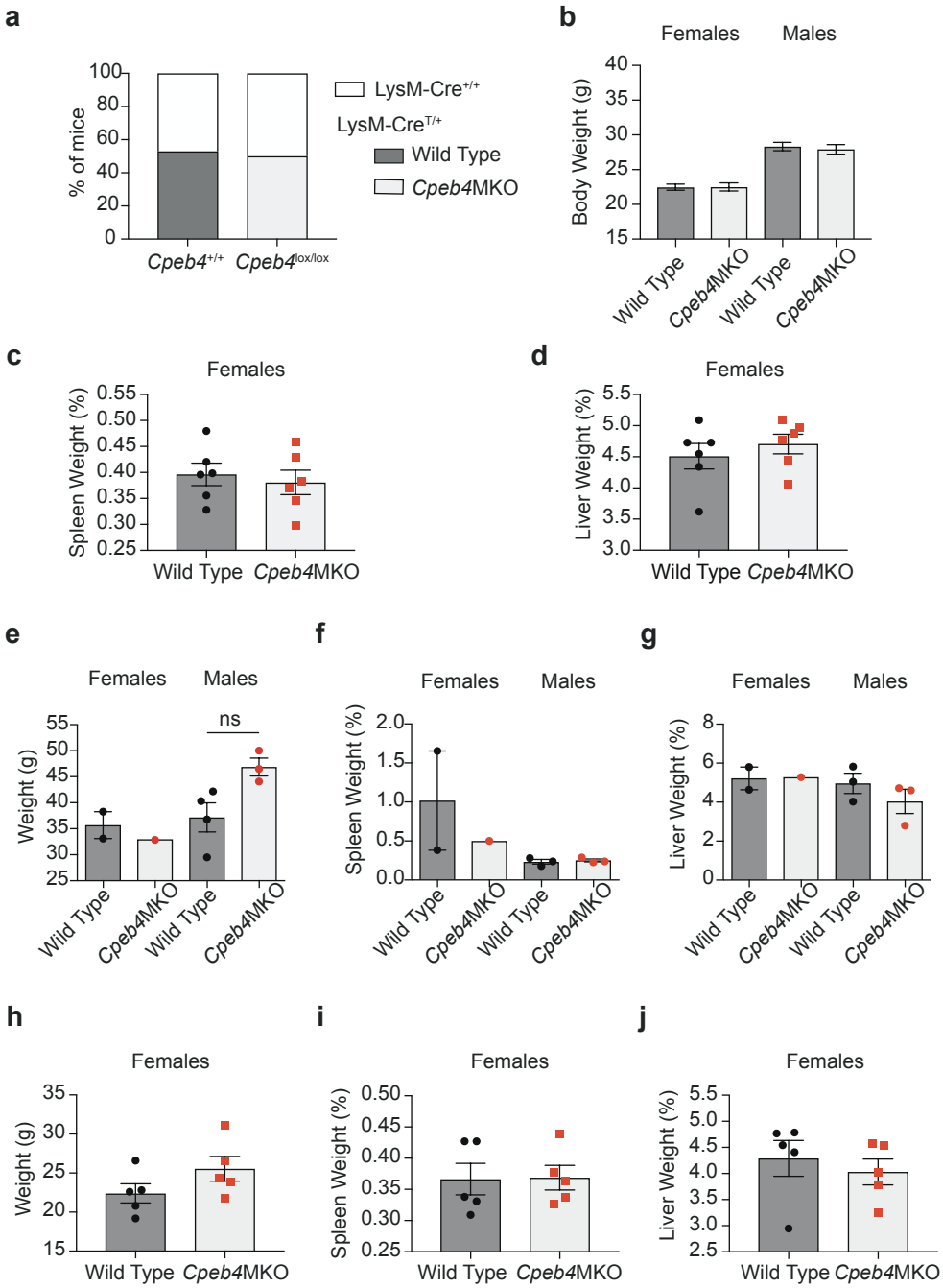

Figure 42. No major abnormalities in *Cpeb4*MKO mice in homeostasis. (a) % of mice of the indicated phenotype born from Cpeb4$^{+/+}$ or Cpeb4l$^{ox/lox}$ matings. **(b,e,h)** Total animal body weight. **(c,d,f,g,l,j)** Normalized organ weight. **(b-d)** 10-18weeks old adult mice maintained in a specific pathogen-free (SPF) facility **(e-g)** 80weeks aged mice maintained in a specific pathogen-free (SPF) facility **(h-j)** 30weeks old adult mice maintained in a non-specific pathogen-free facility. Statistics Mann-Whitney t test ns pv>0,05.

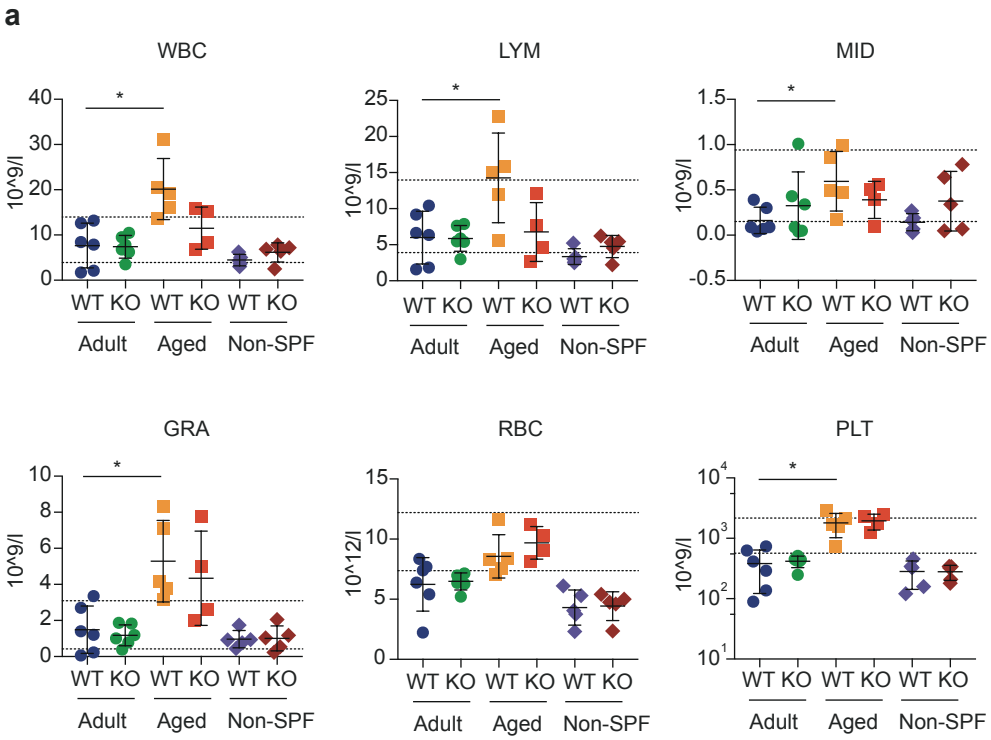

Figure 43. Normal blood counts of *Cpeb4*MKO mice in homeostasis. (a) Complete blood counts from adult (30weeks), aged (80 weeks) and non-SPF mice (30 weeks). 95% interval for 8-10weeks C57BL/6 mice is shown (Charles River®). Abbreviations: WBC (White Blood Cells), LYM (Lymphocytes), MID (Monocytes), GRA (Granulocytes), PLT (Platelets), RBC (Red Blood Cells). Statistics: One-way ANOVA (Kruskall Wallis test) *pv<0.05.

6.2. Decreased survival of *Cpeb4*MKO mice to LPS-induced homeostatic shock

Next, based on our previous results on CPEB4 function during the LPS response, we challenged *Cpeb4*MKO mice with an intraperitoneal dose of LPS. This protocol, known as LPS-induced endotoxic shock, models the systemic inflammatory process that occurs during sepsis. We evaluated *Cpeb4*MKO mice survival upon LPS-induced endotoxic shock and observed that *Cpeb4*MKO mice had increased sensitivity to LPS **(Fig. 44a)**, as they showed decreased survival rates despite having received comparable LPS doses **(Fig. 44b)**. Thus, CPEB4 expression in the myeloid compartment is needed for LPS-induced endotoxic shock survival.

Upon LPS-induced endotoxic shock, mice suffer a dramatic weight loss that can lead to life-threatening conditions. In our case, *Cpeb4*MKO mice lost weight at earlier timepoints and, in higher proportions than wild type mice, lost more than 20% of their initial weight **(Fig. 44c)**, a factor of poor prognosis even if their mean body weight loss was comparable to wild type controls **(Fig. 44d)**.

To better define the origin of our phenotype, we studied the damage after LPS administration for specific organs. Histological analysis revealed that the damage on liver, spleen, lung and thymus was comparable between wild type and *Cpeb4*MKO mice **(Fig. 45a**, see materials and methods for detailed description of the evaluated parameters). Nevertheless, we observed that *Cpeb4*MKO mice developed splenomegaly **(Fig. 45b)**. Importantly, this phenotype has been also described in *Socs1*MKO and *Socs3*MKO mice, two of the previously described CPEB4 targets. These two KO mice also display decreased survival after LPS challenge and the cause of their phenotypes is the development of an exacerbated inflammatory response (Sachithanandan et al. 2011; Qin et al. 2012). Having seen *in vitro* that *Cpeb4*KO BMDMs expressed reduced levels of SOCS1, we hypothesized that the cause of our phenotype could also be related to an impairment in inflammation resolution.

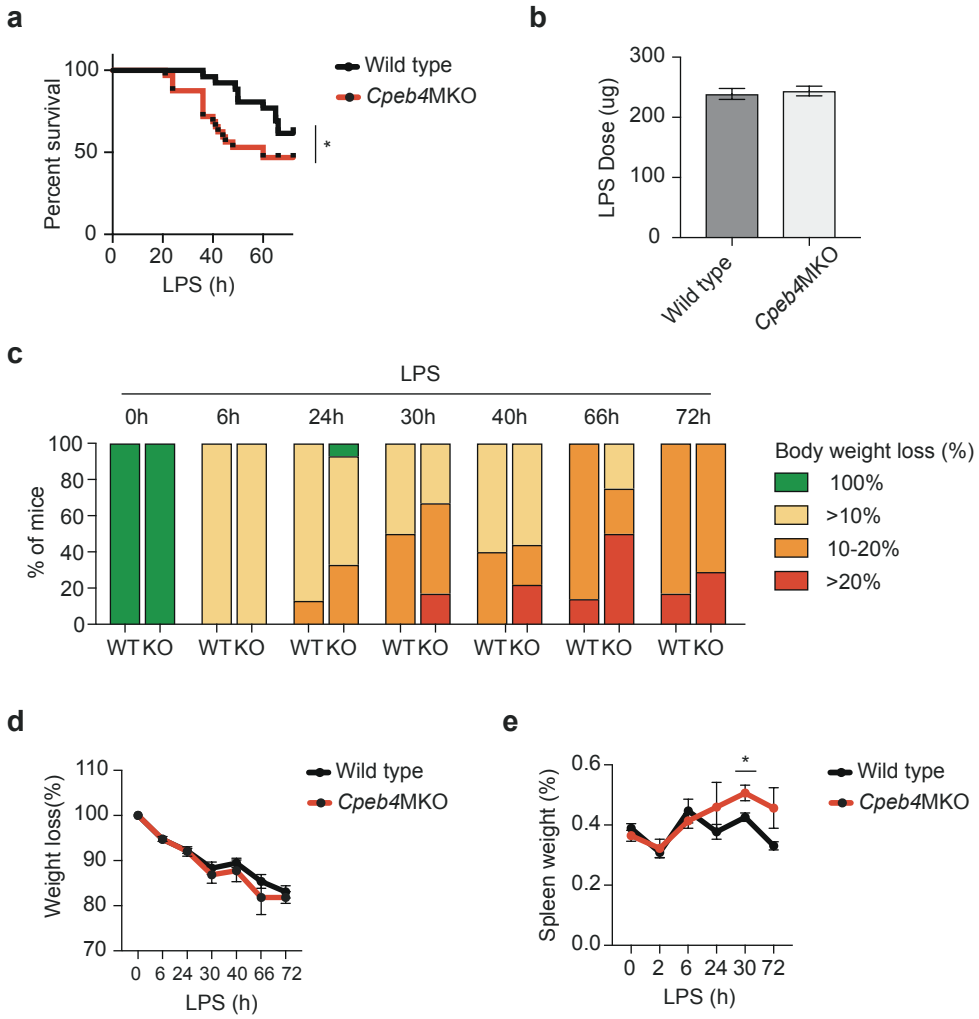

Figure 44. Decreased survival of *Cpeb4*MKO mice to LPS-induced endotoxic shock. (a) Kaplan-Meier survival curves after i.p. injection of LPS (10mg/kg body weight) (n >7/group/experiment). Results represent three independent experiments. *LRT-pv<0.05 **(b)** Micrograms (ug) of LPS administered to WT and MKO mice. **(c)** Weight loss was evaluated after LPS administration at the indicated hours and expressed as % of time zero. **(d)** Weight loss was calculated as described in c and animals were grouped in the indicated categories. **(e)** Spleen weight is shown normalized to total animal weight. Statistics: Mann-Whitney t test.

Therefore, we decided to measure serum cytokine levels, which overall were comparable between wild type and KO mice **(Fig. 45c)**. Looking at wild type animals, though, we detected that animals could be clustered between those expressing high and low IFNγ **(Fig. 45c)**. Interestingly, in *Cpeb4*MKO group there was a higher proportion of mice presenting the IFNγ^{hi} behaviour, and same happened for IL-1β, IL-10 and IL-6 cytokines **(Fig. 45d)**.

Even if we did not observe a significant increase in serum cytokine levels, we considered that these results were very consistent with the penetrance of other phenotypes such as survival or body weight loss. Altogether, these results suggest that, even if *Cpeb4*MKO mice responded deficiently to LPS challenge, some mice could compensate for the CPEB4 absence and survive, while others could not return to the homeostatic state.

Thus, to look for the origin of these alterations, we decided to further study the spleen of *Cpeb4*MKO animals, as splenomegaly development had been so far our most penetrant phenotype. As a first approach, we measured cytokine expression in total spleen mRNA extracts. Interestingly, we observed increased levels of several cytokines, including *Il6*, *Tnf*, *Il10* or *Il1a* **(Fig. 46a)**. These results supported the hypothesis that in the absence of CPEB4 inflammation resolution is impaired. However, further studies should address which cellular compartment in the spleen is expressing these cytokines. Altogether, in this last section we have seen that CPEB4 expression in the myeloid compartment is needed for LPS-induced endotoxic shock survival and to limit inflammatory responses in splenocytes *in vivo*.

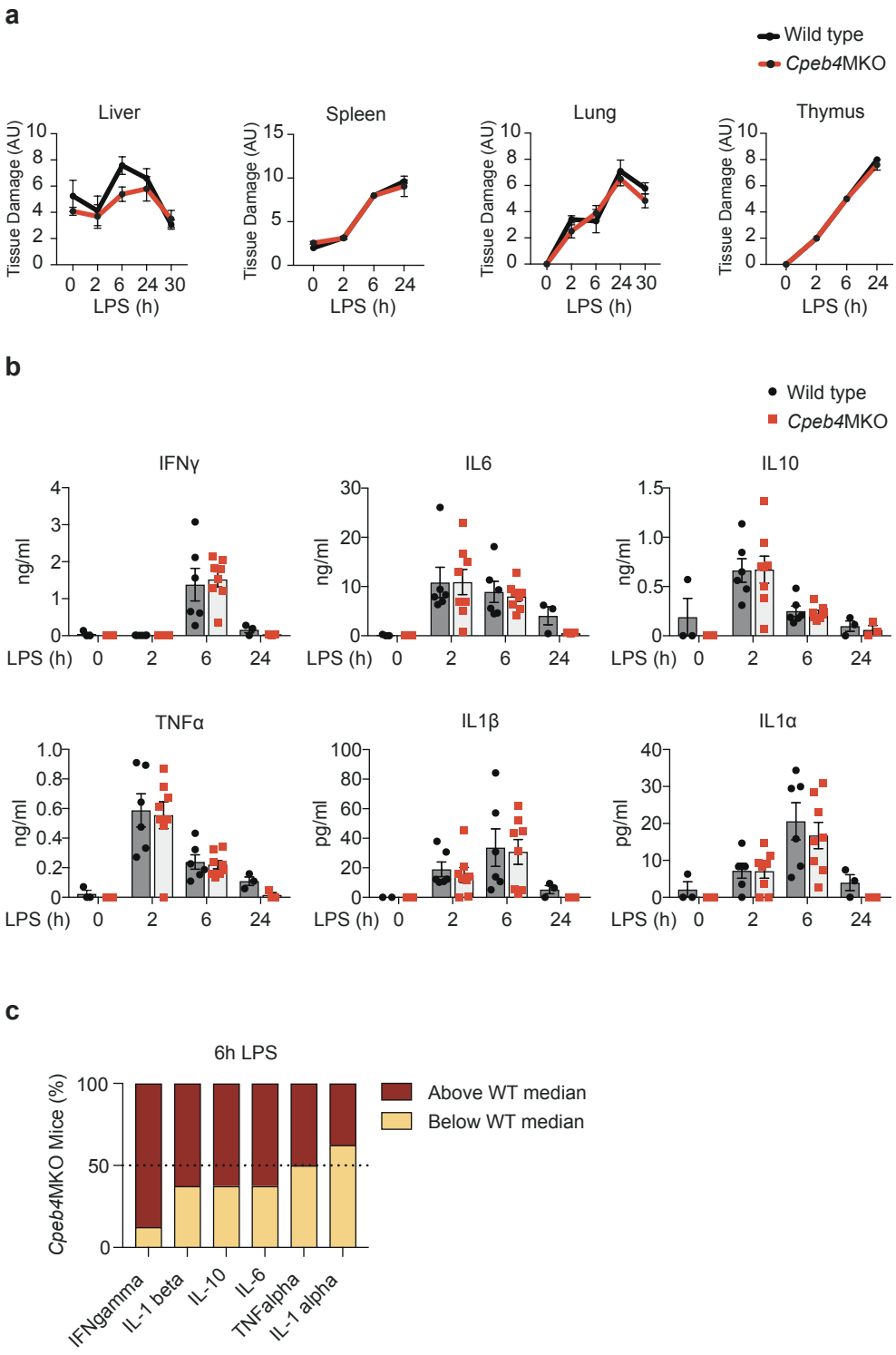

→ Figure 45. *Cpeb4*MKO inflammatory response to LPS-induced endotoxic shock.

← **Figure 45. *Cpeb4*MKO inflammatory response to LPS-induced endotoxic shock.** Wild Type or *Cpeb4*MKO mice were sacrificed after an i.p. injection of LPS (10mg/kg body weight LPS at the indicated hours. **(a)** H&E stained sections of the indicated tissues were evaluated by scoring several parameters from 0 to 4 (highest affectation). Tissue damage for wild type and *Cpeb4*MKO mice was the result of the addition of the different scores. Continues in the next page. **(b)** Serum cytokines levels were measured at the indicated hours after LPS I.P. injection by multiplex bead capture assay. n>3 animals/condition. **(c)** % of Cpeb4MKO displaying serum cytokine levels above or below the wild type median.

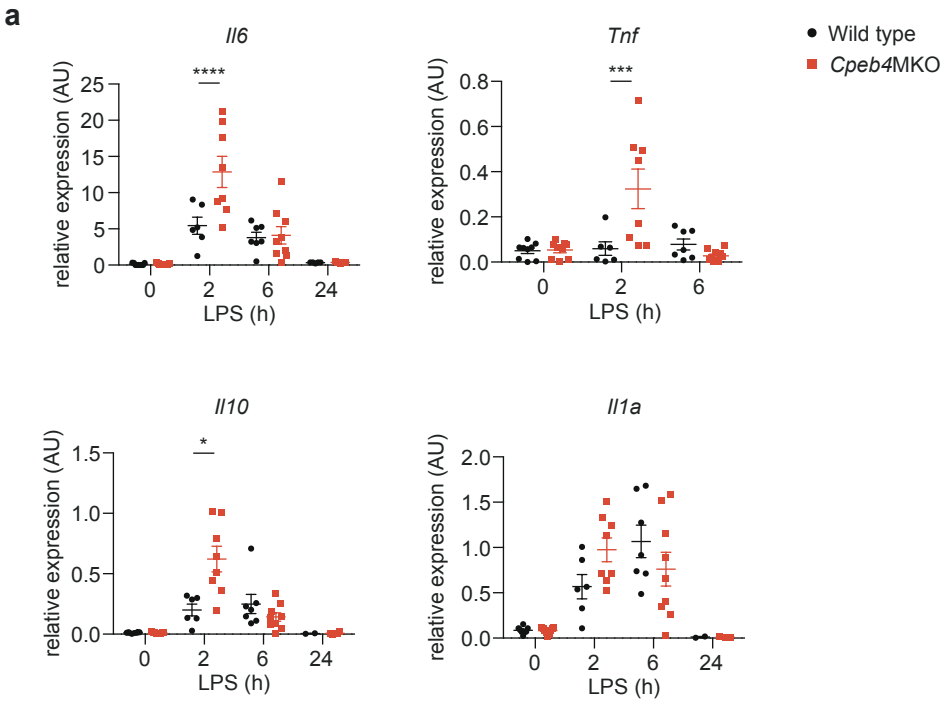

Figure 46. Increased cytokine expression by *Cpeb4*MKO splenocytes during LPS-endotoxemia. (a) Total RNA was isolated from spleens and cytokine levels were measure by RT-qPCR. TBP was used for normalization. n>5 animals/condition. Statistics: Multiple t-test *pv<0,05; ***pv<0,001; ****pv<0,0001.

DISCUSSION

Discussion

In this section, we will discuss different ideas that arise from this work. In the first part (points 1-8), we will comment the results of this study and their biological meaning. In the second (point 9), we will address the open questions that remain unexplored.

1. Inflammation resolution requires CPEB4-mediated translational control

In this work, we have found that CPEB4 is a novel player in macrophage homeostasis and in macrophages response to LPS. We have described how, upon LPS stimulation, the MAPK p38α transiently stabilizes *Cpeb4* mRNA, a process that is mediated by the two ARE-BPs HuR and TTP. We also find a new scenario where CPEB4 protein is regulated by phosphorylation, a modification that regulates its activity (Guillén-Boixet et al. 2016). Downstream CPEB4, we described which are their associated mRNAs during the late phase of the LPS response. Remarkably, our results indicate that CPEB4 participates in inflammation resolution by promoting the expression of negative feedback inhibitors of the inflammatory pathways. Indeed, we have also demonstrated the relevance of CPEB4 contribution to inflammation resolution *in vivo*.

Additionally, we propose that, during the LPS response, TTP and CPEB4 compete to deadenylate or polyadenylate the target mRNAs that they have in common. Moreover, we have uncovered an association between the number of AREs and CPEs in the 3'UTR of mRNAs and their expression pattern after LPS stimulation. These results suggest that the combined action of HuR, TTP and CPEB4 is required to determine different waves of mRNA expression during macrophage activation by LPS.

2. CPEB4, a new player in LPS response

Macrophages are constantly exposed to metabolic, homeostatic and immunoregulatory signals. Unlike other cells, they are specialized in sensing these stimuli and adapt their functions in response to them. For example, upon exposure to danger signals, like LPS, they trigger an inflammatory response that aims to eliminate the invaders, repair the tissue and restore homeostasis.

The development and resolution of inflammatory responses needs to be tightly controlled. Importantly, functional defects in the inflammatory or anti-inflammatory pathways, can lead to pathogenic situations like infections or auto-immune diseases. Thus, macrophages need to carefully balance these two opposite functions. For that, they have a complex network of regulatory mechanisms that control gene expression at multiple levels. Importantly, this network is composed by both positive and negative circuits that cross regulate each other. This way, inflammatory responses present an oscillatory and self-limited behaviour.

So far, extensive studies have described the signalling pathways that are activated in LPS-stimulated macrophages. At the post-transcriptional level, one of the best characterized mechanisms limiting the expression of cytokines is the induction of mRNA deadenylation and decay. Nevertheless, the function of cytoplasmic polyadenylation in this field remained almost unexplored.

In this work, we have studied CPEB4 regulation and function during the LPS response. We have described how the MAPKs pathways regulate CPEB4 levels and activity so that CPEB4 polyadenylating function peaks during the resolutive phase of the LPS response. This way, the expression of CPEB4-regulated mRNAs is also sustained during this period, which is especially relevant for those molecules limiting the activation of the inflammatory pathways. Thus, CPEB4 is a novel player to be included in the regulatory circuits that control macrophage activation in response to LPS.

3. The MAPKs p38α and ERK1/2 regulate CPEB4 levels and activity during the LPS response

To study the role of cytoplasmic polyadenylation in macrophages, we first assessed *Cpebs* expression in macrophages subjected to different stimuli **(Fig. 22)**. We observed that *Cpeb4* mRNA was transiently upregulated after LPS stimulation. CPEB4 protein, however, did not followed the same behaviour, as it was progressively upregulated **(Fig. 22, 25)**. These result suggested that Cpeb4 mRNA was post-transcriptionally regulated. Additionally, we also detected that CPEB4 was phosphorylated during this process, a post-translational modification that enhances CPEB4 polyadenylating activity (Guillén-Boixet et al. 2016) **(Fig. 25)**. Thus, these results suggest that distinct mechanisms regulate CPEB4 expression and activity in a coordinated manner during the LPS response .

Of these regulatory mechanisms, we have shown that, indeed, upon LPS stimulation, the MAPK p38α and the two ARE-BP HuR and TTP regulate *Cpeb4* mRNA. Specifically, during the early times of LPS response, p38α activation stabilizes *Cpeb4* mRNA and promotes its association with HuR **(Fig. 21-22)**, which will probably mediate its stabilization. During the late LPS response, though, TTP associated with *Cpeb4* and promotes its destabilization and downregulation **(Fig. 22,** Sedlyarov et al. 2016). Thus, we have described a novel axis that regulates *Cpeb4* mRNA at the post-transcriptional level through the AREs on its 3'UTR.

Regarding which of the described kinases mediate CPEB4 phosphorylation, our results suggest that ERK1/2 MAPKs could be phosphorylating CPEB4 in this context **(Fig. 25)**. Importantly, it has been shown that phosphorylated CPEB4 can promote the polyadenylation of its own mRNA, creating a positive feedback loop that favours its own expression (Igea & Méndez 2010; Calderone et al. 2016). Pressumably, during the late phase of the LPS response, P-CPEB4 also initiates this feedback loop and polyadenylates its own mRNA to upregulate its own levels.

Importantly, these mechanisms already exemplify that one same mRNA, in this case *Cpeb4*, could be regulated by HuR, TTP and CPEB4 throughout LPS response **(Fig. 47)**.

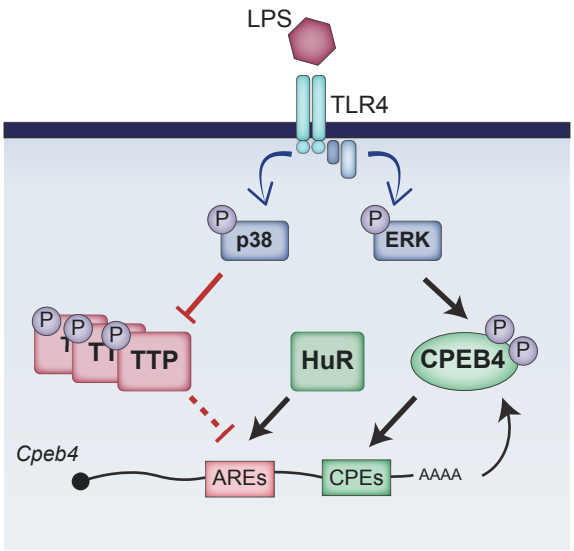

Figure 47. MAPK-dependent regulation of CPEB4 levels and activity during the LPS response in BMDMs. In untreated conditions TTP destabilizes ARE-containing mRNAs like *Cpeb4* (red dashed arrow). Upon LPS stimulation, downstream p38α, TTP is phosphorylated, which favours HuR association with these mRNAs, its stabilization and upregulation. Downstream TLR4, ERK1/2 MAPKs are also activated, which can phosphorylate CPEB4 favouring its polyadenylation activity. Then, CPEB4 activation will promote a positive feedback loop where CPEB4 polyadenylates its own mRNA favouring its progressive upregulation.

4. Relevance of CPEB4 hyperphosphorylation for LPS response

As we have mentioned, CPEB4 polyadenylating function is activated by phosphorylation during the LPS response. However, unlike other proteins, CPEB4 can be hyperphosphorylated in at least twelve sites in its N-terminal domain. Moreover, these twelve phosphorylation events additively activate CPEB4 polyadenylation activity (Guillén-Boixet et al. 2016).

Interestingly, regulation of proteins through hyperphosphorylation like CPEB4 can generate ultrasensitive responses (Guillén-Boixet et al. 2016; Ferrell & Ha 2014a). These type of responses are defined as "a response to an increasing stimulus that is described as a sigmoidal dose-response curve. Low levels of stimulus produce a poor response but, as the stimulus level increases, there is an abrupt increase in the response to near-maximal levels" (Ubersax & Ferrell 2007). Thus, ultrasensitivity allows to create switch-like transitions, where small inputs are initially ignored but, if they surpass a certain threshold, the system responds with a complete output. Besides protein hyperphosphorylation, multiple other mechanisms can generate ultrasensitive responses, for example feedback loops or cooperativity.

Oscillatory processes like inflammatory responses need to delay the induction of inhibitory mechanisms. Thus, they regulate the expression of these molecules via mechanisms that favour this delay, like ultrasensitive responses. In ultrasensitive responses generated by hyperphosphorylation, the timing of the switch is determined by several parameters, such as the ratio between activating sites and total sites, the levels of the substrate or the presence of substrate competitors, among others (Ferrell & Ha 2014a). Therefore, it is probably critical for the LPS response that CPEB4 is regulated via multiple phosphorylating events instead of just one. This way, CPEB4 switch occurs in a delayed manner, creating different temporal windows for the expression of ARE- and CPE-containing mRNAs or, in a broader sense, for the inflammatory and anti-inflammatory phases of the LPS response.

It remains to be explored though, which would be the consequences of an immediate activation of CPEB4 during the early LPS response or the parameters that define the ultrasensitive response generated by CPEB4 in this context.

5. Closing the circuit: CPEB4 targets are enriched in MAPK pathway-related genes

To characterize CPEB4 function in macrophages we performed RNA Immunoprecipitation and Sequencing (RIP-seq) **(Fig. 26-28)**. Once we had defined the mRNAs associated with CPEB4, we observed that the most relevant category in the GO analysis was the MAPK signalling pathway. This result established a regulatory circuit between the MAPK pathway and CPEB4, which could contribute to the oscillatory character of the LPS response.

To generate self-sustained oscillations, a single negative feedback is required and sufficient (Friesen & Block 1984; Ingolia & Murray 2004; Lomnitz & Savageau 2014; Novák & Tyson 2008; Ferrell et al. 2011). However, biological oscillators are usually organized into more complex networks, which include additional elements. Intriguingly, although they are not required to generate oscillations, these elements are evolutionary conserved, highlighting the relevance of their function. Among other properties, biological oscillators need to function properly in noisy environments or, in other words, need to be robust. Consequently, it has been proposed that the function of these additional elements could be related to the oscillator's robustness (Li et al. 2017). For example, the addition of self-positive feedback loops, in which a node can active itself, significantly increases the robustness of a network (Ananthasubramaniam & Herzel 2014; Gérard et al. 2012; Tsai et al. 2008). Alternatively, the addition of nodes receiving incoherent inputs, meaning both positive and negative inputs, also increases the oscillator's robustness (Li et al. 2017).

Interestingly, both features are found in CPEB4 regulation and function during the LPS response. First, CPEB4 is regulated by two incoherent inputs, HuR and TTP. Next, CPEB4 can promote its own expression through a positive feedback loop. Finally, the described competition between CPEB4 and TTP implies that the target mRNAs that they have in common are again subjected to incoherent inputs. Thus, thanks to these features, CPEB4 regulation and function could be increasing the robustness of LPS-driven inflammatory responses **(Fig. 48)**.

Additionally, some cellular systems are formed of multiple interlinked loops rather than single positive feedback loops. Dual-switch systems, for instance, combine loops with distinct temporal properties. Importantly, this combination of different kinetics confers certain advantages to these systems. First, the output is turned on rapidly, as a consequence of the fast loop, but turned off slowly, as a consequence of the slow loop. Thus, this duality allows an independent tuning of the activation and deactivation times. More important, although dual-switch systems exhibit high noise sensitivity when in off state, they become much robust once in its on state, as a result of the properties of its slow loop (Brandman et al. 2005).

Again, the described circuit between the MAPKs pathway and CPEB4 also benefits from these properties. In this system, phosphorylating events between MAPKs involve a rapid positive loop, while CPEB4-mediated translational control mediates a slower loop. This concept, of course, also applies to HuR- and TTP-mediated translational control. Hence, this properties also support that the interregulation between the MAPKs pathway and CPEB4 could increase the robustness of macrophage response to LPS.

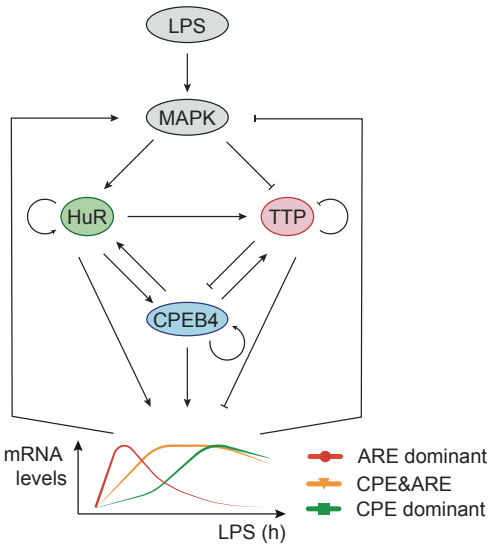

Figure 48. LPS activates a regulatory circuit between the MAPK pathway and CPEB4. LPS recognition by macrophages activates the MAPK pathways, that regulate the levels and activity of HuR, TTP and CPEB4. These three RNA-Binding proteins participate in positive feedback loops, cross regulate each other and also regulate common mRNAs. The number of AREs and CPEs on mRNAs will determine which of these protein preferentially regulate them, thus influencing their expression pattern. Finally, the proteins encoded by these mRNAs will provide new positive and negative feedback to the MAPK circuit.

6. CPEB4 promotes inflammation resolution during the LPS response

Our RIP-seq data also indicated that CPEB4 was associated with the mRNAs of multiple feedback inhibitors of the inflammatory pathways, like SOCS1 and SOCS3, MKP1, TTP, A20 or IL1RA **(Fig. 28)**. This result, together with the fact that CPEB4 activity peaks during the late phase of the LPS response, suggests that CPEB4 promotes inflammation resolution by favouring the expression of these proteins. Supporting this idea, *Cpeb4*KO macrophages presented reduced levels of SOCS1 and TTP **(Fig. 32)**. Additionally, although it has not been validated yet, based on the ARE/CPE score, IL1RA mRNA (*Il1rn*) is a good candidate to be highly dependent on CPEB4 function, and thus downregulated in *Cpeb4*KO BMDMs **(Fig. 36-37)**.

6.1. Decreased survival of *Cpeb4*MKO mice to LPS-induced endotoxemia

To further characterize CPEB4 function in LPS-stimulated macrophages, we subjected *Cpeb4*MKO mice to LPS-induced endotoxic shock. a protocol that models the systemic inflammatory response that occurs in sepsis patients. Importantly, this response needs to be tightly controlled, as it has been described that both an aberrant pro-inflammatory reaction or an extended immune suppression can lead to patient death (van der Poll et al. 2017). In our case, we observed that *Cpeb4*MKO mice presented decreased survival capacity upon LPS-induced endotoxemia. Moreover, they developed splenomegaly and expressed increased levels of several cytokines in their spleens **(Fig. 44-46)**. Again, these results support that CPEB4 function in macrophages is needed to limit inflammatory responses.

Importantly, the same cytokines which expression was dramatically altered *in vivo*, were expressed normally or weakly altered in BMDMs **(Fig. 35, 37, 45)**. Several reasons could account for this difference, such as the distinct features of each type of macrophage or the contribution of other cell types *in vivo*. Regarding this second option, it is important to consider that, *in vivo*, macrophages function as initiators of immune responses. Thus, if macrophages express increased levels of inflammatory cytokines, other immune cell types can sense these signals and overrespond in accordance to them, initiating a process that could dramatically magnify the original phenotype. Related to this concept, the increased expression of MHC class II in *Cpeb4*KO BMDMs could also be relevant for this phenotype **(Fig. 39)**.

7. AREs and CPEs define the kinetics of mRNAs during the LPS response

While studying CPEB4 target mRNAs, we realized that several of them had been also described to be associated with TTP in LPS-stimulated macrophages. Moreover, we detected an inverse correlation between their alterations in TTPMKO and *Cpeb4*KO BMDMs **(Fig. 33, 35)**. These results prompt us to study the AREs and CPEs in the 3'UTR of these mRNAs, to see if we could predict which of the two RBPs would be predominantly regulating each mRNA. Unexpectedly, considering only the number of AREs and CPEs, we clustered 61 mRNAs in three different categories, which followed significantly different expression behaviours during the LPS response **(Fig. 36)**. Briefly, while ARE-dominant (AREd) mRNA levels were rapidly up- and downregulated, CPE-dominant (CPEd) mRNA levels increased in a more progressive manner and they were sustained during the late phase of the LPS response. Finally, the expression of mRNAs containing both AREs and CPEs (A&C mRNAs) presented features of the two behaviours. Importantly, these results uncover the relevance of ARE- and CPE-mediated translational control to establish different temporal mRNA expression patterns during the LPS response **(Fig. 49)**.

7.1. HuR, TTP and CPEB4 define different mRNA expression waves during the LPS response

Interestingly, the described behaviour for each group of mRNAs, was in accordance with how the levels and activity of HuR, TTP and CPEB4 are regulated during the LPS response **(Fig. 49)**. Moreover, we observed that the ARE/CPE score also clustered mRNAs according to their alterations in TTPMKO and *Cpeb4*KO macrophages. For instance, AREd mRNAs were severely upregulated in TTPMKO BMDMs while CPEd mRNAs were barely affected. And, on the contrary, CPEd mRNAs were unaltered in TTPMKO conditions but downregulated in the absence of CPEB4 **(Fig. 33, 35)**.

Altogether, these correlations suggest that HuR, TTP and CPEB4 are indeed the RNA binding proteins reading the combinatorial code between AREs and CPEs on the 3'UTR of mRNAs. Moreover, they also highlight the relevance of the coordinated regulation of the activity and levels of these proteins, in order to define different kinetics of mRNA expression during the LPS response. Finally, it is also worth considering that, by defining these sequential waves of mRNA expression, the function of HuR, TTP and CPEB4 is probably central to delimit the inflammatory and resolutive phases of the LPS response.

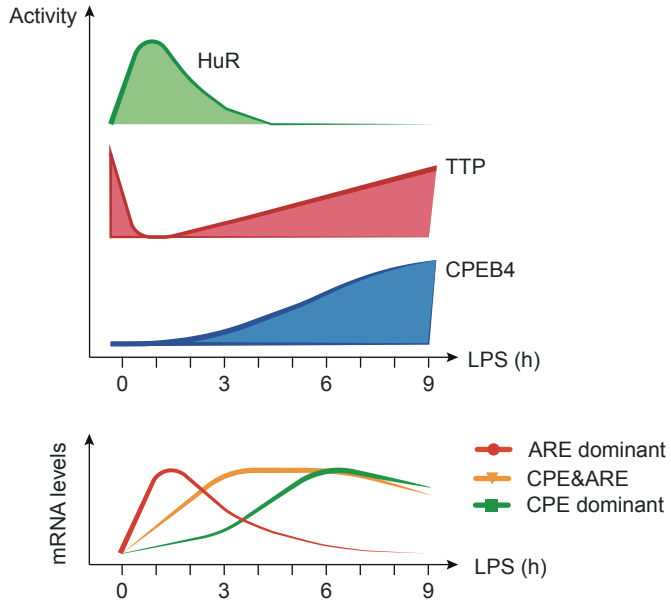

Figure 49. AREs and CPEs define three temporal waves of mRNA expression during the LPS response. The coordinated regulation of the activity and levels of CPEB4, TTP and HuR can explain the behaviour of three type of mRNAs. In turn, these three classes of mRNAs are defined by the number of AREs and CPEs in the 3'UTR of mRNAs. Briefly, during the early LPS response, AREd and A&C mRNAs are stabilized due to the action HuR. CPEd mRNAs, though, are stabilized and upregulated in a more progressive manner, mirroring CPEB4 activity. After 3 hours of LPS, AREd mRNAs are rapidly downregulated, due to the destabilizing activity of TTP, while the expression of ARE&CPE and CPEd mRNAs is more sustained thanks to the polyadenylating function of CPEB4.

7.2. CPEB4 polyadenylating function stabilizes CPE-containing mRNAs during the LPS response

Given the well-established link between mRNA deadenylation and decay, another conclusion derived from these results is that CPEB4-mediated polyadenylation stabilizes CPEd and A&C mRNAs. This hypothesis, although needs to be further confirmed, is in accordance with the established paradigm that the poly(A) tail facilitates mRNA stabilization. If true, it will provide a new mechanism to positively regulate the levels of a specific subset of mRNAs.

Remarkably, none of the published studies on CPEBs function had shown before that mRNA polyadenylation could be coupled to its stabilization. The reason for that, is that this mechanism is probably more relevant in certain scenarios, for example, in cells that display elevated mRNA turnover rates. This is the case of LPS-stimulated macrophages, but could also be valid in differentiating or proliferating cells. Moreover, the magnitude of the effect of CPEBs-mediated polyadenylation on mRNA stability will probably vary among different mRNAs.

7.3. The Combinatorial Code: multiple cis-acting elements collaborate to dynamically regulate gene expression

An emerging idea in the field is that cellular mRNAs could be broadly classified in two categories. The first group includes mRNAs that are very abundant, contain longer poly(A) tails, a high proportion of optimal codons and are overall stable. These mRNAs are transcribed from highly expressed genes and encode for proteins that are needed for basic cellular functions. Thus, their expression does not need to be dynamically regulated. The second group of mRNAs, however, presents the opposite qualities. They are expressed at low levels, contain shorter poly(A) tails, reduced codon optimality and poor stability. Interestingly, these features make these mRNAs highly susceptible to multiple translational regulatory mechanisms, which by slightly modifying their properties can change dramatically their behaviour. Moreover, by coordinating its distinct regulatory mechanisms, these mRNAs can be dynamically regulated.

According with these properties, we would expect that mRNAs in this second category are more susceptible to CPEBs function. It is important to consider, though, that these mRNAs are also highly predisposed to be regulated by multiple other mechanisms. Consequently, to understand how CPEBs regulate its target mRNAs, other regulatory elements may need to be considered. Indeed, our study is not the first one where the combination of CPEs and other elements in the UTRs of mRNAs can explain complex expression patterns. For example, it has been shown that the combination of AREs and CPEs also determines different temporal waves of activation of mRNA translation during meiosis progression (Belloc et al. 2008). Moreover, the combined action of uORFs and CPEs was shown to define two temporal waves of translational activation following ER stress (Maillo et al. 2017).

Altogether, these studies evidence how the combined regulation of mRNAs by two elements in their UTRs can establish different kinetics of gene expression. However, we should consider that mRNAs can contain more than two different elements, that some elements are recognized by more than one RNA Binding protein, and that each protein is subjected to multiple mechanisms that regulate its expression and activity. Hence, the combined regulation of the cis- and trans-acting elements on mRNAs may be able to generate much more complex patterns than the ones that have been described so far.

Finally, we could also think about the biological relevance of this complexity. It is well established that, during animal evolution, the number of protein-coding genes has remained fairly constant; while the length of 3'UTRs and the fraction of genes expressing alternative 3'UTRs have increased substantially (Mayr 2016). Thus, we could hypothesize that these two parameters have increased the complexity of biological regulatory systems, which has in turn contributed to animal evolution.

8. Gene expression is regulated at multiple levels to coordinate LPS response

Finally, looking globally at the LPS response, we can see that multiple mechanisms are involved in the regulation of gene expression. These mechanisms act are very diverse levels, as they are involved in epigenetic, transcriptional, translational and post-translational functions. However, they can be clustered in two groups according to their involvement in pro-inflammatory functions or inflammation resolution. Importantly, these two groups are not independent from each other, as they are activated in a sequential and coordinated manner.

First, during the inflammatory phase of the LPS response, mechanisms that favour the expression of inflammatory genes are activated. These include the activation of signalling pathways via phosphorylation, the degradation of inflammation inhibitors like IκBα, the activation of transcription factors and induction of chromatin relaxation, and also, mechanisms that favour mRNA stability and translation like TTP inactivation, eIF2B dephosphorylation or mTOR activation (appendix III).

Next, in the anti-inflammatory phase, macrophages activate the second battery of mechanisms, which negatively regulate the first ones. Among these, we can find mechanisms that inactivate proteins, like the phosphatase DUSP1, that trigger their degradation, like SOCS1, that promote mRNA decay, like TTP, or that limit translation like mTOR deactivation.

Altogether, then, LPS response could still be seen an oscillatory circuit composed by a single negative feedback loop **(Fig. 50)**.

Considering this criteria of positive and negative regulators gene expression, CPEB4 polyadenylating activity positively regulates mRNAs. Thus, one could expect that is was activated during the initial phase of the LPS response in order to promote the expression of pro-inflammatory molecules. However, CPEB4 is mainly expressed and active during the second anti-inflammatory phase. In this context, given the global reduction in gene expression, it is critical that the upregulation of anti-inflammatory molecules occurs effectively.

Thus, we propose that CPEB4 function in late LPS response is key to preserve the mRNAs coding for anti-inflammatory factors from TTP-mediated deadenylation, thus favouring the expression of a subset of proteins in an environment where gene expression is globally downregulated **(Fig. 50)**.

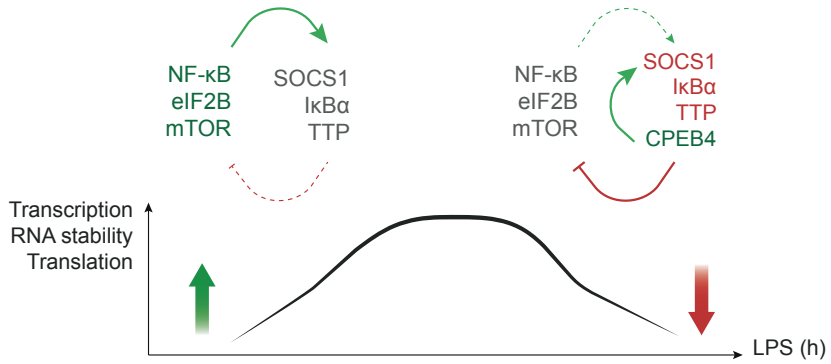

Figure 50. Gene expression regulation during the LPS response. Upon LPS detection, macrophages activate mechanisms that favour gene expression at multiple levels. These mechanisms, besides favouring the expression of inflammatory molecules, also promote the expression of negative regulators of the inflammatory response. These inhibitors, at later timepoints will inhibit gene expression at multiple levels in order to limit the synthesis of pro-inflammatory mediators. During this process, however, their expression could be compromised. Thus, we propose that CPEB4 function is to favour the expression of the molecules in charge of inflammation resolution in this context.

9. Open questions and future directions

In this second part of the introduction we will briefly address some questions that arise from our results and that, so far, remained unanswered.

9.1. CPEBs function in macrophages

In this work we have described CPEB4 function in LPS response. However, several aspects of CPEBs contribution to macrophage physiology remain unexplored. For example, CPEB2 function could be relevant for unstimulated macrophages or CPEB1 for the IL-4 response **(Fig. 22)**. Additionally, we could explore if CPEBs

are involved in macrophages response to other challenges, like infections, tumours or metabolic diseases.

Finally, there are still open questions about the contribution of CPEB1, CPEB2 and CPEB3 to LPS response. CPEB1 has been proposed to repress *Tak1* mRNA in LPS-stimulated macrophages, but the exact timings of its activity or which other mRNAs are repressed by CPEB1 is not known (Ivshina et al. 2015). Moreover, *Cpeb3* mRNA was also transiently upregulated after LPS stimulation **(Fig. 22)**. Finally, in *Cpeb4*KO macrophages, *Cpeb1*, *Cpeb2* and *Cpeb3* are upregulated (Appendix V). We interpret this result as a compensatory mechanism triggered by CPEB4 absence, which suggests that they could partially do overlapping functions. Thus, even if our results suggest that CPEB4 is the main CPEB involved in LPS response, it would be worth to study their contribution to the regulation of CPE-containing mRNAs.

9.2. CPEB4: a stress-response RNA-Binding Protein?

Different stressing stimuli activate the MAPK p38α so that cells adapt their functions to their environment. For example, p38α is activated in front of osmotic shock, radiation and oxidative stress, besides LPS and other cytokines. Thus, the link we have established between *Cpeb4* expression and p38α activation, could actually involve that CPEB4 also participates in the cellular response to these other stimuli that activate p38α. So far, we have evidence that during mitotic cell cycle progression CPEB4 expression is also dependent on the p38α-HuR-TTP axis (data not shown).

In accordance with this, CPEB4 expression and activity has been described in scenarios like oocyte meiosis progression or ER stress (Igea & Méndez 2010; Maillo et al. 2017). Moreover, *in vivo* studies in total *Cpeb4*KO mice suggest that CPEB4 expression is critical in response to a challenge but not under homeostatic conditions, as we observed in Cpeb4MKO mice (Maillo et al. 2017). Thus, given that p38α and other kinases are defined as stress-response kinases, it would be plausible to consider CPEB4 a stress-response RNA binding protein.

9.3. Transcriptional regulation of CPEB4 mRNA

In this work, we have extensively characterized how *Cpeb4* mRNA stability is regulated upon LPS treatment. However, we have not explored how is *Cpeb4* expression regulated at the transcriptional level. According to different databases, the transcription factors PU.1, SMRT, SPI1, CEBPa and CEBPb have been found associated to Cpeb4 promoter in macrophages (ChEA 2016, Enrichr; Chen et al. 2013; Kuleshov et al. 2016). Moreover, Cpeb4 promoter is predicted to have NFKB1 binding sites, one of the major drivers of the LPS response. Thus, any of these factors could be involved in CPEB4 expression in this context.

9.4. Non-MAPK -related CPEB4 functions

9.4.1. CPEB4 maintains ER homeostasis (again)

As shown in **figure 26**, Gene Ontology Analysis revealed that CPEB4 targets were enriched in genes related to the MAPK pathway. However, after LPS stimulation another category significantly enriched was protein processing at the endoplasmic reticulum (ER). The unfolded protein response (UPR) is a pathway that allows cells to manage endoplasmic reticulum (ER) stress that is imposed in periods of high ER-protein-folding demand. In this role, the UPR has increasingly been shown to have crucial functions in inflammatory responses, which are associated to high protein synthesis and secretory charges (Janssens et al. 2014).

CPEB4 has been shown to activate the translation of mRNAs encoding for proteins that participate in the UPR, a function that is required to overcome ER stress periods (Maillo et al. 2017). Therefore, based on the GO data, another function for CPEB4 during the LPS response could be related to favour the expression of UPR related genes to maintain ER homeostasis.

9.4.2. CPEB4 translational control regulates mRNA transcription

We tend to think of gene expression as a linear process where translation acts on the mRNAs served by transcription. However, several studies are showing how multiple processes such as translation or mRNA degradation can signal back to the transcriptional machinery to maintain a balanced proteome. Hence, gene expression should be considered to be circular or bidirectional, but not linear (Gupta et al.

2016; Das et al. 2017).

We have shown that CPEB4 regulates the expression of feedback inhibitors of the inflammatory pathways and thus, to participate in inflammation resolution **(Fig. 28).** However, we also observed some links between CPEB4 function and transcriptional regulation. First, *Cpeb4*KO macrophages presented alterations on NF-κB and STAT1 activation **(Fig. 38)**. Second, CPEB4 was associated to HDAC1 mRNA, which main function is to deacetylase histones and promote chromatin repression **(Fig. 39)**. Therefore, it would be really exciting to study if CPEB4 function could alter certain pathways both at the translational and transcriptional level, and contribute to the bidirectional regulation of gene expression.

9.5. Assessing CPEB4 function by Ribosome profiling

As shown in **figure 30**, our ribosome profiling data suggests that wild type and *Cpeb4*KO macrophages have almost no differences at TE rates. Further experiments should address if this is due to the fact that we did not met all the quality standards **(Fig. 29)** or because of the sensitivity of the technique and the analysis. In the first scenario, we should optimize the RNase digestion and monosome selection steps of the ribosome profiling protocol. For the second, being LPS response such a dynamic process, a possible solution would be to compare mRNA dynamics across different timepoints instead of a single steady state condition. Nevertheless, with the obtained results, it would be worth to further explore the link between CPEB4 and the genes that were significantly altered in *Cpeb4*KO BMDMs, like *Stard13* **(Fig. 30)**.

9.6. Further developing the ARE/CPE Score

9.6.1. Genome wide analysis of the ARE/CPE score

So far, our ARE/CPE score clustered the expression patterns of 61 mRNAs, which included crucial pro- and anti-inflammatory mediators of the LPS response. However, to understand the extent of this regulatory mechanism, we plan to calculate the ARE/CPE score genome wide.

9.6.2. Including other trans-acting factors in our model

According to the literature several other trans-acting factors also regulate mRNA stability during the LPS response. Among them, we can find the miRNA machinery as well as RNA binding proteins such as Roquin, Regnase-1, AUF1, hnRNPC, KSRP or CELF (Díaz-Muñoz & Turner 2018; Turner & Díaz-Muñoz 2018; Lu et al. 2014; Pai et al. 2016; Essandoh et al. 2016). Importantly, some of the mentioned RBPs also recognize AREs and thus, could be contributing to the expression pattern of ARE-dominant mRNAs. Thus, it would be great if future studies included these proteins in our model and revealed their contribution to mRNA dynamics.

9.6.3. Increasing the complexity of the ARE/CPE score

In the same line, another consideration would be if by including other cis-acting elements in the score, we would be able to better understand mRNA dynamics. To tackle this question, we could consider defining a new score computationally. Briefly, this would consist in first clustering mRNAs according to their expression patterns and then defining which cis-elements are dominant in each category.

Nevertheless, it is important to consider that, to understand mRNA dynamics, having a correlation between a regulatory motif and an expression pattern is not enough. It is also necessary to understand which trans-acting factor recognizes this motif, its function, post-translational modifications and expression levels, among other features. In our case, a great number of studies had previously characterized several of these aspects for HuR, TTP and CPEB4. Thanks to them, we could understand and interpret many of our observations and, by putting everything together, get to the ARE/CPE score. Thus, even if we defined a score computationally, characterizing each new element would be beyond our capabilities.

Fifteen years ago The Human Genome project was completed by the collaboration of twenty international institutions and research centres. So far, it is considered the world's largest collaborative biological project. Given the multiple evidence that there is a combinatorial code in the UTRs of mRNAs. Thus, it would be great to design again large collaboratives projects that aimed to understand it.

9.6.4. Considering alternative polyadenylation

Finally, a last consideration on the ARE/CPE score, is that it exclusively considers the number of AREs and CPEs in the 3'UTR of the longest transcript of a gene. However, mRNAs undergoing alternative cleavage and polyadenylation (APA) can generate isoforms with different 3'UTRs, and consequently each 3'UTR should be considered separately as it could have a distinct ARE/CPE score.

As it has been shown that macrophages increase the usage of shorter 3'UTRs in response to bacteria (Pai et al. 2002), it would be really interesting to assess if by undergoing APA, mRNAs could switch from a ARE*d* behaviour to a CPE*d* expression pattern. This way, mRNAs would not be forced to be regulated in different scenarios by the same elements, but they could either be ARE*d* or CPE*d* according to the context.

9.7. Mechanistic basis of the competition between TTP and CPEB4

Another question that remains to be explored is the molecular mechanism of the competition between TTP and CPEB4 for the target mRNAs that they have in common.

First, it would be possible that TTP and CPEB4 are associated with the same mRNAs, where they recruit the deadenylation and polyadenylation machinery, respectively. In this case, the competition between the activities of the recruited complexes would determine the final outcome of the mRNA **(Fig. 51a)**. Alternatively, we could consider that either the deadenylation or the polyadenylation machinery can be present on an mRNA. In this case, the number of TTP or CPEB4 molecules associated with the mRNA could favour the recruitment of one or the other complex **(Fig. 51b).** Moreover, we could also imagine that mRNA association with one protein prevents that the recruitment of the other. Consequently, CPEB4 and TTP would not be associated with the same mRNAs **(Fig. 51c)**. In this case, it would be interesting to address whether the same mRNA molecule can be sequentially associated with the most abundant or active protein throughout the different phases of the LPS response.

Most probably, distinct types of competitions are possible depending on the mRNA features.

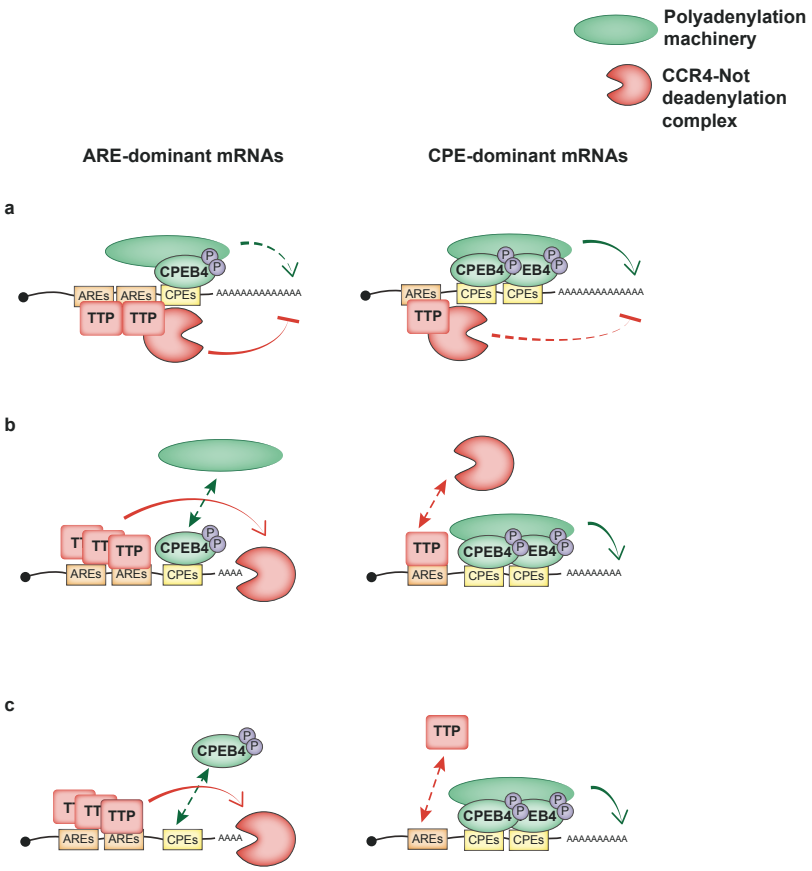

Figure 51. Possible mechanisms behind TTP/CPEB4 mRNA competition. (a) TTP and CPEB4 are associated with the same mRNA and recruit the deadenylation or polyadenylation machinery, respectively. Thus, the final outcome of the mRNA will depend on the activities of these complexes. **(b)** TTP and CPEB4 are associated with the same mRNAs. However, one of them preferentially recruits its corresponding partners. Then, the bound complex will not allow the recruitment of the other. **(c)** TTP and CPEB4 are associated with different mRNAs. Once the mRNA binds one RBP, the other cannot be recruited to this mRNA. This is likely to occur when AREs and CPEs overlap.

9.8. Evaluating the systems used

Finally, I would also like to include a reflexion regarding the systems we have used.

In vitro, Bone Marrow Derived Macrophages display specific features that may be different in monocyte-derived macrophages or tissue-resident macrophages *in vivo*. However, as I have been mentioning throughout this thesis, several mechanistic studies on LPS response have also used BMDMs. Importantly, having a common accepted and robust system to study macrophage biology facilitates that data generated in different laboratories can be contrasted and considered when analysing new results. In this line, I would also like to acknowledge the work performed by Sedlyarov and colleagues, as it has been crucial to understand several pieces in our puzzle **(Fig. 24, 34-37)**. Furthermore, besides their work, their TTP atlas website made the access to their data really straightforward. It would be outstanding if all the published data was as accessible as theirs.

Secondly, regarding the *in vivo* experiments, LPS-induced endotoxemia causes very severe damage in multiple organs. For this reason, and in order to minimize animal use and suffering, we consider that future studies on the role of CPEB4 during the LPS response should consider the use of other models.

CONCLUSIONS

Conclusions

The present study provides new insights into the contribution of CPEB4-mediated translational control to the development and resolution of inflammatory responses in LPS-stimulated macrophages. We describe a new mechanism regulating CPEB4 expression and we propose that CPEB4 function is required for inflammation resolution, in vitro and in vivo. Furthermore, we unveiled that the AREs and CPEs on the 3'UTR of mRNAs define different temporal waves of gene expression during the LPS response.

The main conclusions reached by this work are the following:

1. The MAPK p38α can regulate Cpeb4 mRNA stability during the LPS response. This process is mediated by two ARE binding proteins, HuR and TTP. During early LPS response, p38α promotes HuR binding to Cpeb4 mRNA, which probably mediates the increase in Cpeb4 stability. At later timepoints, though, TTP promotes Cpeb4 mRNA destabilization.

2. Throughout the LPS response, CPEB4 is post-translationally modified by phosphorylation.

3. In BMDMs, CPEB4 is associated with mRNAs related to the MAPK pathway. Thus, during the LPS response, the MAPK pathway and CPEB4 cross regulate each other.

4. During the late phase of the LPS response, CPEB4 regulates the mRNAs of several negative feedback inhibitors of the inflammatory pathways. By promoting the expression of these molecules, CPEB4 participates in inflammation resolution.

5. Throughout the LPS response, HuR, TTP and CPEB4 are associated with common target mRNAs. The AREs and CPEs in the 3'UTR of mRNAs can define their susceptibility to be regulated by TTP or CPEB4 activities. Moreover, during the LPS response, three temporal waves of mRNA expression can be defined by these elements.

6. CPEB4 expression in myeloid cells is dispensable for overall mice homeostasis. However, it is required for LPS-induced endotoxic shock survival. In this context, CPEB4 function is required to limit cytokine expression in splenocytes.

MATERIALS AND METHODS

Materials and methods

Animal Studies. To generate a Myeloid-specific *Cpeb4* KO mice (*Cpeb4*MKO), conditional *Cpeb4* knockout animals (*Cpeb4*$^{lox/lox}$ (Maillo et al. 2017)) were crossed with LysM-Cre$^{T/+}$ (Clausen et al. 1999) transgenic animals obtained from Jackson Laboratory. Offspring was maintained in a C57BL/6J background. Routine genotyping was performed by PCR. Bone Marrow Derived Macrophages (BMDM) were obtained from Wild Type and Myeloid-specific *p38*α KO mice (*p38*αMKO) (Ref Elisa) and full CPEB4 KO mice (Maillo et al. 2017). The mice were given free access to food and water and maintained in individually ventilated cages under specific-pathogen-free conditions (unless otherwise specified). All experimental protocols were approved by the Animal Ethics Committee at the University of Barcelona.

LPS-induced Endotoxic Shock. Wild type (Cre$^{T/+}$) and *Cpeb4*MKO mice were injected intraperitoneally with LPS (10 mg/kg; Santa Cruz SC-3535, E. coli 0111:B4). Animals were monitored and samples were collected at the indicated times. Mice between 2 and 5 months of age were used, matched for age and sex.

Cytokine measurement in serum. Serum was collected after centrifuging clotted blood at 3000g for 30 min. Cytokine levels were measured with a murine ProcartaPlex Assay (Labclinics).

Histological analysis. Tissues were fixed in 10% neutral buffered formalin and stained with H&E. Stained histology sections were visualized with a Nanozoomer 2.0HT – Hamamatsu and the Nanozoomer Digital Pathology Image Software. Disease scores after LPS-induced endotoxic shock were calculated by taking into account the following evaluated parameters (Table I). Each of them was given a score between 0 and 4 and the disease score was calculated by the addition of individual scores.

Table I. Evaluated parameters in the histological analysis	
Liver	Necrosis/Apoptosis of isolated hepatocytes randomly distributed
	Small focal areas of hepatocyte necrosis and mixed inflammatory cell infiltrate
	Increase of cellular inflammatory infiltrate (mainly neutrophils) in sinusoids
	Inflammatory infiltrate portal tracts
	Glycogen depletion
	Gall bladder inflamation
	Hemorrhage (peliosis hepatis)
Lung	Diffuse thickening alveolar septum (neutrophils and some macrophages)
	Perivascular and peribronchial edema
	Congestion alveolar capillaries and alveolar septa
	Neutrophils in vascular lumen
Spleen	Necrosis/apoptosis lymphocytes and increase size white pulp
	Pyogranulomatous inflammatory cell infiltrate white pulp
	Decreased cellularity in red pulp
	Red pulp congestion
Thymus	Necrosis/apoptosis of cortical lymphocytes
	Depletion of lymphocytes in the medulla

Cell culture. BMDMs were isolated from the femurs of adult mice (Celada et al. 1996). Bone marrow cells were differentiated for 7 days on bacteria-grade plastic dishes in DMEM supplemented with 20% (vol/vol) FBS, penicillin (100 units/ml), streptomycin (100 mg/ml), L-glutamine (5mg/ml) and 20% L-cell conditioned medium as a source of M-CSF. DMEM containing 10% FBS, penicillin (100 units/ml), streptomycin (100 mg/ml), L-glutamine (5mg/ml), changing its media on day 5. For stimulation, BMDM were primed with LPS (10ng/ml, E. coli 0111:B4, Santa Cruz SC-3535,), IFNg (low dose 10ng/ml; high dose 100ng/ml, 130-094-047 Milteny Biotec), IL4 (10ng/ml, 550067 Bd Pharmingen) for the indicated time points.

RNA analysis. Total RNA was either extracted by TRIzol reagent (Invitrogen), by phenol-chlorofom or using Maxwell. One microgram of RNA was reverse-transcribed with oligodT and random primers using RevertAid Reverse Transcriptase (ThermoFisher), following the manufacturer's recommendations. Quantitative real-time PCR was performed in a QuantStudio 6flex (ThermoFisher) using PowerUp SYBR Green Master (ThermoFisher). All quantifications were normalized to an endogenous control (TBP or Rpl0).

RNA stability. BMDMs from WT and p38□ KO mice were stimulated with LPS (10ng/ml) for 1h and control cells (time 0) were collected. Fresh medium and Actinomycin D (10ug/ml, Sigma Aldrich A9415) were added and cells were collected at the indicated times. Total RNA was isolated and cDNA was synthesized to perform RT-qPCR analysis, as described below. For each timepoint, remaining *Cpeb4* mRNA was normalized to *Gapdh* mRNA levels. The value at time 0 was set as 100% and for the rest of timepoints the percentage of remaining mRNA was calculated.

Immunoblotting. Protein extracts were quantified by DC Protein assay (Bio-Rad), and equal amounts of proteins were separated by SDS-polyacrylamide gel electrophoresis. After transfer of the proteins onto a nitrocellulose membrane (GE10600001, Sigma) for 1 h at 100mV, membranes were blocked in 5% milk, and specific proteins were labeled with the following antibodies. Quantification was done with ImageStudioLite software.

Immunofluorescence. Cells were fixed with 4% PFA for 10 min followed by permeabilization with 0.1% Triton X-100 for 5 min. Then, cells were blocked with 10% FBS in 0.03% Triton X-100 for 1 h. Primary antibodies were incubated overnight at 4ºC followed by 1 h incubation with the corresponding secondary antibody. Images were obtained on an Olympus ScanR - Xcellence – TIRF with a 60x water objective lense and a Hamamatsu Orca-ER camera. ScanR acquisition software was used.

RNA-immunoprecipitation-sequencing analysis. *Cpeb4*KO and wild type primary Bone Marrow Derived Macrophages, untreated or stimulated for 9h with LPS (10ng/ml), were cultured in DMEM supplemented with 10% FBS, rinsed twice with 10 ml PBS, and incubated with PBS 0.5 % formaldehyde for 5 min at room temperature under constant soft agitation to crosslink RNA-binding proteins to target RNAs. The crosslinking reaction was quenched by addition of glycine to a final concentration of 0.25 M for 5 min. Cells were washed twice with 10 ml PBS, lysed with scraper and RIPA buffer [25 mM Tris-Cl pH7.6, 1% Nonidet P-40, 1% sodium deoxycholate, 0.1% SDS, 100 mM EDTA, 150 mM NaCl, protease inhibitor cocktail, RNase inhibitors], and sonicated for 10 min at low intensity with Standard

Bioruptor Diagenode. After centrifugation (10 min, max speed, 4ºC) supernatants were collected, precleared, and immunoprecipitated (4h, 4ºC, on rotation) with 10 μg of anti-CPEB4 antibody (Abcam), 50 μl of Dynabeads Protein A (Invitrogen). Beads were washed 4 times with cold RIPA buffer supplemented with Protease inhibitors (Sigma-Aldrich), resuspended in 100 μl Proteinase-K buffer with 70 ug of Proteinase-K (Roche), and incubated 60 min at 65ºC. RNA was extracted by standard phenol-chloroform, followed by Turbo DNA-free Kit (Ambion) treatment. Samples were processed at the IRB Functional Genomics Facility following standard procedures. Libraries were sequenced by Illumina 50bp single-end and inputs and IPs were aligned against the mouse reference genome mm10 with Bowtie2 in local mode accepting 1 mismatch in the read seed. Alignments were sorted and indexed with sambamba v0.5.1. Putative over-amplification artifacts (duplicated reads) were assessed and removed with the same software. Coverage tracks in TDF format for IGV were made using IGVTools2. Quality control assessment for unaligned and aligned reads was done with FastQC 0.11. Further quality control steps (Gini/Lorenz/SSD IP enrichment, PCA) was performed in R with the htSeqTools package version 1.12.0. rRNA contamination was assessed using the mm10 rRNA information available at UCSC for both raw and duplicate filtered reads. A preliminary peak calling process was performed for duplicate filtered sequences with the MACS 1.4.2 software using default options to assess overall enrichment in the sequenced samples. The identified peaks (enriched regions) were annotated against the mouse reference genome release mm10 using the ChIPpeakAnno package version 2.16.. Targets were defined combining 3'UTR enriched Regions from MACS peak calling, stablishing as threshold p value < 0,02 and log2(FC) > 1,2. Gene ontology analysis was performed using the DAVID Functional Annotation Bioinformatics Microarray Analysis (Huang et al. 2009b).

BOX 3. OPTIMIZING RIP-SEQ CONDITIONS TO IMPROVE RNA QUALITY

After our first RIP-seq experiment to define CPEB4 targets (n=1, **Fig. 26-28)**, we aimed to repeat this protocol to include more biological replicates in our study. However, given the high level of RNA fragmentation in the first replicate **(Fig. 26)**, we decided to optimize the lysis buffer used for this protocol. As seen in **figure 52a**, by adding more RNase inhibitors, specially ribonucleoside vanadyl complex (RVC) we could highly improve RNA quality. However, when we tried to repeat the RIP-seq experiment with two biological replicates for wild type and Cpeb4KO BMDMs, CPEB4 immunoprecipitation was not highly specific **(Fig 52b, c)**. We hypothesized that the VRC could be interfering with CPEB4 immunoprecipitation and thus, we did an IP test with and without this compound. Unexpectedly, in both conditions CPEB4 IP was again highly inespecific, suggesting that VRC was not the cause of this problem. Finally, we decided to repeat CPEB4 immunoprecipitation using the original buffer with two different batches of CPEB4 antibody (named as 08 and 12). In parallel, we immunoprecipitated HuR to test if these unspecificity was only occurring in CPEB4 IP. We observed that HuR IP was really efficient but in the IPs of both CPEB4 antibodies or the IgG an unspecific smear was again detected **(Fig.52 d)**.

a

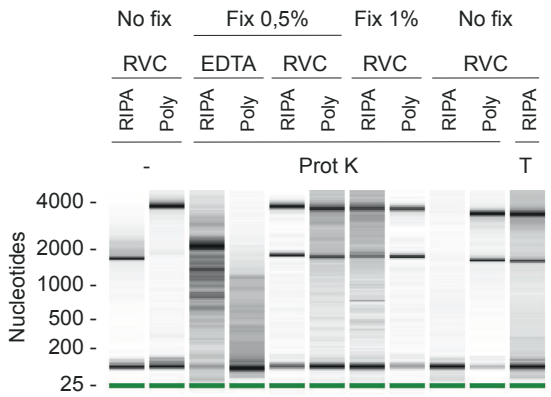

Figure 52. RIP-seq optimization process. (a) After BMDMs lysis with different buffers, mRNA was isolated and RNA integrity was evaluated with an Agilent 2100 BioAnalyzer with the RNA 6000 Pico kit. **(b)** RIP-seq protocol was followed as described but using RIPA buffer supplemented with RVC. Immunoblot for CPEB4 from inputs and immunoprecipitated fractions with anti-CPEB4 antibody in BMDMs obtained from Wild type or *Cpeb4*KO mice (n=2) is shown; Vinculin served as a loading control. Ponceau staining is shown. **(c)** Immunoblot for CPEB4 from inputs and immunoprecipitated fractions with anti-CPEB4 antibody in BMDMs obtained from Wild type. RIPA buffer with and without RVC was used. IgG served as control. **(d)** Immunoblot for CPEB4 and HuR from inputs, immunoprecipitated and unbound fractions from Wild type BMDMs. Two different batches of anti-CPEB4 antibody were used (08 and 12). RIPA buffer with and without RVC was used. IgG served as control. →

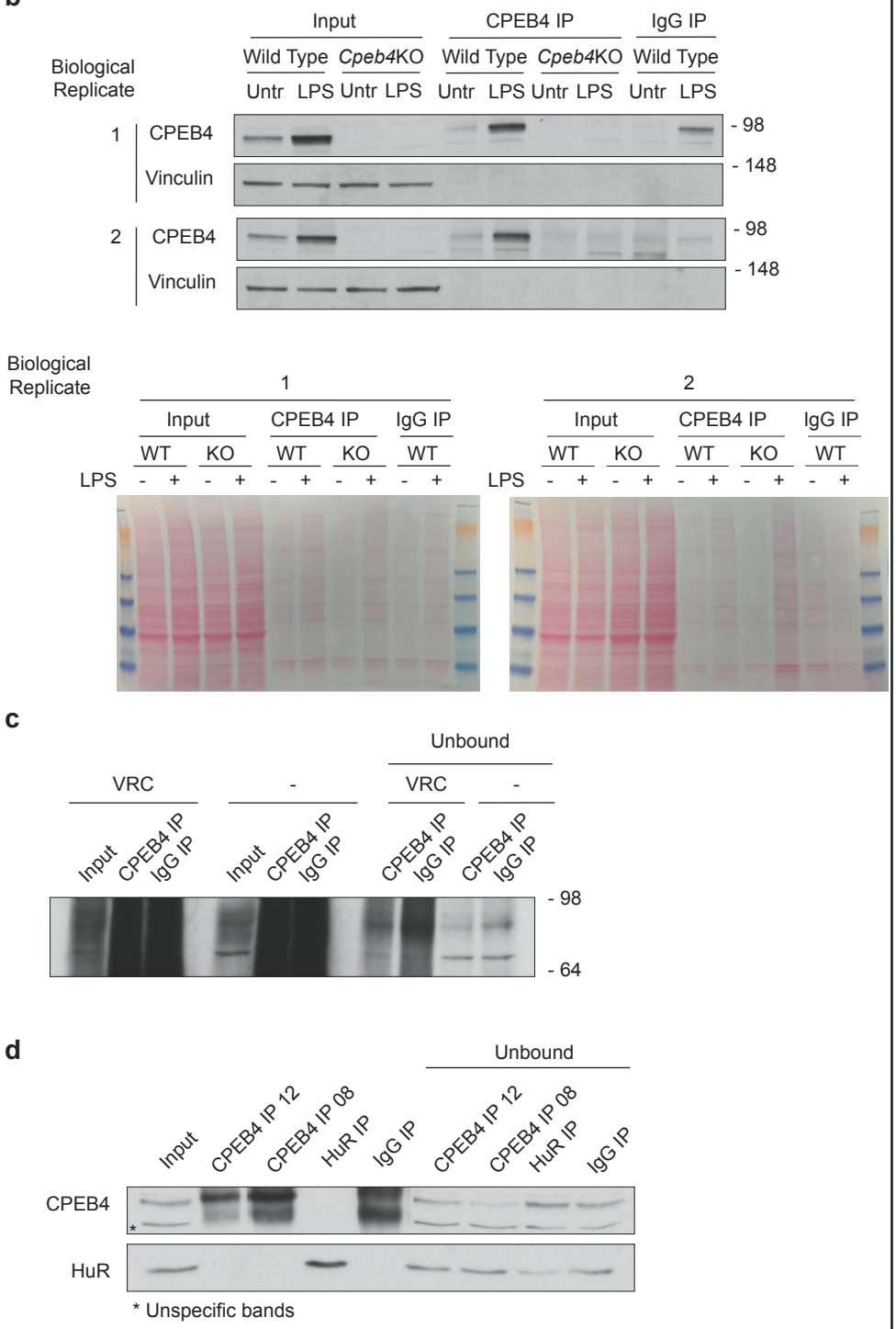

← Figure 52. RIP-seq optimization process.

RIP-seq optimization. Buffers Optimization process: RIPA: 50mM Tris pH=8, 150mM NaCl, 1mM MgCl2, 1% NP40, 0,1% SDS. POLY: 10mM HEPES pH=7, 100mM KCl, 5mM MgCl2, 0,5% NP40. RIPA/POLY buffers were supplemented with 2mM DTT, Protease inhibitors, Riboblock (200U/ml), SUPErase In (100U/ml), 0,5mg/ml Heparin and either 25mM EDTA or 10mM VRC. For proteinase K treatment, fresh add riboblock, heparin, superase IN and VRC were added. Proteinase K was performed for 30min at 42ºC followed by 30min at 65ºC. Befor RNA precipitaton, 1ul of EDTA 0,5M was added.

Script CPE-G. To calculate CPE-G containing mRNAs the following modifications were included in the CPE script defined by Piqué and colleagues (Piqué et al. 2008). We substituted CPEc definition by TTTTGT, removed CPEnc and PBE and maintained the distances to the hexanucleotide.

Statistics. Data are expressed as means±SEM. Dataset statistics were analyzed using the GraphPad Prism software. For two group comparisons, column statistics were calculated and based on Standard Deviation and d'Agostino&Pearson normality test, parametric t test (assuming or not same SD) or non-parametric t-test (Mann-Whitney) was performed. For multiple comparisons, one-way ANOVA Kruskal Wallis test or two-way ANOVA followed by the Bonferroni post-hoc test were used. To asses survival, Kaplan-Meier survival curves were done with Disease Free Survival using R2.15 and the survival package version 2.37-2, adjusting by Gender, Weight and LPS ug. Fisher's exact test was used for contingency analysis. Differences under $p<0.05$ were considered statistically significant (*P<0.05, **P<0.01, ***P<0.001). For animal studies, same sample size tried to include always more than five mice in each group. Animals were grouped in blocks to control for experimental variability. Furthermore, wild-type and knockout animals were bred in the same cages whenever possible and the experimenter was blinded until the conclusion of the experimental analysis. Experiments were repeated independently with similar results as indicated in the figure legends.

Phagocytosis assay. BMDM were incubated with AlexaFluor 594 E. coli Bioparticles (ThermoFisher) for 90 min at 37°C. For cytometry analysis, cells were washed with PBS to remove free particles, then scraped and collected on ice. Samples were run on a Gallios flow cytometer, and data was analyzed using FlowJo software.

For microscopy analysis, cells were washed with PBS and fixed with 4% PFA for 10 min, permeabilized with 0.1% Triton X-100 for 5 min and stained with Dapi. The amount of particle-positive cells was analyzed by fluorescence microscope, with five random fields per condition (n > 200).

Lambda protein phosphatase assay (l-PPase). BMDM were lysed with l-PPase reaction buffer (New England BioLabs, Ipswich, MA) supplemented with 0.4% NP-40 and EDTA-free protease inhibitors (Sigma-Aldrich). l-PPase (New England BioLabs) reactions were performed following manufacturer's instructions.

Ribosome Profiling. Ribosome profiling (RP) was performed as previously described (Loayza-Puch et al. 2016; Slobodin et al. 2017). Briefly, sucrose gradients for separation of polysomes were usually prepared by gentle sequential addition of 2.2ml of the different sucrose solutions (e.i., 47, 37, 27, 17 and 7% in Tris-HCl pH = 7.5 (f.c. 20mM), MgCl2 (f.c. 10mM) and KCl (f.c. 100mM), supplemented with 2mM DTT, Ribosafe RNase inhibitor (Bioline, 1 ml/ml) and CHX (100 mg/ml) into a 12 mL tube (Beckman, 13,2ml 14x89mm) and left overnight at 4ºC to achieve continuous gradient prior to the centrifugation. CHX (100 μg/ml) was added to the medium of 80-85% confluent BMDM (untreated or after 9h of LPS) and incubated for 5min at 37°C. $10x10^6$ cells were collected in ice-cold PBS and lysed in lysis buffer (20 mM Tris-HCl pH 7.8, 10 mM $MgCl_2$, 100 mM KCl, 1% Triton X-100, 2 mM DTT, 100 μg/ml CHX, cOmplete protease inhibitors (Roche). An aliquot was kept for RNA sequencing. Lysates were passed through a 26G needle (BD bioscience) for further homogenization, and centrifuged at 4°C 1300xg for 10 min. Supernatants were treated with 2.5U/μl of RNase I (Ambion) for 45 min at room temperature in gentle constant rotation. Lysates were loaded onto a linear sucrose gradient (7%–47%,(Slobodin et al. 2017)), and fractionated by ultracentrifugation, using a SW-41Ti rotor at 36000 rpm (221632.5g) during 2 hr. The sucrose gradient was divided into 14 fractions of 840 μl. The monosome-enriched sucrose fractions (7 to 10) were collected and treated with proteinase K (PCR grade, Roche), in presence of 1% SDS. The so-released ribosome protected fragments (RPFs) were purified using TRIsure reagent (Bioline), following the manufacturer's instructions. RPFs between 30 and 33 nucleotides in length were size-selected in 10% acrylamide gel and isolated. The 3' ends of the RPFs were dephosphorylated by treatment with

T4 polynucleotide kinase (New England Biolabs) for 6 hr at 37°C in MES-NaOH buffer (100mM MES-NaOH, pH 5.5, 10mM $MgCl_2$, 10mM β-mercaptoethanol, 300mM NaCl). 3' adaptor (RA3) was ligated using T4 RNA ligase 1 (New England Biolabs) for 3.5 hr at 37°C, in absence of ATP. Ligation products were size selected in 10% acrylamide gel, and the 5' ends were phosphorylated by treatment with T4 polynucleotide kinase for 30 min at 37°C, in presence of 1mM ATP. 5' adaptor (RA5) was ligated using T4 RNA ligase 1 (New England Biolabs) during 2.5h at 37°C, and the ligation products were selected in 10% acrylamide gel. Ribosomal RNA depletion was performed by biotin-streptavidin affinity purification using biotinylated ribosomal RNA probes and streptavidin dynabeads. Retro-transcription of the ligation products into cDNA was performed using Super Script III reverse-transcriptase (Invitrogen) following the manufacturer's instructions, and the primer RTP. PCR amplification was performed using the forward primer RP1, and the reverse primer RPI that contained a hexanucleotide index used to multiplex different samples during next generation sequencing (NGS). PCR products were size selected by E-Gel electrophoresis (Invitrogen), and submitted to Illumina 50bp single-end sequencing. After sequencing, Cutadapt was used to remove Illumina 3' adapter and Bowtie2 local 1 mismatch was performed against rRNA. Non-rRNA reads were aligned using bowtie1 (-n1 -m1 -l24)against: CDS+/-18bp(UCSC canonical transcripts), 5'UTR +/- 18bp, or 3'UTR +/- 18bp. Non-rRNA reads were also aligned against whole genome with STAR2.3.0e (mismatch 0.05, minlength 20). Tx- level counts for CDS/UTR reads was imported in R with Rsamtools. CDS/UTR read proportion, read length and periodicity were checked for all reads and for several subsets taking into account different read length (28-31bp). Raw counts and periodicity was checked. DESeq2 was used to identify differentially expressed transcripts between conditions. The RiboProfiling package was used to perform further quality control steps from genome aligned reads.

The sequence of the nucleotide markers, 3' and 5' adapters, RTP, RP1 and different RPI primers is shown in Table I).

Table II. Oligos Ribosome Profiling	
26 nt marker	5′ AGCGUGUACUCCGAAGAGGAUCCAAA
29 nt marker	5′ AGCGUGUACUCCGAAGAGGAUCCAAAAGC
32 nt marker	5′ GGCAUUAACGCGAACUCGGCCUACAAUAGUGA
35 nt marker	5′ GGCAUUAACGCGAACUCGGCCUACAAUAGUGACGA
RNA 5' Adapter (RA5)	5‘ rGrUrU rCrArG rArGrU rUrCrU rArCrA rGrUrC rCrGrA rCrGrA rUrC
RNA 3' Adapter (RA3)	5‘ /5rApp/TGG AAT TCT CGG GTG CCA AGG /3ddC/
RNA RT Primer (RTP)	5' GCCTTGGCACCCGAGAATTCCA
RNA PCR Primer (RP1)	
5' AATGATACGGCGACCACCGAGATCTACACGTTCAGAGTTCTACAGTCCGA	
RNA PCR Primer, Index 1 (RPI1)	
5'CAAGCAGAAGACGGCATACGAGATCGTGATGTGACTGGAGTTCCTTGGCACCCGAGAATTCCA	
RNA PCR Primer, Index 2 (RPI2)	
5'CAAGCAGAAGACGGCATACGAGATACATCGGTGACTGGAGTTCCTTGGCACCCGAGAATTCCA	
RNA PCR Primer, Index 3 (RPI3)	
5'CAAGCAGAAGACGGCATACGAGATGCCTAAGTGACTGGAGTTCCTTGGCACCCGAGAATTCCA	
RNA PCR Primer, Index 4 (RPI4)	
5'CAAGCAGAAGACGGCATACGAGATTGGTCAGTGACTGGAGTTCCTTGGCACCCGAGAATTCCA	
RNA PCR Primer, Index 5 (RPI5)	
5'CAAGCAGAAGACGGCATACGAGATCACTGTGTGACTGGAGTTCCTTGGCACCCGAGAATTCCA	
RNA PCR Primer, Index 6 (RPI6)	
5'CAAGCAGAAGACGGCATACGAGATATTGGCGTGACTGGAGTTCCTTGGCACCCGAGAATTCCA	
RNA PCR Primer, Index 7 (RPI7)	
5'CAAGCAGAAGACGGCATACGAGATGATCTGGTGACTGGAGTTCCTTGGCACCCGAGAATTCCA	
RNA PCR Primer, Index 8 (RPI8)	
5'CAAGCAGAAGACGGCATACGAGATTCAAGTGTGACTGGAGTTCCTTGGCACCCGAGAATTCCA	

Reagents.

Table III. Antibodies		
Anti-Mouse CD11b FITC	557396	Bd Bioscience
Anti-Mouse F4/80 Antigen PE	12-4801-82	eBioscience
Anti-Mouse MHC Class II (I-A/I-E) PC	17-5321-81	eBioscience
CHOP	SC-575	Santa Cruz
COX2	D5H5	Cell Signalling
CPEB4	Ab83009	Abcam
CyclinD1	SC-8396	Santa Cruz
Hif1a	10006421	Cayman
IkB-alpha (6A920)	NB100-56507SS-0.025	Novus Biologicals
P-S6	Clon D68F8, 5364	Cell Signaling
Phospho-p44/42 MAPK (Erk1/2) (Thr202/Tyr204)	Clon E10, 9106	Cell Signaling
SOCS1	Ab9870	Abcam
Tubulin	T9026	Sigma
Vinculin	Ab18058	Abcam

Table IV. RT-qPCR primers

Gene	Forward	Reverse
dtVNN	ccccccccccccccccccVNN	
m18S	cgccccccacccggccgac	gagcgaccaaaggaaccaca
mCcl2	agccgcagcccccgccaccaagc	gcgccgaagaccccagggca
mCiita	ccccaggacacccagcccga	ggccccagaggcgggcacca
mCpeb1	cgccgcaaagaggcacaggc	caaggcaccaacaaacacc
mCpeb2	caccaccagcccccccgaa	cccccgcggcgacccccgc
mCpeb3	gaccggagcaggccccacga	cgccacccgcccccggacggcgg
mCpeb4	gcacgccccaaaacccaccgg	cggaaaccagccgcgaccccaccc
mCxcl1	acccaaaccgaagccacagcc	ccgccagaagccagcgccc
mCxcl2	cccgccccgaccccgaagcc	ccccggcccccccgccgaggga
mElavl1	accggcgaggccgaacccgc	ccacaaaaccgcagcccaag
mH2-Aa	cgccccccgagcccggccaa	ggaacacagccgcccgagga
mH2-Ab1	ggcccacacccgccacgcgg	cgacgccgcccaacaccccg
mH2-Eb1	cgccacggccgagcggaaag	aagcagacgaacagccccgc
mHif1a	ccccggcagcgacgacacag	aagcggccccggagcccccg
mIl10	ggccgccaagccccaccgga	gagaaaccacgacagcgcc
mIl1a	cgccgcaggccacccaaccaagcg	cgccgcaggccacccaaccaagcg
mIl6	ccacccccacgacccccccagag	cgggaccgacgccggcgaca
mNfkbia	gagacccggccccccccaac	ccccggagcccaggaccaca
mNos2	aaccccggagcgagccgcgg	caggaagcaggcgagggcccg
mPtgs2	tgagtaccgcaaacgcttct	cagccatttccttctctcctgt
mRpl0	ccgcaggggcagcagcggc	aagcgcgccccggaccgccc
mSocs1	cgccccccggggcccgcc	gagaccgcaccgccggcc
mSocs3	agcccccccgcagaccccacg	agccagccccgaagcgaaacc
mTbp	agaacaacccagaccagcagca	gggaaccccacaccacagccc
mTnf	ccacggcccagacccccacaccc	gccggcaccaccagccggccgcccc
mZfp36	ccccccccaccaaggccacccg	cgacaggccacggcccaccg

REFERENCES

References

Abernathy, E. & Glaunsinger, B., 2015. Emerging roles for RNA degradation in viral replication and antiviral defense. Virology, 479–480, pp.600–608.

Afroz, T. et al., 2014. A fly trap mechanism provides sequence-specific RNA recognition by CPEB proteins. Genes and Development, 28, pp.1498–1514.

Aguilera, A., 2005. Cotranscriptional mRNP assembly: From the DNA to the nuclear pore. Current Opinion in Cell Biology, 17(3), pp.242–250.

Ananthasubramaniam, B. & Herzel, H., 2014. Positive feedback promotes oscillations in negative feedback loops. PLoS ONE, 9(8).

Arthur, J.S. & Ley, S.C., 2013. Mitogen-activated protein kinases in innate immunity. Nat Rev Immunol, 13(9), pp.679–692.

Barbosa, C., Peixeiro, I. & Romão, L., 2013. Gene Expression Regulation by Upstream Open Reading Frames and Human Disease. PLoS Genetics, 9(8), pp.1–12.

Barillot, E. et al., 2012. Computational Systems Biology of Cancer. Chapman & Hall/CRC Mathematical & Computational Biology.

Beisang, D. & Bohjanen, P.R., 2012. Perspectives on the ARE as it turns 25 years old. Wiley Interdisciplinary Reviews: RNA, 3(5), pp.719–731.

Belloc, E. & Méndez, R., 2008. A deadenylation negative feedback mechanism governs meiotic metaphase arrest. Nature, 452(7190), pp.1017–1021.

Belloc, E., Piqué, M. & Méndez, R., 2008. Sequential waves of polyadenylation and deadenylation define a translation circuit that drives meiotic progression. Biochemical Society Transactions, 36(4), pp.665–670.

Bhatt, D. & Ghosh, S., 2014. Regulation of the NF-κB-mediated transcription of inflammatory genes. Frontiers in Immunology, 5(FEB), pp.1–9.

Bode, J.G., Ehlting, C. & Häussinger, D., 2012. The macrophage response towards LPS and its control through the p38 MAPK-STAT3 axis. Cellular Signalling, 24(6), pp.1185–1194.

Brandman, O. et al., 2005. Systems biology: Interlinked fast and slow positive feedback loops drive reliable cell decisions. Science, 310(5747), pp.496–498.

Brook, M. et al., 2006. Posttranslational Regulation of Tristetraprolin Subcellular Localization and Protein Stability by p38 Mitogen-Activated Protein Kinase and Extracellular Signal-Regulated Kinase Pathways. Molecular and Cellular Biology, 26(6), pp.2408–2418.

Brown, T., 2011. Introduction to Genetics: A Molecular Approach, Taylor & Francis Group.

Burns, D.M. et al., 2011. CPEB and two poly(A) polymerases control miR-122 stability and p53 mRNA translation. Nature, 473(7345), pp.105–8.

Caldeira, J. et al., 2012. CPEB1, a novel gene silenced in gastric cancer: a Drosophila approach. Gut, 61(8), pp.1115–23.

Calderone, V. et al., 2016. Sequential Functions of CPEB1 and CPEB4 Regulate Pathologic Expression of Vascular Endothelial Growth Factor and Angiogenesis in Chronic Liver Disease. Gastroenterology, 150(4), p.982–997.e30.

Carpenter, S. et al., 2014. Post-transcriptional regulation of gene expression in innate immunity.

Nature reviews. Immunology, 14(6), pp.361–76.

Celada, A. et al., 1996. The Transcription Factor PU,1 is Involved in Macrophage Proliferation. Journal of Experimental Medicine, 184(July), pp.61–69.

Chao, H.-W. et al., 2013. Deletion of CPEB3 enhances hippocampus-dependent memory via increasing expressions of PSD95 and NMDA receptors. The Journal of neuroscience : the official journal of the Society for Neuroscience, 33(43), pp.17008–22.

Chao, H.W. et al., 2012. NMDAR signaling facilitates the IPO5-mediated nuclear import of CPEB3. Nucleic Acids Research, 40(June), pp.8484–8498.

Charlesworth, A., Meijer, H. a. & De Moor, C.H., 2013. Specificity factors in cytoplasmic polyadenylation. Wiley Interdisciplinary Reviews: RNA, 4(August), pp.437–461.

Chen, E.Y. et al., 2013. Enrichr: Interactive and collaborative HTML5 gene list enrichment analysis tool. BMC Bioinformatics, 14.

Chen, P.-J. & Huang, Y.-S., 2012. CPEB2-eEF2 interaction impedes HIF-1α RNA translation. The EMBO journal, 31(4), pp.959–71.

Chin, A. & Lécuyer, E., 2017. RNA localization: Making its way to the center stage. Biochimica et Biophysica Acta - General Subjects, 1861(11), pp.2956–2970.

Chu, J. & Pelletier, J., 2015. Targeting the eIF4A RNA helicase as an anti-neoplastic approach. Biochimica et Biophysica Acta - Gene Regulatory Mechanisms, 1849(7), pp.781–791.

Cláudio, N. et al., 2013. Mapping the crossroads of immune activation and cellular stress response pathways. The EMBO journal, 32(9), pp.1214–24.

Clausen, B.. et al., 1999. Conditional gene targeting in macrophage and granulocytes using LysMcre mice. Transgenic Research, 8, pp.265–277.

Clement, S.L. et al., 2011. Phosphorylation of Tristetraprolin by MK2 Impairs AU-Rich Element mRNA Decay by Preventing Deadenylase Recruitment. Molecular and Cellular Biology, 31(2), pp.256–266.

Crick, F., 1970. Central Dogma of Molecular Biology. Nature, 227, p.561.

Crick, F.H.C., 1958. On Protein Synthesis. The Symposia of the Society for Experimental Biology, 12, pp.138–163.

Cycon, K.A. et al., 2013. Histone deacetylase inhibitors activate CIITA and MHC class II antigen expression in diffuse large B-cell lymphoma. Immunology, 140(2), pp.259–272.

Das, S., Sarkar, D. & Das, B., 2017. The interplay between transcription and mRNA degradation in Saccharomyces cerevisiae. Microbial Cell, 4(7), pp.212–228.

Das, T. et al., 2018. A20/tumor necrosis factor α-induced protein 3 in immune cells controls development of autoinflammation and autoimmunity: Lessons from mouse models. Frontiers in Immunology, 9(FEB).

Decker, C.J. & Parker, R., 2012. P-bodies and stress granules: Possible roles in the control of translation and mRNA degradation. Cold Spring Harbor Perspectives in Biology, 4(9).

Dever, T.E. & Green, R., 2015. Phases of Translation in Eukaryotes. , pp.1–16.

Díaz-Muñoz, M.D. & Turner, M., 2018. Uncovering the role of RNA-binding proteins in gene expression in the immune system. Frontiers in Immunology, 9(MAY).

Doller, A., Pfeilschifter, J. & Eberhardt, W., 2008. Signalling pathways regulating nucleo-cytoplasmic shuttling of the mRNA-binding protein HuR. Cellular Signalling, 20(12), pp.2165–2173.

Drisaldi, B. et al., 2015. SUMOylation Is an Inhibitory Constraint that Regulates the Prion-like Aggregation and Activity of CPEB3. Cell Reports, pp.1–9.

Eckmann, C.R., Rammelt, C. & Wahle, E., 2011. Control of poly(A) tail length. Wiley Interdisciplinary Reviews: RNA, 2(3), pp.348–361.

Elkon, R., Ugalde, A.P. & Agami, R., 2013. Alternative cleavage and polyadenylation: Extent, regulation and function. Nature Reviews Genetics, 14(7), pp.496–506.

Essandoh, K. et al., 2016. MiRNA-Mediated Macrophage Polarization and its Potential Role in the Regulation of Inflammatory Response. Shock, 46(2), pp.122–131.

Fabian, M.R. et al., 2013. Structural basis for the recruitment of the human CCR4-NOT deadenylase complex by tristetraprolin. Nature Structural and Molecular Biology, 20(6), pp.735–739.

Fan, H.K. & Cook, J.A., 2004. Molecular mechanisms of endotoxin tolerance. Journal of Endotoxin Research, 10(2), pp.71–84.

Fernández-Miranda, G. & Méndez, R., 2012. The CPEB-family of proteins, translational control in senescence and cancer. Ageing research reviews, 11(4), pp.460–72.

Ferrell, J.E. & Ha, S.H., 2014a. Ultrasensitivity part II: Multisite phosphorylation, stoichiometric inhibitors, and positive feedback. Trends in Biochemical Sciences, 39(11), pp.556–569.

Ferrell, J.E. & Ha, S.H., 2014b. Ultrasensitivity part III: Cascades, bistable switches, and oscillators. Trends in Biochemical Sciences, 39(12), pp.612–618.

Ferrell, J.E., Tsai, T.Y.C. & Yang, Q., 2011. Modeling the cell cycle: Why do certain circuits oscillate? Cell, 144(6), pp.874–885.

Fioriti, L. et al., 2015. The Persistence of Hippocampal-Based Memory Requires Protein Synthesis Mediated by the Prion-like Protein CPEB3. Neuron, pp.1–16.

Fong, S.W. et al., 2016. CPEB3 deficiency elevates TRPV1 expression in dorsal root ganglia neurons to potentiate thermosensation. PLoS ONE, 11(2), pp.1–19.

Friesen, W.O. & Block, G.D., 1984. What is a biological oscillator? The American journal of physiology, 246(6 Pt 2), pp.R847–R853.

Fu, M. & Blackshear, P.J., 2017. RNA-binding proteins in immune regulation: A focus on CCCH zinc finger proteins. Nature Reviews Immunology, 17(2), pp.130–143.

Fu, Y. et al., 2014. Gene expression regulation mediated through reversible m 6 A RNA methylation. Nature Reviews Genetics, 15(5), pp.293–306.

van Furth; et al., 1972. Le systeme phagocytaire mononucleaire: nouvelle classification des macrophages, des monocytes et de leurs cellules souches.

Gallouzi, I.E. & Wilusz, J., 2013. A DIStinctively novel exoribonuclease that really likes U. EMBO Journal, 32(13), pp.1799–1801.

Gebauer, F. & Hentze, M.W., 2004. Molecular mechanisms of translational control. Nature Reviews Molecular Cell Biology, 5(10), pp.827–835.

Geissmann, F. et al., 2010. Unravelling mononuclear phagocyte heterogeneity. Nature Reviews Immunology, 10(6), pp.453–460.

Gérard, C., Gonze, D. & Goldbeter, A., 2012. Effect of positive feedback loops on the robustness of oscillations in the network of cyclin-dependent kinases driving the mammalian cell cycle. FEBS Journal, 279(18), pp.3411–3431.

Di Giammartino, D.C., Nishida, K. & Manley, J.L., 2011. Mechanisms and Consequences of Alternative Polyadenylation. Molecular Cell, 43(6), pp.853–866.

Giangarrà, V. et al., 2015. Global Analysis of CPEBs Reveals Sequential and Non-Redundant Functions in Mitotic Cell Cycle. Plos One, 10(9), p.e0138794.

Goldstrohm, A.C. & Wickens, M., 2008. Multifunctional deadenylase complexes diversify mRNA control. Nature Reviews Molecular Cell Biology, 9(4), pp.337–344.

Guillén-Boixet, J. et al., 2016. CPEB4 is regulated during cell cycle by ERK2/Cdk1-mediated phosphorylation and its assembly into liquid-like droplets. eLife, 5(Nov 2016), pp.1–26.

Gupta, I. et al., 2016. Translational Capacity of a Cell Is Determined during Transcription Elongation via the Ccr4-Not Complex. Cell Reports, 15(8), pp.1782–1794.

Das Gupta, K. et al., 2016. Histone deacetylases in monocyte/macrophage development, activation and metabolism: refining HDAC targets for inflammatory and infectious diseases. Clinical & Translational Immunology, 5(1), p.e62.

Hägele, S. et al., 2009. Cytoplasmic polyadenylation-element-binding protein (CPEB)1 and 2 bind to the HIF-1alpha mRNA 3'-UTR and modulate HIF-1alpha protein expression. The Biochemical journal, 417(1), pp.235–46.

Hajishengallis, G. & Lambris, J.D., 2010. Crosstalk pathways between Toll-like receptors and the complement system. Trends in Immunology, 31(4), pp.154–163.

Hake, L.E., Mendez, R. & Richter, J.D., 1998. Specificity of RNA binding by CPEB: requirement for RNA recognition motifs and a novel zinc finger. Molecular and cellular biology, 18(2), pp.685–693.

Halbeisen, R.E. et al., 2008. Post-transcriptional gene regulation:From genome-wide studies to principles. Cell. Mol. Life Sci., 65, pp.798–813.

Hayden, M.S. & Ghosh, S., 2011. NF-κB in immunobiology. Cell Research, 21(2), pp.223–244.

Herdy, B. et al., 2012. Translational control of the activation of transcription factor NF-κB and production of type i interferon by phosphorylation of the translation factor eIF4E. Nature Immunology, 13(6), pp.543–550.

Hinnebusch, A.G. & Lorsch, J.R., 2012. The mechanism of eukaryotic translation initiation: New insights and challenges. Cold Spring Harbor Perspectives in Biology, 4(10), pp.1–26.

Hitti, E. et al., 2006. Mitogen-activated protein kinase-activated protein kinase 2 regulates tumor necrosis factor mRNA stability and translation mainly by altering tristetraprolin expression, stability, and binding to adenine/uridine-rich element. Molecular and cellular biology, 26(6), pp.2399–2407.

Hoffmann, A. & Baltimore, D., 2006. Circuitry of nuclear factor κB signaling. Immunological Reviews, 210, pp.171–186.

Hu, W., Yuan, B. & Lodish, H.F., 2014. Cpeb4-mediated translational regulatory circuitry controls terminal erythroid differentiation. Developmental cell, 30(6), pp.660–72.

Hu, X., Chakravart, S.D. & Lionel B. Ivashkiv, 2008. Regulation of IFN and TLR Signaling During

Macrophage Activation by Opposing Feedforward and Feedback Inhibition Mechanisms. Immunological Reviews, pp.41–56.

Huang, D.W., Sherman, B.T. & Lempicki, R.A., 2009a. Bioinformatics enrichment tools: Paths toward the comprehensive functional analysis of large gene lists. Nucleic Acids Research, 37(1), pp.1–13.

Huang, D.W., Sherman, B.T. & Lempicki, R.A., 2009b. Systematic and integrative analysis of large gene lists using DAVID bioinformatics resources. Nature Protocols, 4(1), pp.44–57.

Huang, W.-H. et al., 2014. Elevated activation of CaMKIIÎ± in the CPEB3-knockout hippocampus impairs a specific form of NMDAR-dependent synaptic depotentiation. Frontiers in Cellular Neuroscience, 8(November), pp.1–12.

Huang, Y.-S. et al., 2006. CPEB3 and CPEB4 in neurons: analysis of RNA-binding specificity and translational control of AMPA receptor GluR2 mRNA. The EMBO journal, 25(20), pp.4865–76.

Huntzinger, E. & Izaurralde, E., 2011a. Gene silencing by microRNAs: Contributions of translational repression and mRNA decay. Nature Reviews Genetics, 12(2), pp.99–110.

Huntzinger, E. & Izaurralde, E., 2011b. Gene silencing by microRNAs: Contributions of translational repression and mRNA decay. Nature Reviews Genetics, 12(2), pp.99–110.

Hurt, J.A. & Silver, P.A., 2008. mRNA nuclear export and human disease. Disease Models and Mechanisms, 1(2–3), pp.103–108.

Hutchins, A.P., Diez, D. & Miranda-Saavedra, D., 2013. The IL-10/STAT3-mediated anti-inflammatory response: Recent developments and future challenges. Briefings in Functional Genomics, 12(6), pp.489–498.

Igea, A. & Méndez, R., 2010. Meiosis requires a translational positive loop where CPEB1 ensues its replacement by CPEB4. The EMBO journal, 29(13), pp.2182–93.

Imataka, H., Gradi, A. & Sonenberg, N., 1998. A newly identified N-terminal amino acid sequence of human eIF4G binds poly(A)-binding protein and functions in poly(A)- dependent translation. EMBO Journal, 17(24), pp.7480–7489.

Inada, T., 2013. Quality control systems for aberrant mRNAs induced by aberrant translation elongation and termination. Biochimica et Biophysica Acta - Gene Regulatory Mechanisms, 1829(6–7), pp.634–642.

Ingolia, N.T. & Murray, A.W., 2004. The ups and downs of modeling the cell cycle. Current Biology, 14(18), pp.771–777.

Ivshina, M. et al., 2015. CPEB regulation of TAK1 synthesis mediates cytokine production and the inflammatory immune response. Molecular and cellular biology, 35(3), pp.610–8.

Iwasaki, A. & Medzhitov, R., 2015. Control of adaptive immunity by the innate immune system. Nature Immunology, 16(4), pp.343–353.

Jackson, R.J., Hellen, C.U.T. & Pestova, T. V., 2010. The mechanism of eukaryotic translation initiation and principles of its regulation. Nature Reviews Molecular Cell Biology, 11(2), pp.113–127.

Janssens, S., Pulendran, B. & Lambrecht, B.N., 2014. Emerging functions of the unfolded protein response in immunity. Nature Immunology, 15(10), pp.910–919.

Jurado, A.R. et al., 2014. Structure and function of pre-mRNA 5′-end capping quality control and

3′-end processing. Biochemistry, 53(12), pp.1882–1898.

Kaczmarczyk, L. et al., 2016. New phosphospecific antibody reveals isoform-specific phosphorylation of CPEB3 protein. PLoS ONE, 11(2).

Kahvejian, A. et al., 2005. Mammalian poly (A) -binding protein is a eukaryotic translation initiation factor , which acts via multiple mechanisms. Genes and Development, 19, pp.104–113.

Kapp, L.D. & Lorsch, J.R., 2004. The Molecular Mechanics of Eukaryotic Translation. Annual Review of Biochemistry, 73(1), pp.657–704.

Kaul, G., Pattan, G. & Rafeequi, T., 2011. Eukaryotic elongation factor-2 (eEF2): Its regulation and peptide chain elongation. Cell Biochemistry and Function, 29(3), pp.227–234.

Kawasaki, T. & Kawai, T., 2014. Toll-like receptor signaling pathways. Frontiers in Immunology, 5(SEP), pp.1–8.

Ke, Y. et al., 2017. PARP1 promotes gene expression at the post-transcriptiona level by modulating the RNA-binding protein HuR. Nature Communications, 8.

Kim, J.H. & Richter, J.D., 2006. Opposing Polymerase-Deadenylase Activities Regulate Cytoplasmic Polyadenylation. Molecular Cell, 24(2), pp.173–183.

Kojima, S., Sher-Chen, E.L. & Green, C.B., 2012. Circadian control of mRNA polyadenylation dynamics regulates rhythmic protein expression. Genes and Development, 26(24), pp.2724–2736.

Kozak, M., 2002. Pushing the limits of the scanning mechanism for initiation of translation. Gene, 299(1–2), pp.1–34.

Kozomara, A. & Griffiths-Jones, S., 2011. MiRBase: Integrating microRNA annotation and deep-sequencing data. Nucleic Acids Research, 39(SUPPL. 1), pp.152–157.

Kuleshov, M. V. et al., 2016. Enrichr: a comprehensive gene set enrichment analysis web server 2016 update. Nucleic acids research, 44(W1), pp.W90–W97.

Kumagai, Y. et al., 2016. Genome-wide map of RNA degradation kinetics patterns in dendritic cells after LPS stimulation facilitates identification of primary sequence and secondary structure motifs in mRNAs. BMC Genomics, 17(Suppl 13).

Lackner, D.H. & Bähler, J., 2008. Chapter 5 Translational Control of Gene Expression. From Transcripts to Transcriptomes. International Review of Cell and Molecular Biology, 271(C), pp.199–251.

Lavin, Y. & Merad, M., 2013. Macrophages: Gatekeepers of Tissue Integrity. Cancer Immunology Research, 1(4), pp.201–209.

Lawrence, T. & Fong, C., 2010. The resolution of inflammation: Anti-inflammatory roles for NF-??B. International Journal of Biochemistry and Cell Biology, 42(4), pp.519–523.

LeibundGut-Landmann, S. et al., 2004. Specificity and expression of CIITA, the master regulator of MHC class II genes. European Journal of Immunology, 34(6), pp.1513–1525.

Leppek, K., Das, R. & Barna, M., 2018. Functional 5′ UTR mRNA structures in eukaryotic translation regulation and how to find them. Nature Reviews Molecular Cell Biology, 19(3), pp.158–174.

Li, Z., Liu, S. & Yang, Q., 2017. Incoherent Inputs Enhance the Robustness of Biological Oscillators. Cell Systems, 5(1), p.72–81.e4.

Liu, J., Qian, C. & Cao, X., 2016. Post-Translational Modification Control of Innate Immunity. Immunity, 45(1), pp.15–30.

Loayza-Puch, F. et al., 2016. Tumour-specific proline vulnerability uncovered by differential ribosome codon reading. Nature, 530(7591), pp.490–494.

Lomnitz, J.G. & Savageau, M.A., 2014. No Title. , (1).

Lopez-Pelaez, M. et al., 2012. Cot/tpl2-MKK1/2-Erk1/2 controls mTORC1-mediated mRNA translation in Toll-like receptor-activated macrophages. Molecular Biology of the Cell, 23(15), pp.2982–2992.

Lu, W.H., Yeh, N.H. & Huang, Y.S., 2017. CPEB2 Activates GRASP1 mRNA Translation and Promotes AMPA Receptor Surface Expression, Long-Term Potentiation, and Memory. Cell Reports, 21(7), pp.1783–1794.

Lu, Y.-C. et al., 2014. ELAVL1 Modulates Transcriptome-wide miRNA Binding in Murine Macrophages. Cell reports, 9(6), pp.2330–43.

Lykke-Andersen, J. & Wagner, E., 2005. Recruitment and activation of mRNA decay enzymes by two ARE-mediated decay activation domains in the proteins TTP and BRF-1. Genes and Development, 19(3), pp.351–361.

Maillo, C. et al., 2017. Circadian- and UPR-dependent control of CPEB4 mediates a translational response to counteract hepatic steatosis under ER stress. Nature Cell Biology, (January).

Malumbres, M. & Barbacid, M., 2009. Cell cycle, CDKs and cancer: A changing paradigm. Nature Reviews Cancer, 9(3), pp.153–166.

Markmiller, S. et al., 2018. Context-Dependent and Disease-Specific Diversity in Protein Interactions within Stress Granules. Cell, 172(3), p.590–604.e13.

Martinez, F.O. & Gordon, S., 2014. The M1 and M2 paradigm of macrophage activation: time for reassessment. F1000prime reports, 6(March), p.13.

Marzluff, W.F., Wagner, E.J. & Duronio, R.J., 2008. Metabolism and regulation of canonical histone mRNAs: Life without a poly(A) tail. Nature Reviews Genetics, 9(11), pp.843–854.

Mayr, C., 2016. Evolution and Biological Roles of Alternative 3 0 UTRs. Trends in Cell Biology, 26(3), pp.227–237.

Mayr, C., 2017. Regulation by 3 -Untranslated Regions. Annu. Rev. Genet.

McCormick, S.M. & Heller, N.M., 2015. Regulation of macrophage, dendritic cell, and microglial phenotype and function by the SOCS proteins. Frontiers in Immunology, 6(OCT).

Mendez, R., Hake, L.E., et al., 2000. Phosphorylation of CPE binding factor by Eg2 regulates translation of c-mos mRNA. Nature, 404(6775), pp.302–7.

Mendez, R., Murthy, K.G., et al., 2000. Phosphorylation of CPEB by Eg2 mediates the recruitment of CPSF into an active cytoplasmic polyadenylation complex. Molecular cell, 6(5), pp.1253–9.

Merkel, D.J. et al., 2013. The C-terminal region of cytoplasmic polyadenylation element binding protein is a ZZ domain with potential for protein-protein interactions. Journal of Molecular Biology, 425(11), pp.2015–2026.

Miller, S. et al., 2002. Disruption of dendritic translation of CaMKIIalpha impairs stabilization of synaptic plasticity and memory consolidation. Neuron, 36(3), pp.507–519.

Mills, C.D., 2015. Anatomy of a discovery: m1 and m2 macrophages. Frontiers in immunology, 6(May), p.212.

Mino, T. et al., 2015. Regnase-1 and roquin regulate a common element in inflammatory mRNAs by spatiotemporally distinct mechanisms. Cell, 161(5), pp.1058–1073.

Morgan, M., Iaconcig, A. & Muro, A.F., 2010. CPEB2, CPEB3 and CPEB4 are coordinately regulated by miRNAs recognizing conserved binding sites in paralog positions of their 3'-UTRs. Nucleic acids research, 38(21), pp.7698–710.

Moynagh, P.N., 2005. TLR signalling and activation of IRFs: Revisiting old friends from the NF-κB pathway. Trends in Immunology, 26(9), pp.469–476.

Murray, P.J. & Wynn, T. a, 2011. Protective and pathogenic functions of macrophage subsets. Nature reviews. Immunology, 11(11), pp.723–37.

Muzumdar, M.D. et al., 2007. A Global Double-Fluorescent Cre Reporter Mouse. Genesis (New York, N.Y. : 2000), 45, pp.593–605.

Novák, B. & Tyson, J.J., 2008. Design principles of biochemical oscillators. Nature Reviews Molecular Cell Biology, 9(12), pp.981–991.

Novoa, I. et al., 2010. Mitotic cell-cycle progression is regulated by CPEB1 and CPEB4-dependent translational control. Nature cell biology, 12(5), pp.447–56.

Nürenberg, E. & Tampé, R., 2013. Tying up loose ends: Ribosome recycling in eukaryotes and archaea. Trends in Biochemical Sciences, 38(2), pp.64–74.

Oakley, F. et al., 2005. Nuclear factor-kappaB1 (p50) limits the inflammatory and fibrogenic responses to chronic injury. The American journal of pathology, 166(3), pp.695–708.

Ortiz-Zapater, E. et al., 2012. Key contribution of CPEB4-mediated translational control to cancer progression. Nature medicine, 18(1), pp.83–90.

Van Overmeire, E. et al., 2014. Mechanisms driving macrophage diversity and specialization in distinct tumor microenvironments and parallelisms with other tissues. Frontiers in immunology, 5(March), p.127.

Pai, A.A. et al., 2016. Widespread Shortening of 3' Untranslated Regions and Increased Exon Inclusion Are Evolutionarily Conserved Features of Innate Immune Responses to Infection. PLoS Genetics, 12(9), pp.1–24.

Pai, R.K. et al., 2002. Regulation of Class II MHC Expression in APCs: Roles of Types I, III, and IV Class II Transactivator. The Journal of Immunology, 169(3), pp.1326–1333.

Pakos-Zebrucka, K. et al., 2016. The integrated stress response. EMBO reports, 17(10), pp.1374–1395.

Papasaikas, P. & Valcárcel, J., 2015. The Spliceosome: The Ultimate RNA Chaperone and Sculptor. Trends in biochemical sciences, 41(1), pp.33–45.

Parker, R. & Sheth, U., 2007. P Bodies and the Control of mRNA Translation and Degradation. Molecular Cell, 25(5), pp.635–646.

Parras, A. et al., 2018. Autism-like phenotype and risk gene mRNA deadenylation by CPEB4 mis-splicing. Nature, 560(7719), pp.441–446.

Pascual R. et al, under review. The RNA-binding protein CPEB2 regulates mammary hormone sensing in homeostasisand tumourigenesis.

Pavlopoulos, E. et al., 2011. Neuralized1 activates CPEB3: a function for nonproteolytic ubiquitin in synaptic plasticity and memory storage. Cell, 147(6), pp.1369–83.

Peer, E., Rechavi, G. & Dominissini, D., 2017. Epitranscriptomics: regulation of mRNA metabolism through modifications. Current Opinion in Chemical Biology, 41, pp.93–98.

Peng, S.-C. et al., 2010. A novel role of CPEB3 in regulating EGFR gene transcription via association with Stat5b in neurons. Nucleic acids research, 38(21), pp.7446–57.

Perdiguero, E.G. & Geissmann, F., 2016. The development and maintenance of resident macrophages. Nature Immunology, 17(1), pp.2–8.

Piqué, M. et al., 2008. A Combinatorial Code for CPE-Mediated Translational Control. Cell, 132, pp.434–448.

van der Poll, T. et al., 2017. The immunopathology of sepsis and potential therapeutic targets. Nature Reviews Immunology, 17(7), pp.407–420.

Pollard, J.W., 2009. Trophic macrophages in development and disease. Nature reviews. Immunology, 9(4), pp.259–270.

Popp, M.W.-L. & Maquat, L.E., 2013. Organizing Principles of Mammalian Nonsense-Mediated mRNA Decay. Annual Review of Genetics, 47(1), pp.139–165.

Preis, A. et al., 2014. Cryoelectron microscopic structures of eukaryotic translation termination complexes containing eRF1-eRF3 or eRF1-ABCE1. Cell Reports, 8(1), pp.59–65.

Proudfoot, N.J., 2011. Ending the message : poly (A) signals then and now. Genes & development, 25, pp.1770–1782.

Qin, H. et al., 2012. SOCS3 deficiency promotes M1 macrophage polarization and inflammation. Journal of immunology (Baltimore, Md. : 1950), 189(7), pp.3439–3448.

Reith, W., LeibundGut-Landmann, S. & Waldburger, J.-M., 2005. Regulation of MHC class II gene expression by the class II transactivator. Nature reviews. Immunology, 5, pp.793–806.

Richter, J.D., 2007. CPEB: a life in translation. Trends in Biochemical Sciences, 32(6), pp.279–285.

Richter, J.D. & Coller, J., 2015. Pausing on Polyribosomes: Make Way for Elongation in Translational Control. Cell, 163(2), pp.292–300.

Richter, J.D. & Sonenberg, N., 2005. Regulation of cap-dependent translation by eIF4E inhibitory proteins. Nature, 433(7025), pp.477–480.

Roignant, J.Y. & Soller, M., 2017. m6A in mRNA: An Ancient Mechanism for Fine-Tuning Gene Expression. Trends in Genetics, 33(6), pp.380–390.

Roundtree, I.A. et al., 2017. Dynamic RNA Modifications in Gene Expression Regulation. Cell, 169(7), pp.1187–1200.

Roux, P.P. & Blenis, J., 2004. ERK and p38 MAPK-Activated Protein Kinases : a Family of Protein Kinases with Diverse Biological Functions ERK and p38 MAPK-Activated Protein Kinases : a Family of Protein Kinases with Diverse Biological Functions. Microbiology and molecular biology reviews : MMBR, 68(2), pp.320–344.

Roux, P.P. & Topisirovic, I., 2018. Signaling pathways involved in the regulation of mRNA translation. Molecular and Cellular Biology, p.MCB.00070-18.

Sachithanandan, N. et al., 2011. Macrophage deletion of SOCS1 increases sensitivity to LPS and

palmitic acid and results in systemic inflammation and hepatic insulin resistance. Diabetes, 60(8), pp.2023–2031.

Sachs, A.B., Sarnow, P. & Hentze, M.W., 1997. Starting at the beginning, middle, and end: Translation initiation in eukaryotes. Cell, 89(6), pp.831–838.

Saraiva, M. & O'Garra, A., 2010. The regulation of IL-10 production by immune cells. Nature Reviews Immunology, 10(3), pp.170–181.

Scharer, C.D. et al., 2015. Genome-wide CIITA-binding profile identifies sequence preferences that dictate function versus recruitment. Nucleic Acids Research, 43(6), pp.3128–3142.

Schneider, W.M., Chevillotte, M.D. & Rice, C.M., 2014. Interferon-Stimulated Genes: A Complex Web of Host Defenses William. Annual Review of Immunology, pp.513–545.

Schoenberg, D.R. & Maquat, L.E., 2009. Re-capping the message. Trends in Biochemical Sciences, 34(9), pp.435–442.

Schuller, A.P. & Green, R., 2018. Roadblocks and resolutions in eukaryotic translation. Nature Reviews Molecular Cell Biology, pp.1–16.

Sedlyarov, V. et al., 2016. Tristetraprolin binding site atlas in the macrophage transcriptome reveals a switch for inflammation resolution. Molecular systems biology, 12(5), p.868.

Serhan, C.N., Chiang, N. & Van Dyke, T.E., 2008. Resolving inflammation: dual anti-inflammatory and pro-resolution lipid mediators. Nature reviews. Immunology, 8(5), pp.349–61.

Shakespear, M.R. et al., 2011. Histone deacetylases as regulators of inflammation and immunity. Trends in Immunology, 32(7), pp.335–343.

Shatkin, A.J. & Manley, J.L., 2000. The ends of the affair: Capping and polyadenylation. Nature Structural Biology, 7(10), pp.838–842.

Shatsky, I.N. et al., 2018. Cap-Independent Translation : What ' s in a Name ? , pp.1–14.

Shi, Z. et al., 2017. Heterogeneous Ribosomes Preferentially Translate Distinct Subpools of mRNAs Genome-wide. Molecular Cell, 67(1), p.71–83.e7.

Simsek, D. et al., 2017. The Mammalian Ribo-interactome Reveals Ribosome Functional Diversity and Heterogeneity. Cell, 169(6), p.1051–1065.e18.

Slobodin, B. et al., 2017. Transcription Impacts the Efficiency of mRNA Translation via Co-transcriptional N6-adenosine Methylation. Cell, 169(2), p.326–337.e12.

Smallie, T. et al., 2015. Dual-Specificity Phosphatase 1 and Tristetraprolin Cooperate To Regulate Macrophage Responses to Lipopolysaccharide. The Journal of Immunology, 195(1), pp.277–288.

Sonenberg, N. & Hinnebusch, A.G., 2007. New Modes of Translational Control in Development, Behavior, and Disease. Molecular Cell, 28(5), pp.721–729.

Sonenberg, N. & Hinnebusch, A.G., 2009. Regulation of Translation Initiation in Eukaryotes: Mechanisms and Biological Targets. Cell, 136(4), pp.731–745.

Stepien, B.K. et al., 2016. RNA-binding profiles of Drosophila CPEB proteins Orb and Orb2. Proceedings of the National Academy of Sciences, 113(45), pp.E7030–E7038.

Stoecklin, G. et al., 2004. MK2-induced tristetraprolin:14-3-3 Complexes prevent stress granule association and ARE-mRNA decay. EMBO Journal, 23(6), pp.1313–1324.

Sun, L. et al., 2007. Tristetraprolin (TTP)-14-3-3 complex formation protects TTP from dephosphorylation by protein phosphatase 2a and stabilizes tumor necrosis factor-□ mRNA. Journal of Biological Chemistry, 282(6), pp.3766–3777.

Tang, T. et al., 2017. Macrophage responses to lipopolysaccharide are modulated by a feedback loop involving prostaglandin E2, dual specificity phosphatase 1 and tristetraprolin. Scientific Reports, 7(1), pp.1–13.

Tarun, S. & Sachs, A.B., 1995. A common function for mRNA 5'and 3'ends in translation initiation in yeast. Genes & development, 9(23), p.2997.

Tiedje, C. et al., 2012. The p38/MK2-Driven Exchange between Tristetraprolin and HuR Regulates AU-Rich Element-Dependent Translation. PLoS Genetics, 8(9).

Ting, J.P.-Y. & Trowsdale, J., 2002. Genetic Control of MHC Class II Expression. Cell, 109(2), pp.S21–S33.

Topisirovic, I. & Sonenberg, N., 2011. mRNA Translation and Energy Metabolism in Cancer : The Role of the MAPK and mTORC1 Pathways mRNA Translation and Energy Metabolism in Cancer : The Role of the MAPK and mTORC1 Pathways. Cold Spring Harbor Symposia on Quantitative Biology, LXXVI, pp.355–367.

Tsai, T.Y. et al., 2008. Robust, Tunable Biological Oscillations from Interlinked Positive and Negative Feedback Loops Tony. Science, 321(JULY), pp.126–130.

Tugal, D., Liao, X. & Jain, M.K., 2013. Transcriptional control of macrophage polarization. Arteriosclerosis, Thrombosis, and Vascular Biology, 33(6), pp.1135–1144.

Turner, M. & Díaz-Muñoz, M.D., 2018. RNA-binding proteins control gene expression and cell fate in the immune system. Nature Immunology, 19(2), pp.120–129.

Ubersax, J.A. & Ferrell, J.E., 2007. Mechanisms of specificity in protein phosphorylation. Nature Reviews Molecular Cell Biology, 8(7), pp.530–541.

Vairo, G.I.N., Royston, A.K. & Hamilton, J.A., 1992. Macrophage Activation and the Inhibition of Macrophage Proliferation by Tumor Necrosis. , 641.

Wang, C.-F. & Huang, Y.-S., 2012. Calpain 2 Activated through N-Methyl-D-Aspartic Acid Receptor Signaling Cleaves CPEB3 and Abrogates CPEB3-Repressed Translation in Neurons. Molecular and Cellular Biology, 32(August), pp.3321–3332.

Wang, N., Liang, H. & Zen, K., 2014. Molecular mechanisms that influence the macrophage m1-m2 polarization balance. Frontiers in immunology, 5(November), p.614.

Wang, X.-P. & Cooper, N.G.F., 2009. Characterization of the transcripts and protein isoforms for cytoplasmic polyadenylation element binding protein-3 (CPEB3) in the mouse retina. BMC molecular biology, 10, p.109.

Wang, X.P. & Cooper, N.G.F., 2010. Comparative in Silico analyses of Cpeb1-4 with functional predictions. Bioinformatics and Biology Insights, 4, pp.61–83.

Weichhart, T., Hengstschläger, M. & Linke, M., 2015. Regulation of innate immune cell function by mTOR. Nature Reviews Immunology, 15(10), pp.599–614.

Weill, L. et al., 2012. Translational control by changes in poly(A) tail length: recycling mRNAs. Nature structural & molecular biology, 19(6), pp.577–85.

Weinstein, S.L. et al., 1992. Bacterial lipopolysaccharide induces tyrosine phosphorylation and

activation of mitogen-activated protein kinases in macrophages. J Biol Chem, 267(21), pp.14955–14962.

Wells, S.E., et al. & al., E., 1998. Circularization of mRNA by Eukaryotic Translation Initiation Factors. Molecular Cell, 2(1), pp.135–140.

Wertz, I.E. & Dixit, V.M., 2010. Signaling to NF- B: Regulation by Ubiquitination. Cold Spring Harbor Perspectives in Biology, 2(3), pp.a003350–a003350.

Wilson, H.M., 2014. SOCS proteins in macrophage polarization and function. Frontiers in Immunology, 5(JUL), pp.1–5.

Woo, C.W. et al., 2009. Adaptive suppression of the ATF4-CHOP branch of the unfolded protein response by toll-like receptor signalling. Nature Cell Biology, 11(12), pp.1473–1480.

Woo, C.W. et al., 2012. Toll-like receptor activation suppresses ER stress factor CHOP and translation inhibition through activation of eIF2B. Nature Cell Biology, 14(2), pp.192–200.

Xaus, J. et al., 1999. Interferon □ induces the expression of p21(waf-1) and arrests macrophage cell cycle, preventing induction of apoptosis. Immunity, 11(1), pp.103–113.

Xu, S., Tyagi, S. & Schedl, P., 2014. Spermatid Cyst Polarization in Drosophila Depends upon apkc and the CPEB Family Translational Regulator orb2. PLoS genetics, 10(5), p.e1004380.

Yan, Y. Bin, 2014. Deadenylation: Enzymes, regulation, and functional implications. Wiley Interdisciplinary Reviews: RNA, 5(3), pp.421–443.

Yiakouvaki, A. et al., 2012. Myeloid cell expression of the RNA-binding protein HuR protects mice from pathologic inflammation and colorectal carcinogenesis. Journal of Clinical Investigation, 122(1), pp.48–61.

Yona, S. & Gordon, S., 2015. From the reticuloendothelial to mononuclear phagocyte system - The unaccounted years. Frontiers in Immunology, 6(JUL), pp.1–7.

Yoshimura, A., Naka, T. & Kubo, M., 2007. SOCS proteins, cytokine signalling and immune regulation. Nature Reviews Immunology, 7(6), pp.454–465.

Youn, J.Y. et al., 2018. High-Density Proximity Mapping Reveals the Subcellular Organization of mRNA-Associated Granules and Bodies. Molecular Cell, 69(3), p.517–532.e11.

Youssif, C. et al., 2018. Myeloid p38□ signaling promotes intestinal IGF-1 production and inflammation-associated tumorigenesis. EMBO molecular medicine, p.e8403.

Zhang, X., Virtanen, A. & Kleiman, F.E., 2010. To polyadenylate or to deadenylate: That is the question. Cell Cycle, 9(22), pp.4437–4449.

Zika, E. et al., 2003. Histone Deacetylase 1 / mSin3A Disrupts Gamma Interferon-Induced CIITA Function and Major Histocompatibility Complex Class II Enhanceosome Formation. Molecular and cellular biology, 23(9), pp.3091–3102.

APPENDIX

APPENDIX I. CPEB4 target mRNAs in Untreated BMDMs

0610007P14Rik
1110059E24Rik
1110059G10Rik
1810030O07Rik
2310022A10Rik
2510009E07Rik
2510039O18Rik
2810417H13Rik
3110002H16Rik
4931406P16Rik
5730508B09Rik
9530068E07Rik
Abca1
Abcc5
Abhd17c
Abi1
Abi2
Acap2
Acer3
Actn4
Adam10
Adam9
Adgrl2
Adnp2
Adprhl2
Adrbk1
Aebp2
Agpat9
AI597479
AI606181
Akt1
Alcam
Ampd2
Ank
Ankrd27
Ankrd33b
Ankrd40
Ankrd44
Ano6
Ap1ar
Ap1s2
Ap3s1
Apaf1
Aph1a
Api5
Arf1
Arf4
Arf5
Arfgap3
Arhgap17
Arhgap18
Arid1b
Arid4a
Arih1
Arl2bp
Arl5a
Arl5b
Arl6ip6
Arl8a
Arl8b
Armc10
Arnt
Arpc5
Arrdc3
Arrdc4
Arsk
Asb7
Atad1
Atf1
Atf2
Atg5
Atg7
Atp11b
Atp13a3
Atp1a1
Atp2a2
Atp2b1
Atp8b2
Atxn1
Atxn3
Atxn7
Atxn7l3
Azin1
B3gnt2
B4galt1
B4galt3
B4galt5
B4galt6
B630005N14Rik
Baz2a
Bbc3
Bbx
BC028528
Bcl10
Bcl2l11
Bcl3
Bcl7b
Bfar
Bmp2k
Bod1
Brd3
Brox
Bsdc1
Btbd1
Btbd2
Btg2
C2cd5
Caap1
Cab39
Cadm1
Calcrl
Calm3
Calu
Capn12
Capza1
Carm1
Casd1
Casp2
Cat
Cav1
Cav2
Cbfb
Ccdc117
Ccdc126
Ccdc127
Ccdc43
Ccl2
Ccl3
Ccl4
Ccl7
Ccnd1
Ccng2
Ccnt1
Ccny
Ccz1
Cd200r1
Cd274
Cd300lb
Cd44
Cd47
Cd82
Cd93
Cdc27
Cdc34
Cdc40
Cdc42ep3
Cdca4
Cdca7
Cdca7l
Cdk17
Cdk19
Cdk9
Cdyl2
Cebpg
Celf2
Cep120
Cept1
Cercam
Cerkl
Cers6
Cflar
Cggbp1
Chfr
Chmp2b
Chmp4b
Chst11
Chst14
Chsy1
Cks1b
Cldnd1
Clec12a
Clic1
Clint1
Cmip
Cmtm3
Cmtm7
Cnga3
Cnot6
Cnot7
Cnot8
Coa5
Coprs
Cops7b
Coq10b
Cotl1
Cpd
Cpeb2
Cpeb3
Cpeb4
Cpne1
Cpne3
Cpped1
Cpsf4
Creb1
Creb3l1
Crebrf
Crem
Crtc3
Csgalnact2
Csnk1a1
Csnk1g2
Csnk1g3
Csnk2a1
Csrnp1
Ctdp1
Ctdsp2
Ctdspl2
Ctnnd1
Ctns
Ctso
Cul2
Cux1
Cwc25
Cxcr4
Cyfip2
Cyp51
Cyth3
D030056L22Rik
D1Ertd622e
D230025D16Rik
Dab2ip
Dag1
Dapk1
Dcp1a
Dcp2
Ddi2
Ddit4
Ddost
Ddx10
Dek
Dennd6a
Desi2
Dffb
Dip2a
Dlc1
Dnah11
Dnaja3
Dnajb5
Dnajb6
Dnajc10
Dnajc14
Dnal4
Dohh
Dpm3
Dr1
Dram1
Dscr3
Dusp1
Dusp6
Dusp7
Dyrk1a
Dyrk2
E2f3
E2f4
Edem1
Eea1
Efcab14
Efhd2
Efr3a
Egr2
Eif1
Eif2ak3
Elf1
Elf2
Elk3
Emp1
Ensa
Ep300
Epb41
Erbb2ip
Erf
Ergic1
Erh
Erlin1
Ero1l
Esyt1
Etaa1
Ets2
Etv5
Etv6
Exoc5
Extl3
Eya1
Eya3
Faf2
Fam102a
Fam107b
Fam117b
Fam120a
Fam134b
Fam20b
Fam35a
Fam3c
Fam46a
Fam49b
Fam60a
Fam63b
Fam76a
Fam76b
Fam78a

APPENDIX I. CPEB4 target mRNAs in Untreated BMDMs

Fam96a
Far1
Fbxl14
Fbxo21
Fbxo25
Fbxo30
Fcgr2b
Fchsd2
Flcn
Fli1
Fmnl1
Fndc3b
Fnip1
Fos
Foxj2
Foxn2
Foxp1
Foxred2
Frat2
Fzd7
G3bp1
Gab1
Gabpb1
Galnt1
Galnt2
Galnt7
Gas2l3
Gas6
Gatad1
Gatsl2
Gclm
Gdpd1
Ggta1
Ginm1
Gk
Glg1
Gltp
Gltscr1l
Glud1
Glul
Gm10401
Gm20388
Gm28036
Gm28048
Gm5900
Gmcl1
Gmeb1
Gnai2
Gnaq
Gng12
Gnpda1
Golga7
Golph3
Golph3l
Golt1b
Gosr1
Gosr2
Gpbp1l1
Grb2
Gsk3b
Gsr
Gtf2h3
Gtpbp10
H2afv
H2afx
H3f3b
Hacd2
Hcfc1
Hcfc2
Hdac1
Hdac7
Heatr5a
Hells
Helz
Herpud2
Hif3a
Hilpda
Hipk1
Hipk3
Hira
Hist1h1c
Hk2
Hlx
Hmga2
Hmgcl
Hmgcr
Hmgn2
Hmox1
Hnrnpd
Hnrnpf
Hpse
Hspa13
Hus1
Hyou1
Id2
Idh1
Ids
Ier3ip1
Ifnar1
Ifngr1
Igf1
Igfbp4
Ikzf5
Il1rn
Il2rg
Impad1
Ints9
Ipmk
Irf2
Irf5
Irf8
Isca1
Isg20l2
Itga4
Itgav
Jag1
Jak2
Jarid2
Jdp2
Jun
Jund
Kat2b
Katnbl1
Kbtbd2
Kcnj2
Kcnk13
Kctd13
Kctd20
Kctd5
Kdelc2
Kdelr2
Kdm2a
Kdm6b
Kdsr
Khdrbs1
Kifc3
Klf2
Klf6
Klf7
Klhl12
Klhl20
Klhl21
Klhl5
Klhl9
Klra2
Kmt2e
Kmt5a
Kras
Krcc1
Lamc1
Lamp2
Lamtor3
Lasp1
Lats1
Lats2
Ldlrad3
Lemd3
Leprot
Leprotl1
Lgals8
Lin7c
Lix1l
Lman1
Lmnb1
Lnpep
Loxl2
Lpcat2
Lpgat1
Lrp6
Lsm12
Lsm14a
Lsm3
Lsm6
Luzp1
M6pr
Mafg
Mafk
Mak16
Maml1
Man1a
Man2a1
Manea
Manf
Map2k3
Map4k3
Mapkapk3
Mat2b
Max
Mbnl2
Mccc2
Mcm4
Mdfic
Med13l
Mef2a
Mef2c
Men1
Mesdc1
Metap2
Metrnl
Mettl14
Mettl6
Mex3c
Mfap3
Mfsd14a
Mfsd14b
Mfsd4b4
Mfsd7b
Mgat2
Midn
Mier1
Mitf
Mkl1
Mknk1
Mknk2
Mllt10
Mllt6
Mlx
Mmp13
Mob1b
Mob3c
Mob4
Mospd2
Mrpl10
Ms4a6c
Msi2
Msl1
Msl2
Msmo1
Msr1
Mt2
Mta1
Mtdh
Mtf2
Mthfd2
Mtm1
Mtpn
Mxd1
Mxd4
Myadm
Myc
Myd88
Myh9
Myl12a
Myl12b
Mylip
Mzt1
N4bp1
Naa30
Nacc1
Nadk
Naf1
Naga
Nampt
Ncbp1
Ncbp2
Nck2
Ncoa5
Ncoa7
Nde1
Ndrg1
Ndst1
Nectin2
Nedd1
Nek6
Nelfb
Nf1
Nfe2l2
Nfia
Nfkb1
Nfkbia
Nfya
Nfyb
Nin
Nipa2
Nkap
Nlk
Nmt2
Notch1
Npc1
Nptn
Nptx1
Nr2f6
Nr3c1
Nrbf2
Nrp1
Nt5c3
Nt5dc1
Nudt4
Nufip2
Nup153
Nup188
Nup54
Nup62
Nus1
Nxt2
Oraov1
Ormdl2
Osbp
Ostc
Ostm1
Otud1
P2rx4
P2rx7
P4ha1
Pacs2
Pafah1b2
Paip1
Paip2
Pan3
Pank2
Pank3
Papd7
Papola
Papolg
Pbrm1
Pbx2
Pcbp4
Pcid2
Pcnp
Pdcd7
Pdcl
Pde4a
Pde8a
Pdgfa
Pdgfb
Pdia6
Pdik1l
Pdpk1
Peli1
Pgam5
Phc1
Phc2
Phf2
Phf21a
Pias4
Pik3ca
Pim1
Pim3
Pip5k1a
Pkdcc
Pkig
Pkn2
Pla2g4a
Plau
Plaur
Plekha1
Plekha2
Plekha3
Plekha8
Plekhf2
Plxna1
Plxna2
Plxnb2
Plxnc1
Pmp22
Pnrc1
Pnrc2
Poc1b
Pofut2
Pold3
Polr2d
Polr2h
Ppfibp1
Ppib
Ppif
Ppil4
Ppip5k2
Ppm1a
Ppm1k
Ppp1r18
Ppp1r3b
Ppp3ca
Ppp3r1
Ppp4c
Ppp6c
Ppp6r3
Pprc1
Pptc7
Pqlc1
Prkaa1
Prkaca
Prkacb
Prkar2b
Prkch
Prkx
Prosc
Prpsap2
Prrc1
Psen2
Psmc3ip
Psmd11
Psme3
Ptbp1
Ptbp3
Ptms
Ptp4a1
Ptpn1
Ptpn12
Pum2
Pura
Pycr2
Qtrtd1
R3hdm2
Rab10
Rab13
Rab18
Rab1a
Rab22a
Rab31
Rab40b
Rab6a
Rabgef1
Rad21
Rad9b
Rae1
Rai14
Rala
Ralb
Rap1a
Rap1b

APPENDIX I. CPEB4 target mRNAs in Untreated BMDMs

Rap2a
Rap2c
Rarg
Rasa2
Raver1
Rbbp9
Rbl2
Rbm15
Rbm15b
Rbm7
Rbms1
Rbms2
Rc3h2
Rcc1
Rcn2
Reep3
Reep4
Rell1
Rest
Rffl
Rfx7
Rgmb
Rgs1
Rgs2
Rhbdf2
Rhoa
Rhob
Ric1
Rin2
Rnf11
Rnf111
Rnf13
Rnf149
Rnf150
Rnf166
Rnf38
Rock2
Rora
Rpf2
Rpgrip1
Rpia
Rpl34
Rpn1
Rprd1b
Rps27l
Rps6ka3
Rqcd1
Rsl24d1
Rtf1
Runx1
Rwdd4a
Rybp
S1pr1
S1pr2
Sacm1l
Samd8
Sar1a
Sav1
Sbf2
Scap
Scarb2
Scmh1
Scn8a
Scpep1
Scyl2
Sdc4
Sdf2l1
Sec11a
Sec61a1
Selk
Senp3
Sept9
Sep15
Serinc3
Sertad2
Sertad3
Sesn2
Set
Setd1b
Setd2
Setd5
Sf3a1
Sgk1
Sgk3
Sgms1
Sgpp1
Sh3bgrl
Sh3bgrl2
Sh3glb1
Shisa5
Shoc2
Shtn1
Siah1a
Siah2
Sipa1l2
Siva1
Skil
Skp2
Slc12a6
Slc16a1
Slc16a10
Slc17a5
Slc19a2
Slc20a1
Slc25a15
Slc25a16
Slc25a24
Slc25a25
Slc25a32
Slc25a51
Slc2a1
Slc2a12
Slc30a1
Slc30a10
Slc30a5
Slc31a2
Slc35a1
Slc35a2
Slc35c1
Slc35d1
Slc40a1
Slc41a2
Slc44a1
Slc4a7
Slc6a8
Slc7a8
Slc9a6
Slmap
Smad5
Smarca5
Smarcd2
Smim15
Smndc1
Smurf2
Snap23
Snapin
Snx18
Snx22
Snx3
Snx5
Socs3
Socs5
Sos2
Sp1
Sp3
Spata13
Spcs2
Spcs3
Spg21
Spop
Sppl3
Spred1
Spred2
Spry2
Spryd7
Sptssa
Sqrdl
Srd5a3
Srebf2
Srf
Srpr
Srsf4
Srsf9
Ss18
Ssbp3
Ssh1
Ssh2
Ssr1
Ssr2
Ssr3
St13
St3gal1
St6gal1
St8sia4
Stard13
Stard3nl
Stat5b
Stk24
Stk4
Stk40
Strap
Strn3
Stt3a
Stx3
Stx4a
Stx6
Stx7
Sumf2
Sumo1
Sumo2
Supt16
Surf4
Susd6
Suz12
Syap1
Syf2
Syne3
Syngr2
Sypl
Tab2
Tada1
Taf1
Taf2
Taf5l
Tagln2
Tap1
Tapt1
Tbc1d10a
Tbc1d2b
Tbc1d8
Tbcel
Tbl1x
Tbl1xr1
Tbpl1
Tcea1
Tceanc
Tceb1
Tcf12
Tcf3
Terf2
Tfap4
Tgfbr1
Tgfbr2
Tgif1
Tgoln1
Thbs1
Thoc2
Tirap
Tm7sf3
Tm9sf1
Tm9sf2
Tm9sf3
Tma7
Tmcc1
Tmed2
Tmed5
Tmed9
Tmem106b
Tmem123
Tmem127
Tmem131
Tmem165
Tmem167
Tmem167b
Tmem170
Tmem170b
Tmem18
Tmem184b
Tmem189
Tmem230
Tmem254c
Tmem30a
Tmem33
Tmem38b
Tmem39a
Tmem64
Tmem65
Tmem87a
Tmem87b
Tmod3
Tmx2
Tmx3
Tmx4
Tnfaip2
Tnfaip8
Tnfrsf1b
Tnfrsf21
Tnks2
Tnpo1
Tob2
Tollip
Tomm22
Tomm5
Tomm70a
Tor1aip1
Tor3a
Tpm1
Tpm4
Tpra1
Tprgl
Trabd
Trappc10
Trib3
Trim30d
Trp53
Trp53inp1
Tsc22d3
Tshz1
Tspan14
Tspan31
Tusc1
Tvp23b
Twsg1
Txndc5
Txnip
Txnrd1
Uap1
Ubald2
Ube2b
Ube2d1
Ube2f
Ube2h
Ube2r2
Ube2w
Ubfd1
Ublcp1
Ugcg
Ugdh
Usb1
Usf3
Usp12
Usp45
Utp15
Uxs1
Vasp
Vegfa
Vezf1
Vimp
Vkorc1l1
Vma21
Vprbp
Wac
Wbp5
Wdr73
Wdr82
Wfdc12
Wnk1
Wsb1
Wwc2
Xpot
Yipf2
Yipf4
Yipf6
Yy1
Zbtb12
Zbtb7a
Zcchc10
Zcchc24
Zdhhc20
Zdhhc21
Zdhhc7
Zdhhc8
Zfand6
Zfp148
Zfp26
Zfp275
Zfp326
Zfp36
Zfp367
Zfp395
Zfp422
Zfp706
Zhx1
Zmiz1
Zmynd11
Znrd1
Zranb3
Zwilch
Zyx

APPENDIX II. CPEB4 target mRNAs after 9h LPS in BMDMs

0610007P14Rik
0610010F05Rik
1110004F10Rik
1110038F14Rik
1110059E24Rik
1190002N15Rik
1600014C10Rik
1810030O07Rik
2510009E07Rik
2510039O18Rik
2610001J05Rik
2810474O19Rik
3110043O21Rik
3830406C13Rik
4930453N24Rik
4931406P16Rik
4932438A13Rik
9430076C15Rik
9530068E07Rik
A630033H20Rik
Aaed1
Abca1
Abcb10
Abcc1
Abce1
Abhd13
Abhd16a
Abhd17c
Abi1
Acap2
Acer3
Acly
Aco1
Acsl4
Actn4
Actr2
Actr3
Acvr1
Acvr1b
Adam10
Adam17
Adam9
Adgrl2
Adipor1
Adipor2
Adrbk1
Aebp2
Ago2
Agpat1
Agpat9
Ahr
AI597479
AI607873
Ak2
Ak4
Akap7
Akirin1
Akna
Akt1
Alcam
Aldh18a1
Aldh3a2
Alg10b
Alg14
Alkbh5
Alkbh8
Ammecr1
Ampd3
Angel2
Ankfy1
Ankrd13c
Ankrd27
Ankrd40
Ankrd44
Ankrd52
Anpep
Antxr1
Anxa2
Anxa5
Ap1ar
Ap1g1
Ap1m1
Ap1s2
Ap2b1
Ap3m1
Ap3s1
Ap4e1
Ap5m1
Apaf1
Apbb2
Aph1a
Aph1b
Api5
Appbp2
Aprt
Arf4
Arf5
Arfgef1
Arg1
Arhgef3
Arhgef4
Arid2
Arid3a
Arid4a
Arih1
Arl2bp
Arl5a
Arl5b
Arl6ip1
Arl6ip5
Arl8a
Arl8b
Armc10
Arnt
Arpc4
Arpc5
Arpp19
Arrdc3
Arrdc4
Arsk
Asah1
Asb7
Asph
Atad1
Atf1
Atf2
Atf4
Atg5
Atg7
Atl2
Atl3
Atp11b
Atp11c
Atp13a3
Atp1a1
Atp2a2
Atp2b1
Atp2c1
Atp7a
Atp8b2
Atp8b4
Atxn1
Atxn3
Atxn7l3
AU019823
Axl
B230219D22Rik
B3gnt2
B3gnt9
B4galt1
B4galt3
B4galt5
B4galt6
B630005N14Rik
Bambi
Batf
Bax
Baz1b
Baz2a
Baz2b
Bbx
BC005537
BC023829
BC030336
BC048403
Bccip
Bcl10
Bcl2l11
Bcl3
Bend6
Bfar
Bhlhe40
Bmi1
Bmp2k
Bod1
Bpnt1
Braf
Brd3
Brox
Bsdc1
Btbd1
Btbd7
Btf3l4
Btg1
Btg2
Bzw1
C330018D20Rik
C5ar1
Caap1
Cab39
Calcrl
Calm2
Calu
Canx
Cap1
Capn12
Caprin1
Capza1
Capza2
Capzb
Car13
Carhsp1
Carm1
Carnmt1
Casd1
Casp2
Cat
Cav1
Cav2
Cbarp
Cbfb
Cbl
Cbx3
Ccdc126
Ccdc127
Ccdc43
Ccdc47
Ccdc50
Ccdc71l
Ccdc90b
Ccl2
Ccl22
Ccl3
Ccl6
Ccl7
Ccnc
Ccnd1
Ccnd2
Ccng2
Ccni
Ccnt1
Ccny
Ccrl2
Cd200
Cd200r4
Cd274
Cd300lb
Cd300lf
Cd33
Cd38
Cd40
Cd44
Cd47
Cd48
Cd69
Cd82
Cd86
Cd93
Cdc37l1
Cdc42
Cdc42ep3
Cdc42se2
Cdc73
Cdk12
Cdk13
Cdk17
Cdk2ap1
Cdk2ap2
Cdk6
Cdkn1a
Cdkn2aipnl
Cdyl
Cebpg
Celf1
Celf2
Cep192
Cep83
Cept1
Cerkl
Cers6
Cflar
Cggbp1
Ch25h
Chd1
Chdh
Chfr
Chic2
Chmp2b
Chmp4b
Chp1
Chpt1
Chsy1
Chtf8
Chuk
Cinp
Cisd2
Cks1b
Cks2
Clcn5
Cldnd1
Clec12a
Clec5a
Clic1
Clic4
Clic5
Clint1
Cln5
Clock
Cmip
Cmtm3

APPENDIX II. CPEB4 target mRNAs after 9h LPS in BMDMs

Cmtm6
Cmtm7
Cnot6
Cnot6l
Cnot7
Coa5
Cog3
Col18a1
Commd10
Comt
Copb1
Cops2
Coq10b
Coro1c
Cotl1
Cox15
Cox18
Cpd
Cpeb2
Cpeb4
Cpne1
Cpne2
Cpne3
Cpox
Cpped1
Cpsf2
Cpsf4
Creb1
Creb3l1
Crebl2
Crebrf
Crtc3
Csde1
Csf3
Csgalnact2
Csnk1a1
Csnk1g2
Csnk1g3
Csnk2a1
Csrnp1
Ctbp2
Ctnnb1
Ctnnd1
Ctss
Ctu2
Cul5
Cux1
Cxcl1
Cxcl10
Cxcl11
Cxcl16
Cxcl2
Cxcl3
Cyb5b
Cybb
Cyhr1
Cyld
Cyp51
Cysltr1
D030056L22Rik
D16Ertd472e
D1Ertd622e
D230025D16Rik
Dach1
Dag1
Dazap2
Dbf4
Dbt
Dcaf8
Dcbld2
Dcp1a
Dcp2
Dcun1d1
Ddit4
Ddx21
Ddx3y
Ddx42
Dek
Dennd1b
Dennd6a
Desi2
Dfna5
Dhx33
Diaph1
Diaph2
Dip2c
Dirc2
Dnaja1
Dnajb1
Dnajb11
Dnajb5
Dnajb9
Dnajc10
Dnajc5
Dnajc8
Dnmt3a
Dock4
Dolpp1
Dph6
Dpy19l4
Dpysl2
Dr1
Dram1
Dram2
Dscr3
Dusp1
Dusp11
Dusp6
Dusp7
Dync1li2
Dynlt3
Dyrk1a
Dyrk2
E2f3
E2f4
Eaf1
Ece1
Edem1
Edem3
Edn1
Eea1
Eed
Eef1e1
Efhd2
Efr3a
Egln1
Eif1a
Eif2ak2
Eif4ebp2
Eif5a
Elavl1
Elf1
Elf2
Elk1
Elk3
Elk4
Ell2
Elovl5
Emc4
Eml4
Emp1
Eng
Enpp4
Ensa
Entpd7
Ep300
Epc2
Epm2a
Epn2
Eps15
Erbb2ip
Erf
Ergic1
Erh
Erlin1
Erlin2
Ern1
Ero1l
Esrp2
Esyt1
Esyt2
Etnk1
Ets2
Etv6
Evi2a
Evl
Exoc5
Exosc3
Fabp3
Faf2
Fam102b
Fam103a1
Fam107b
Fam118b
Fam120a
Fam134b
Fam168b
Fam174a
Fam179b
Fam192a
Fam204a
Fam206a
Fam20b
Fam210a
Fam234b
Fam3c
Fam43a
Fam45a
Fam46a
Fam49b
Fam60a
Fam63b
Fam76b
Fam96a
Far1
Fbxl14
Fbxl3
Fbxo22
Fbxo28
Fbxo33
Fbxo34
Fbxo9
Fcho2
Fchsd2
Fermt3
Fgfr1op2
Fip1l1
Flcn
Fli1
Flrt2
Fmnl1
Fmr1
Fnbp1
Fnbp1l
Fndc3b
Fnip1
Fnta
Fos
Fosl2
Foxn2
Foxp1
Fpgs
Frmd4b
Fubp3
Fundc1
Fut8
Fyb
Fyttd1
Fzd1
Fzd7
G3bp1
Gab1
Gabpa
Gabpb1
Gadd45a
Galnt1
Galnt11
Galnt2
Galnt7
Ganab
Gas2l3
Gatad2b
Gbas
Gbp3
Gbp9
Gca
Gcc1
Gch1
Gclm
Gcsh
Gdap2
Gdpd1
Gfpt1
Ggh
Ggps1
Ggta1
Gid4
Ginm1
Gja1
Gk
Gltp
Glud1
Glul
Gm10282
Gm10401
Gm12184
Gm12942
Gm20388
Gm20521
Gm28035
Gm28036
Gm28048
Gm29394
Gm37240
Gm6377
Gm6563
Gm7367
Gm9845
Gmcl1
Gmeb1
Gmfb
Gna13
Gnai3
Gnaq
Gng12
Gng2
Gng5
Gnl3l
Gnpda1
Gnpnat1
Golga5
Golga7
Golph3
Golph3l
Golt1b
Gopc
Gosr1
Gosr2
Gpbp1l1
Gpd2

APPENDIX II. CPEB4 target mRNAs after 9h LPS in BMDMs

Gpr85
Grb2
Gsk3b
Gsr
Gtf2a1
Gtf2h1
Gtf2h3
Gtpbp10
H1f0
H2-T24
H2afv
H2afx
Hacd2
Hacd3
Hcfc1
Hcfc2
Hdac5
Hdgf
Heatr5a
Helz
Herc4
Herpud2
Hif1a
Hilpda
Hipk1
Hipk3
Hist1h1c
Hk2
Hlx
Hmga2
Hmgcl
Hmgcr
Hmgcs1
Hmgn2
Hmgxb4
Hn1l
Hnrnpa0
Hnrnpa2b1
Hnrnpab
Hnrnpd
Hnrnpf
Hnrnpk
Hnrnpu
Hnrnpul1
Hnrnpul2
Hook3
Hprt
Hpse
Hs2st1
Hsd17b7
Hspa13
Hspa1b
Hspd1
Hsph1
Hus1
Hyal2
Hyou1
Iah1
Ibtk
Id1
Id2
Id3
Idh1
Idi1
Ids
Ier3ip1
Ier5
Ifi44
Ifit2
Ifnar1
Ifnar2
Ifngr1
Ifngr2
Ifrd1
Ift80
Igf1
Igf1r
Igf2bp2
Igfbp4
Ikbkb
Ikbkg
Ikzf1
Ikzf5
Il12b
Il13ra1
Il1a
Il1rn
Il2rg
Il6
Ilf3
Impa1
Impact
Impad1
Ing3
Ing5
Insig1
Ints12
Ints5
Ints9
Ipmk
Ipo8
Irak4
Irf2
Irf5
Irf9
Isg20
Isg20l2
Isoc1
Itch
Itga4
Itgal
Itgav
Itgax
Itgb1
Itgb8
Itpripl2
Iws1
Jag1
Jak2
Jarid2
Jdp2
Jrkl
Jun
Jund
Kat2b
Kat6a
Katnbl1
Kbtbd2
Kcnj2
Kctd12
Kctd13
Kctd20
Kdelc2
Kdelr1
Kdelr2
Kdm2a
Kdm4a
Kdm4c
Kdm6b
Kdm7a
Khdrbs1
Kif5b
Kin
Klf10
Klf13
Klf2
Klf6
Klf7
Klhl20
Klhl5
Klhl7
Klhl8
Klhl9
Klra2
Kmt2a
Kmt2e
Kmt5a
Kras
Krcc1
l7Rn6
Lacc1
Lamc1
Lamp2
Lamtor3
Larp4
Larp4b
Lasp1
Lats1
Lats2
Lcp2
Ldlr
Ldlrad3
Lemd3
Leprot
Leprotl1
Lgals8
Lif
Lig3
Limd2
Lims1
Lin52
Lin54
Lin7c
Lipa
Lix1l
Lman1
Lman2
Lmbr1l
Lmo4
Lnpep
Lpar1
Lpcat1
Lpcat2
Lpgat1
Lpl
Lpp
Lrp12
Lrp6
Lrrc57
Lrrc8b
Lrrc8c
Lrrc8d
Lrrfip1
Lrrk2
Lsm12
Lsm14a
Lsm3
Lsm8
Luc7l2
Ly96
Lyrm5
Lztfl1
M6pr
Macf1
Mad2l1
Maea
Maf
Maff
Mafg
Mafk
Magohb
Magt1
Mak16
Maml1
Man1a
Man2a1
Manf
Map2k3
Map2k7
Map3k2
Map4k3
Mapk14
Mapk6
Mapk8
Mapkapk3
Mapre1
Marc2
Marcks
Marf1
Max
Mbnl2
Mcl1
Mctp1
Mdfic
Mdm2
Med1
Med11
Med13
Med14
Med17
Mef2a
Mef2c
Men1
Mesdc1
Met
Metap2
Metrnl
Mettl14
Mettl21a
Mettl6
Mex3c
Mfap3
Mfap3l
Mfsd1
Mfsd14a
Mfsd14b
Mfsd4b4
Mfsd7b
Mgat2
Mib1
Midn
Mier1
Mif4gd
Mink1
Mitd1
Mitf
Mknk1
Mknk2
Mkrn1
Mllt1
Mlx
Mmd
Mmp12
Mmp13
Mmp9
Mob1a
Mob1b
Mob3b
Mob3c
Mob4
Mospd2
Mphosph6
Mpv17
Mpv17l
Mrc1
Mrfap1
Mrgbp
Mrpl10
Mrpl36
Mrpl50
Msi2
Msl1
Msl2
Msmo1
Msn
Msr1
Mta1
Mta2
Mtdh
Mtf2
Mtm1
Mtmr14
Mtpn
Mtss1
Mxd1
Myadm
Myd88
Myh9
Myl12a
Myl12b
Mylip
Mynn
Myo10
Myof
Mzt1
N4bp1
N4bp2l1
Naa30
Naa40
Naa50
Nab1
Nacc1
Nadk
Naf1
Naga
Naif1
Nampt
Nap1l4
Nbeal1
Ncbp1
Ncbp2
Ncoa3
Ncoa4
Ndrg1
Ndst1
Ndufaf4
Nedd1
Nedd9
Nek7
Nelfa
Neurl3
Nf1
Nfatc2ip
Nfatc3
Nfe2l2
Nfix
Nfkb1
Nfxl1
Nfya
Nfyb
Nfyc
Nin
Nip7
Nipa2
Nkx6-2
Nlk
Nmt2
Nol11
Nol4l
Nos2
Notch1
Notch2
Npc1
Nploc4
Npm3
Nptn
Nr1h2
Nr3c1
Nrbp1
Nrg4
Nrp1
Nrp2
Nsun3
Nt5c3
Nt5dc1
Nucks1
Nudcd2
Nudt4
Nufip2
Nup153
Nup160
Nup54
Nupl1
Nus1
Nutf2
Nxt2
Oas2
Ogfrl1
Ola1
Opn1sw
Orai2
Oraov1
Orc6
Osm
Ostc
Ovca2
Oxsm
P2rx7
P4ha1
Pabpc1
Pabpn1
Pacs2
Pafah1b1
Pafah1b2
Pag1
Paip1
Pak4
Pan3
Pank2
Pank3

APPENDIX II. CPEB4 target mRNAs after 9h LPS in BMDMs

Papd5
Papd7
Papola
Papss1
Parp14
Parp6
Paxip1
Pbx2
Pcdh7
Pcgf3
Pcgf5
Pcid2
Pcmtd2
Pcnp
Pdcd6
Pdcl
Pddc1
Pde10a
Pde4a
Pde4b
Pde6d
Pde8a
Pdia4
Pdik1l
Pdpk1
Pdzd8
Peak1
Peli1
Pex11a
Pfkfb3
Pfn1
Pgap2
Pggt1b
Pgm1
Phb2
Phc1
Phc2
Phf2
Phf6
Phip
Phtf2
Pias1
Pias4
Piezo1
Pigf
Pigm
Pign
Pik3c2a
Pik3ca
Pik3r5
Pilra
Pim3
Pip4k2b
Pip4k2c
Pip5k1a
Pip5k1c
Pkig
Pkn2
Pla2g12a
Pla2g4a
Plagl2
Plau
Plaur
Plcb3
Plek
Plekha1
Plekha3
Plekha8
Plekhf2
Plod2
Plpp3
Pls3
Plxna1
Plxnc1
Plxnd1
Pnrc1
Pnrc2
Poc1b
Pofut1
Pofut2
Pold3
Polr2d
Polr2h
Pom121
Pon2
Pou2f2
Pp2d1
Ppard
Ppfibp1
Ppif
Ppig
Ppil4
Ppm1b
Ppm1f
Ppm1h
Ppp1cc
Ppp1r12b
Ppp1r15b
Ppp1r18
Ppp1r2
Ppp1r3b
Ppp1r9b
Ppp2r4
Ppp2r5a
Ppp2r5e
Ppp3ca
Ppp3r1
Ppp4r2
Ppp6c
Ppp6r3
Ppt1
Pptc7
Pqlc1
Prex1
Prkaa1
Prkaca
Prkacb
Prkar2b
Prkch
Prkci
Prkrir
Prkx
Pros1
Prosc
Prpf40a
Prpsap2
Prrc2a
Psip1
Psmc3ip
Psmd11
Psmd3
Psmd7
Psme3
Ptbp1
Ptbp3
Ptges
Ptgs2
Ptma
Ptms
Ptp4a1
Ptp4a2
Ptpn1
Ptpn12
Ptprc
Ptpre
Ptprj
Ptprs
Pum1
Pum2
Pura
Pvr
Pygo2
Pyhin1
Pym1
Qk
Qtrtd1
R3hdm2
Rab10
Rab12
Rab14
Rab18
Rab1a
Rab21
Rab31
Rab32
Rab33b
Rab5a
Rab6a
Rab7
Rab8b
Rabgef1
Rac1
Rad21
Rad54l2
Rad9b
Raf1
Rala
Ralb
Rap1a
Rap2b
Rap2c
Rapgef2
Rarg
Rasa2
Rasgrp1
Raver1
Rbbp9
Rbfox2
Rbl1
Rbm10
Rbm15
Rbm22
Rbm26
Rbm27
Rbm33
Rbm47
Rbm7
Rbms1
Rbms2
Rbpj
Rbpms
Rc3h1
Rc3h2
Rcan3
Rcc1
Rcc2
Rcn2
Rcor3
Rdh10
Rec114
Reep3
Reep5
Rell1
Rffl
Rgs19
Rhbdf2
Rhob
Rhoq
Rin2
Rlim
Rnf11
Rnf111
Rnf115
Rnf13
Rnf145
Rnf149
Rnf166
Rnf2
Rnf213
Rnf24
Rnf38
Rnf4
Rnf44
Rnf6
Rock2
Rp2
Rpf2
Rpgrip1
Rpia
Rpn1
Rprd1a
Rprd1b
Rps27rt
Rps6ka3
Rqcd1
Rrm2b
Rrs1
Rsad2
Rsbn1
Rsbn1l
Rsl1d1
Rsl24d1
Rtf1
Rtn4
Runx1
Rwdd4a
Rybp
S100a10
S1pr1
Sacm1l
Samd1
Samd10
Samd8
Samsn1
Sar1a
Sart3
Sash1
Sav1
Sbno1
Sc5d
Scaf4
Scamp1
Scoc
Scpep1
Sde2
Sdf2l1
Sec11a
Sec14l1
Sec22a
Sec22b
Sec23a
Sec24a
Sec61a1
Sec62
Sec63
Seh1l
Selk
Sema4c
Sema4d
Senp1
Senp5
Sephs1
Sept7
Sept8
Sept11
Sep15
Serbp1
Serf2
Serinc3
Serpinb2
Serpine1
Sertad2
Sertad3
Sesn2
Set
Setd1b
Setd2
Setd5
Sfmbt1
Sgk1
Sgk3
Sgms1
Sgms2
Sgpp1
Sh3bgrl
Sh3bgrl2
Sh3gl1
Sh3glb1
Sh3pxd2b
Sh3rf1
Shc1
Shisa3
Shoc2
Shtn1
Siah1a
Siah1b
Siah2
Sipa1l3
Sirpa
Siva1
Skil
Skp2
Slain2
Slc12a6
Slc16a1
Slc16a10
Slc16a6
Slc19a2
Slc20a1
Slc20a2
Slc22a5
Slc25a15
Slc25a16
Slc25a24
Slc25a25
Slc25a32
Slc25a37
Slc25a38
Slc25a46
Slc25a51
Slc26a2
Slc2a1
Slc2a12
Slc31a2
Slc33a1
Slc35a1
Slc35a3
Slc35a5
Slc35c1
Slc36a1
Slc39a1
Slc39a6
Slc40a1
Slc41a2
Slc44a1
Slc4a7
Slc6a6
Slc6a8
Slc7a11
Slc7a2
Slc7a8
Slco3a1
Slfn5
Slmap
Slmo2
Slx4ip
Smad5
Smarcad1
Smarcc2
Smarcd2
Smco4
Smcr8
Smek2
Smg8
Smim10l1
Smim13
Smim14
Smim15
Smndc1
Sms
Smurf2
Snap23
Snrnp40
Snrpa
Snrpd1
Snrpg
Snx10
Snx18
Snx22
Snx3
Snx5
Soat1
Socs1
Socs3
Socs4
Soga1
Sos2
Sp1
Sp3
Spast
Spata13
Spcs2
Spcs3
Specc1l
Spg21
Spin1
Spint2
Spop
Sppl2a
Sppl3

APPENDIX II. CPEB4 target mRNAs after 9h LPS in BMDMs

Spred1
Spred2
Spryd7
Sptssa
Srd5a3
Srebf2
Srek1
Srek1ip1
Srf
Srpk2
Srpr
Srsf1
Srsf2
Srsf4
Srsf5
Srsf6
Srsf7
Srsf9
Ss18
Ssh2
Ssh3
Ssna1
Ssr1
Ssr2
Ssr3
St13
St18
St3gal1
St3gal4
St3gal5
St3gal6
St8sia4
Stag2
Stam
Stambp
Stambpl1
Stard13
Stat2
Stat3
Stat5b
Stat6
Stau1
Stim2
Stk3
Stk4
Stk40
Strn3
Stt3a
Stx12
Stx4a
Stx6
Stx7
Stxbp1
Suco
Sumf2
Sumo1
Sumo2
Supt16
Surf2
Surf4
Susd6
Suz12
Syap1
Syf2
Syncrip
Syngr2
Sypl
Szrd1
Tab2
Tacc1
Taf1
Taf12
Taf2
Taf5l
Taf7
Taf8
Taok1
Tap1
Tapt1
Tars
Tbc1d10a
Tbc1d14
Tbc1d15
Tbc1d20
Tbc1d23
Tbc1d2b
Tbcel
Tbl1x
Tbl1xr1
Tbpl1
Tcea1
Tceanc
Tceb1
Tcf12
Tfrc
Tgds
Tgfbr1
Tgfbr2
Tgif1
Tgm2
Tgoln1
Tgs1
Thbs1
Thg1l
Thoc2
Ticam1
Tifa
Tigar
Timm17a
Timm8b
Tiparp
Tiprl
Tirap
Tle4
Tln1
Tlr3
Tlr4
Tm6sf1
Tm7sf3
Tm9sf1
Tm9sf3
Tma7
Tmbim6
Tmcc1
Tmco1
Tmed2
Tmed5
Tmem101
Tmem106b
Tmem123
Tmem127
Tmem131
Tmem164
Tmem165
Tmem167b
Tmem168
Tmem170b
Tmem185b
Tmem2
Tmem216
Tmem230
Tmem243
Tmem30a
Tmem33
Tmem38b
Tmem39a
Tmem41b
Tmem50a
Tmem59
Tmem64
Tmem65
Tmem67
Tmem68
Tmem87a
Tmem87b
Tmod3
Tmtc2
Tmtc3
Tmx2
Tmx3
Tmx4
Tnfaip3
Tnfaip8
Tnfrsf21
Tnks
Tnks2
Tnpo1
Tns3
Tob2
Tollip
Tomm22
Tomm34
Tomm40
Tomm5
Top1
Tor1aip1
Tor1aip2
Tpd52l2
Tpm1
Tpm3
Tpm4
Tpp2
Tprgl
Tram1
Trem3
Trim25
Trim30d
Trim36
Trmt11
Trp53
Trp53inp2
Trpt1
Trrap
Tshz1
Tsn
Tspan14
Tspan31
Tsr2
Ttc39b
Ttf1
Tusc1
Tvp23b
Twf1
Twsg1
Txndc5
Txnip
Txnrd1
U2surp
Uap1
Uba3
Uba6
Ubac2
Ubald2
Ube2a
Ube2d1
Ube2h
Ube2j1
Ube2k
Ube2n
Ube2q2
Ube2r2
Ube2w
Ube2z
Ube4b
Ubfd1
Ubl3
Ubtd2
Ubtf
Ugcg
Ugdh
Uhmk1
Urb1
Urb2
Usb1
Usf2
Usf3
Usp21
Usp31
Usp39
Usp7
Usp9x
Utp11l
Utp23
Uxs1
Vamp3
Vasp
Vbp1
Vcl
Vdac1
Vdac2
Vegfa
Vezf1
Vgll4
Vhl
Vimp
Vkorc1l1
Vma21
Vprbp
Vps26a
Vps37a
Vps72
Wac
Wapl
Wasf2
Wasl
Wbp5
Wdfy2
Wdfy3
Wdr36
Wdr45b
Wdr82
Wdr89
Wipf1
Wls
Wnk1
Wsb1
Wwp1
Xiap
Xpo7
Xpot
Xpr1
Xrn1
Yaf2
Ybey
Yipf2
Yipf4
Yipf6
Ykt6
Yod1
Ypel2
Yrdc
Ythdf2
Ythdf3
Ywhab
Ywhaz
Yy1
Zak
Zbed3
Zbtb14
Zbtb41
Zbtb44
Zbtb6
Zbtb7a
Zc3h12c
Zc3hav1
Zcchc3
Zcchc8
Zdhhc13
Zdhhc18
Zdhhc20
Zdhhc21
Zdhhc5
Zdhhc8
Zfand6
Zfhx3
Zfp111
Zfp266
Zfp36
Zfp367
Zfp36l1
Zfp36l2
Zfp422
Zfp451
Zfp518a
Zfp652
Zfp654
Zfp687
Zfp706
Zfp740
Zfp790
Zfp871
Zfp91
Zfx
Zhx1
Zmiz1
Zmpste24
Zmynd11
Zmynd8
Znrd1
Zranb1
Zranb3
Zswim6

APPENDIX III. TTP target mRNAs during the LPS response

We considered as TTP targets the iCLIP-defined TTP targets in BMDMs stimulated for 3h or 6h with LPS. Only those mRNAs with detected binding sites in its 3'UTR were included (Sedlyarov et al., 2016)

5730508B09Rik
9530068E07Rik
Abcc1
Actb
Aff1
Anxa5
App
Arf4
Arl8a
Asb1
Atf3
Atp6v0b
Atp6v1e1
Atxn2l
Atxn7l1
B2m
Bcl10
Brd4
Ccdc50
Ccl12
Ccl2
Ccl3
Ccl4
Ccl7
Ccl9
Ccng2
Ccr5
Ccrl2
Cd274
Cd44
Cd69
Cdkn1a
Cebpb
Cep170
Cflar
Cish
Cklf
Clec4e
Cmpk2
Cmtm6
Cox17
Cpd
Cpne3
Csf3
Csrnp1
Cxcl1
Cxcl10
Cxcl2
D1Ertd622e
Dck
Dda1
Degs1
Dennd4b
Dock8
Dusp1
Dusp11
Dusp2
Edn1
Ehd1
Eno2
Errfi1
Ets2
Etv3
Etv6
Evl
Fam49b
Fgl2
Fos
Fth1
Gch1
Gdf15
Gnb2
Golga7
H2-T24
H3f3b
Hif1a
Hmox1
Icam1
Ier3
Ifit2
Il10
Il10ra
Il12b
Il1a
Il1b
Il1rn
Il27
Il6
Inpp4a
Irf1
Junb
Ldlr
Lgals3
Lipg
Lpl
March5
Maf
Mafk
Mapk1ip1l
Mapk6
Marcks
Mcl1
Mdm2
Mllt11
Mmp13
Mpeg1
Mxd1
Myadm
Myl12a
Myl12b
Nab2
Nfkbia
Nfkbiz
Nlrp3
Nos2
Notch1
Nt5c3
Papd7
Pcgf3
Pde4b
Peli1
Picalm
Pim1
Pim3
Plaur
Pld2
Plek
Ppp1r15a
Ppp3r1
Prdx1
Ptgs2
Pvr
Rab18
Rab5c
Rabep1
Ralgds
Rasgef1b
Rassf4
Rbm33
Rhob
Rusc2
Sdc4
Sdcbp
Serpine1
Sfmbt1
Sgk3
Slamf7
Slc16a10
Slc4a7
Slfn4
Slfn5
Smpdl3a
Socs1
Socs3
Sp100
Spp1
Spred1
Stat1
Stip1
Stx7
Tbc1d13
Tiparp
Tmed4
Tmem171
Tmem2
Tmem55b
Tnf
Tnfaip2
Tnfaip3
Tnfrsf11a
Tnfrsf1b
Tnfsf9
Tns3
Tor1aip1
Tpm4
Trim30a
Txnrd1
Ufd1l
Usp12
Usp18
Ywhaz
Zeb2
Zfp36
Zfp36l2

APPENDIX IV. ARE/CPE Score

Gene Symbol	AREs	CPEs	ARE/CPE Score
Il1rn	0	7	-
Ptges	0	5	-
Socs1	0	1	-
Ccnd2	2	11	-2.46
Slco3a1	2	7	-1.81
Maf	4	12	-1.58
Mxd1	5	12	-1.26
Picalm	9	21	-1.22
Mapk6	4	9	-1.17
Cpeb4	17	35	-1.04
Klra2	2	4	-1.00
Ccl2	1	2	-1.00
Ccl7	2	4	-1.00
Nfkbia	2	4	-1.00
Peli1	5	9	-0.85
Txnrd1	4	7	-0.81
Notch1	4	7	-0.81
Hif1a	8	14	-0.81
Nos2	3	5	-0.74
Ccrl2	2	3	-0.58
Pim1	5	7	-0.49
Pyhin1	5	7	-0.49
St3gal6	3	4	-0.42
Il1a	3	4	-0.42
Zfp36	3	4	-0.42
Aff1	9	12	-0.42
Il10ra	3	4	-0.42
Cflar	13	16	-0.30
Stx7	5	6	-0.26
Pilra	3	3	0.00
Ccl22	2	2	0.00
Ccl4	2	2	0.00
Dusp1	4	4	0.00
Stip1	1	1	0.00
Tor1aip1	8	7	0.19
Antxr1	5	4	0.32
Mllt11	10	8	0.32
Nlrp3	5	4	0.32
Socs3	4	3	0.42
Cd274	11	8	0.46
Slc4a7	25	18	0.47
Ifi44	7	5	0.49
Slc7a2	3	2	0.58
Tiparp	9	6	0.58
Il6	6	4	0.58
Ccl3	5	3	0.74
Tnfaip3	5	3	0.74
Ptgs2	14	8	0.81
Cxcl1	7	4	0.81
Cd69	2	1	1.00
Tnfsf9	2	1	1.00
Cxcl2	11	5	1.14
Il1b	4	1	2.00
Cmpk2	7	1	2.81
Ralgds	1	0	-
Usp18	2	0	-
Cish	3	0	-
Il27	5	0	-
Ier3	5	0	-
Il10	6	0	-
Tnf	8	0	-

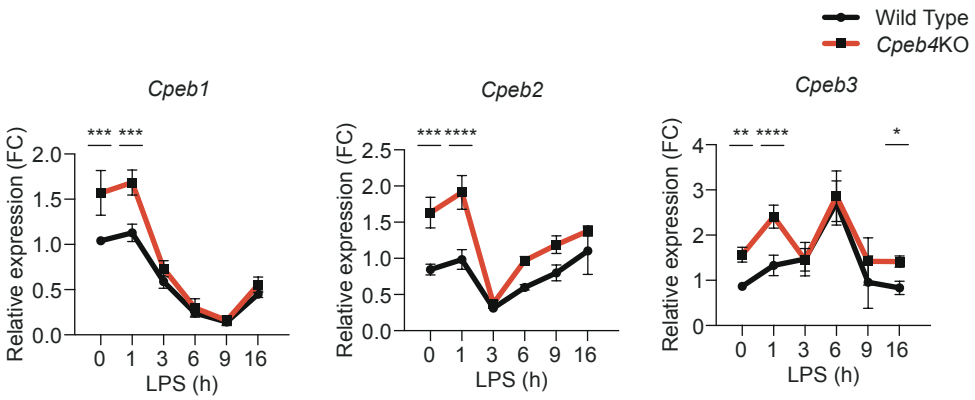

Figure 53. Increased *Cpeb1-3* levels in *Cpeb4*KO BMDMs. Wild type or *Cpeb4*KO BMDMs were stimulated with LPS (10ng/ml) for 0-24h and mRNA was measured by RT-qPCR. *Tbp* was used to normalize and relative levels to untreated wild type were calculated. Data are shown as mean and s.e.m.; n=6. Statistics: Two-way ANOVA *pv<0.05; **pv<0.01; *** pv<0.001; ****pv<0.0001.

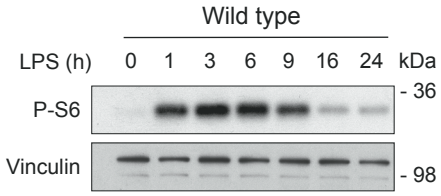

Figure 54. mTOR activation during the LPS response. BMDMs were treated with LPS (10ng/ml) for the indicated hours. Immunoblot analysis of phospho-S6 as a readout of mTOR activity is shown. Vinculin was used as loading control.

1. Publications

Clara Suñer*, Annarita Sibilio*, Judit Martín, Ivan Dotu, Oscar Reina, Vittorio Calderone, Elisa Rivas, Ángel Nebreda, Raúl Méndez. Inflammation resolution requires CPEB-mediated translational control in macrophages. Manuscript in preparation.

Annarita Sibilio*, **Clara Suñer***, Judit Martín, Toni Berenguer, Ángel Nebreda, Raúl Méndez. CPEB-mediated translational control in intestinal homeostasis and diseases. Manuscript in preparation.

In this work, we have studied CPEB4 contribution to intestinal homeostasis and disease. Our results suggest that CPEB4 could control the immune intestinal environment. Indeed, in stressed-colitis conditions Cpeb4KO mice present enhanced inflammation and a delay in the recovery of colon epithelia. However, in tumoral circumstances CPEB4-mediated immune compartment could help the adaptive tumoral response to struggle against cancer cells, as Cpeb4KO mice show less colitis-associated tumorigenesis when treated with chemical carcinogens.

Rosa Pascual, Judit Martín, Fernando Salvador, Oscar Reina, **Clara Suñer**, Gonzalo Fernández-Miranda, Yi-Shuian Huang, Roger R. Gomis and Raúl Méndez. The RNA-binding protein CPEB2 regulates mammary hormone sensing in homeostasis and tumourigenesis. Under review

2. Other projects

Novel functions for CPEB3 in mammalian organisms during homeostasis

Anna Ferrer*, **Clara Suñer***, Judít Martín, Neus Prats, Rosa Pascual, Gonzalo Fernández Miranda, Raúl Méndez.

This project aimed to describe new functions for CPEB3 using distinct ubiquitous Cpeb3KO mouse models. Given all the literature about CPEB3 function in the nervous system, here we focused on the other organs. Interestingly, we observed that CPEB3 was highly expressed in testis. Additionally CPEB3 was also expressed in retina, pancreas, prostate, muscle, heart, liver and mammary gland. In accordance with that, two Cpeb3KO models, inducible and constitutive, showed displayed defects in testis and retina. Importantly, in these two tissues the four members of the CPEB family are expressed, suggesting a possible collaboration between them to regulate CPE-containing mRNAs in different cell types or at different stages.

Interplay between CPEBs functions in mammalian organisms

Judit Martín*, Rosa Pascual*, **Clara Suñer***, Neus Prats, Gonzalo Fernández Miranda, Raúl Méndez.

This project aimed to study the interplay between the different members of the CPEB family in mammalian organism in vivo. Using an ubiquitous inducible system, we generated and characterized the single Cpeb1-4KO mouse models, which overall showed mild phenotypes in homeostasis. Moreover, we also combined CPEBs deletions and generated double, triple and quadruple Cpeb1-4KO mouse models. Interestingly, as we depleted the expression of more CPEBs, mice developed more aggressive phenotypes. These results indicated that CPEBs function partially overlap and, in single CpebKO mice, CPEBs can possibly compensate the absence of one of them.

*Equally contributing

ACKNOWLEDGMENTS

Mil Gràcies

Dicen que el cerebro de los niños es como una esponja, que absorbe todo lo que hay a su alrededor. En mi experiencia, durante el doctorado tu cerebro vuelve un poco a ese estado de absorción y se va empapando de todo lo que te rodea. Por eso es tan importante quién te rodea durante esta etapa.

Todos vosotros, los que me habéis acompañado estos años, me habéis enseñado, mejorado, llevado a nuevos sitios, corregido, ayudado, divertido…y todo eso es mucho más importante que ser doctora. O quizás ser doctora sea eso. Por eso, mil gracias. Os admiro de una manera que no podéis imaginar y que, en unas pocas páginas, voy a intentar que entendáis.

THE COVER

THE COVER

En la bahía de Cadaqués descansa el Cucurucú. Para la mayoría, es una roca con forma de aleta. Para unos pocos, es la aleta de un pez gigante sumergido.

Los investigadores a menudo no somos los primeros en observar un fenómeno...

…sino los primeros en ver qué hay debajo del agua.

A la badia de Cadaqués descansa el Cucurucuc. Per la majoria, és una roca amb forma d'aleta. Per uns pocs, és l'aleta d'un peix gegant submergit.

Els investigadors sovint no som els primers en observar un fenòmen…

…sinó els primers en veure què hi ha sota l'aigua.

On Cadaqués bay, lays the Cucurucuc. For most, it is a fin-shaped rock. For a few, it is the fin of a giant submerged fish.

Researchers are often not the first to observe a phenomenon…

…but the first to see what lays under water.

AMB L'AJUDA DE´

Cucurupeix	Ilich Roimeser instagram.com/ilich_roimeser
Diseño de la portada	Friedel Scholten www.scholtenstudio.com
Disseny de l'interior	Marta Ferrer www.vausestudio.com